ASTROGEOLOGIC STUDIES

ANNUAL PROGRESS REPORT

July 1, 1965 to

July 1, 1966

PART C: COSMIC CHEMISTRY AND PETROLOGY

October 1966

This report concerns work done on behalf of the National Aeronautics and Space Administration.

DEPARTMENT OF THE INTERIOR
UNITED STATES GEOLOGICAL SURVEY

CONTENTS

PART C--COSMIC CHEMISTRY AND PETROLOGY

INTRODUCTION

This Annual Report is the seventh of a series describing the results of research conducted by the U.S. Geological Survey on behalf of the National Aeronautics and Space Administration. The report is in four volumes corresponding to four main areas of research: Part A, Lunar and Planetary Investigations; Part B, Crater Investigations; Part C, Cosmic Chemistry and Petrology; Part D, Space Flight Investigations; and a map supplement. An additional volume presents abstracts of the papers in Parts A, B, C, and D.

The major long-range objectives of the astrogeologic studies program are to determine and map the stratigraphy and structure of the Moon's crust, to work out from these the sequence of events that led to the present condition of the Moon's surface, and to determine the processes by which these events took place. Work that leads toward these objectives includes a program of lunar geologic mapping; studies on the discrimination of geologic materials on the lunar surface by their photometric, polarimetric, and infrared properties; field studies of structures of impact, explosive, and volcanic origin; laboratory studies on the behavior or rocks and minerals subjected to shock; and study of the chemical, petrographic, and physical properties of materials of possible lunar origin and the development of special techniques for their analysis.

Part C, Cosmic Chemistry and Petrology, includes reports on techniques of study, analysis, and interpretation of data on materials of known or suspected extraterrestrial origin. The results of a study in which metallic spherules and glass in tektites are compared with spherules and glass in impactites are presented. Conclusions are drawn as to the partial pressure of oxygen during tektite formation. New chemical analyses of the Martha's Vineyard and Georgia tektites reveal that these tektites are genetically related to the Texas tektites (bediasites) and that they were probably formed by the same event. A study done

in cooperation with the Smithsonian Institution reveals that troilite lamellae in iron meteorites crystallized from a melt, and that some of the meteorites containing these lamellae apparently cooled extremely rapidly. Further data are presented on the search for cosmic dust as part of the Luster Project, done in cooperation with NASA. A review article on the latest techniques available in geochemical analysis is included. The work was done in cooperation with the Branch of Analytical Services, U.S. Geological Survey. Finally, new techniques are presented for the analysis of trace amounts of Cs, Hf, and Ta by neutron activation and of Zn and Ag by spectrography.

METALLIC SPHERULES IN IMPACTITE AND TEKTITE GLASSES

By Robin Brett

INTRODUCTION

Impactite bombs consist predominantly of glass that formed from rock and soil when a meteorite hit the earth. These impactite bombs, which have been described by several authors, commonly contain small Ni-Fe spherules.

Previous analyses of metallic spherules from meteorite impact craters indicate that the spherules are richer in Ni than the parent meteorite from which they were derived. The Ni content of metallic spherules in tektites is consistently low with respect to that in impactite spherules.

In this paper, the possible causes of the Ni enrichment are examined, and oxidation, which the spherules in tektites have not undergone, is proposed as the most likely one.

ACKNOWLEDGMENTS

I should like to thank F. Wood, Goddard Space Flight Center, NASA, Greenbelt, Md., for help in the analytical work, and T. J. Abercrombie, National Geographic Society, Washington, D.C.; T. E. Bunch, University of Pittsburgh; E. C. T. Chao, U.S. Geological Survey, Washington, D.C.; and E. P. Henderson, U.S. National Museum, Washington, D.C., for supplying specimens for study.

DESCRIPTION OF SPHERULES

Ni-Fe spherules in impactite bombs from the Wabar and Meteor Crater meteorite impact craters have been described by several authors (Spencer, 1933; Nininger, 1954; Park and Reid, 1964; Larson and others, 1964). The spherules consist of Ni-Fe finely intergrown with subordinate troilite (FeS) and schreibersite $(Fe, Ni)_3P$ in a fine-grained texture characteristic of rapid cooling from a melt.

Spherules occur both within impactite glass bombs (Spencer, 1933) and as discrete individuals coated with a thin layer of oxide and siliceous glass (Mead and others, 1965). The spherules within the impactite glass bombs commonly occur in dark rather than light-colored glass. Spherules range in diameter from 0.5 mm to less than a micron. Within any given impactite bomb, spherules are highly irregular in size and concentration; they are as common near the surface of bombs as in the interior. Unlike spherules in tektites, not all metal particles in impactites are spherical. A small percentage of these particles in Meteor Crater impactites are irregular in shape; among these, a dumbbell shape is especially common.

Metallic spherules in the Wabar and Meteor Crater impactites are undoubtedly of meteoritic origin, since metallic meteorites are the only available source of Ni-Fe.

Spherules similar in size and mineralogy to those in impactites occur within tektites from Dalat, South Viet Nam, and Mandaluyong, Philippine Islands (Chao and others, 1964). They have also been reported in australites by Schüller and Ottemann (1963). Spherules are considerably rarer in tektites than in impactite glasses. The presence of coesite, which appears to be indicative of meteoritic impact (Chao and others, 1960), in tektites (Walter, 1965) and the resemblance of the metallic spherules in tektites to impactite spherules suggest that the spherules are of meteoritic origin.

IRON AND NICKEL CONTENT OF SPHERULES AND GLASS

Previous Work

Analyses by previous workers of the Ni content of impactite and tektite spherules are given in table 1. Some Wabar spherules are greatly enriched in Ni with respect to the parent meteorite, containing 7.3 wt percent Ni (Spencer, 1933). One spherule in suevite glass from the Bosumtwi Crater (El Goresy, 1966) is low in Ni with respect to impactite spherules from other craters. The composition of the parent meteorite is, however, unknown.

Table 1.--Analyses of nickel in metallic spherules from impactite glass and tektites

[Analysis by electron microprobe unless otherwise stated]

Locality	Ni, wt percent	Reference
Wabar Crater	8 - 11	Park and Reid (1964).
	10 - 48	Larson and others (1964).
	*8.8	Spencer (1933).
Bosumtwi Crater	5.2	El Goresy (1966).
Philippinites	1.2 - 3.2	Chao and others (1962).
	2.1 - 4.9	Chao and others (1964).
Indochinites	4.4 - 13.2	Chao and others (1964).

*Wet chemical analysis.

Analyses of Meteor Crater spherules that were not enclosed in glass also show enrichment of Ni with respect to the composition of the parent meteorite. Ni contents are as high as 45 wt percent (Nininger, 1956; Park and Reid, 1964; Mead, and others, 1965).

No analyses have been made of the Fe or Ni content of the impactite or tektite glasses containing spherules, although Spencer (1933) included a bulk analysis of Wabar black glass with spherules (table 2). Spencer calculated that the Fe-Ni ratio in the black glass (including spherules) is close to that of the parent meteorite. Table 2 also lists analyses of some tektite glasses.

Table 2.--Composition of selected tektites, impactites, and impactite source material

[Tektite analyses from Chao (1963), Wabar analyses from Spencer (1933)]

	Indochinites	Philippinites	Avg. tektite	Wabar white glass	Wabar black glass*	Wabar sandstone
SiO_2	73.0	70.8	73.87	92.88	87.45	92.06
Al_2O_3	12.83	13.85	12.69	2.64	1.77	2.80
NiO	---	---	---	---	.35	---
Fe_2O_3	.64	.70	.47	.23	.28	.60
FeO	4.37	4.30	4.16	.53	5.77	.19
MgO	2.48	2.60	2.18	.47	.60	.45
CaO	1.91	3.09	2.23	1.46	1.90	1.19
SrO	---	---	---	---	---	.01
Na_2O	1.45	1.38	1.38	.42	.39	1.03
K_2O	2.40	2.40	2.28	1.61	.58	1.04
TiO_2	.73	.79	.75	.12	.15	.12
P_2O_5	---	---	---	tr.	tr.	---
CO_2	---	---	---	---	---	.58
MnO	.09	.09	.10	.01	.01	.01
H_2O+	---	---	---	.32	.04	.20
H_2O-	---	---	---	.11	.08	.22
Total	99.90	100.00	100.11	100.80	99.37	100.50

*Includes Ni-Fe spherules.

Present Analyses

In the present study, glass and spherules from both the Mandaluyong, Philippine Islands, and Dalat, South Viet Nam, tektite localities and impactite glass from the meteorite craters at Wabar, Saudi Arabia, and Meteor Crater, Ariz., were examined for Fe and Ni with an ARL electron microprobe. Some spherules were also analyzed for Si, using pure Fe as a standard. The spherules analyzed had not been oxidized by weathering, since they showed no characteristic oxide veinlets or preferential oxidation of troilite.

Fe-Ni standards for spherule analysis were those used by Goldstein and Ogilvie (1965). Synthetic glasses (total Fe = 1.4, 3.1, 4.2, 4.4, 4.9, 6.7 wt percent), pyroxenes (total Fe = 8.5, 14.7, 16.5, 19.9, 24.3 wt percent), chromite (total Fe = 10.9 wt percent), and fayalite (total Fe = 44.2 wt percent) were used as standards in determining the Fe content of the impactite and tektite glasses. The accuracy for the quantitative analysis of Ni in the Ni-Fe spherules is conservatively estimated as within ± 5 percent of the amount present, and for the Fe analyses of the glasses within ± 10 percent of the amount present.

Results are listed in table 3 and figure 1. At least 10 points were analyzed within each spherule, both by traverse and spot analysis. At least 12 points were analyzed within the glass surrounding each spherule by traversing from 0-100 microns out from the spherule at either 2- or 5-micron intervals. At least 10 spot analyses of glass more than 500 microns distant from any spherule were also made for most specimens. The above figure of 500 microns is correct only if it is assumed that there were no spherules within 500 microns below the surface analyzed. The assumption is probably not correct in some measurements of impactite glass, which explains the high Fe content of some of the glass.

Table 3.--Microprobe analyses of Ni in spherules and Fe in surrounding glass of tektites and impactites

[More than one listing for a given specimen corresponds to analyses of more than one spherule in that specimen. All analyses in wt percent, given as mean plus std deviation and range of values. Ranges of values are in parentheses]

Locality	Ni in metal	Fe in glass	Fe content of glass at least 500 microns from any spherule	Comments
Philippinite A	1.5 ± 0.1 (1.3 - 1.7)	4.4 ± 0.2 (3.8 - 4.8)	4.0 ± 0.5 (3.3 - 4.5)	
Philippinite B	2.7 ± 0.3 (2.5 - 3.5)	5.4 ± 0.5 (4.8 - 5.8)	5.4 ± 0.3 (5.0 - 5.7)	
Indochinite A	5.0 ± 0.5 (4.5 - 6.5)	3.6 ± 0.2 (3.2 - 4.0)	3.5 ± 0.2 (3.3 - 3.7)	
Meteor Crater A	22.8 ± 1.9 (19.7 - 23.5)	24.9 ± 1.6 (23.2 - 27.4)	---	Ni content of Canyon Diablo meteorite is 7-8.5 wt percent (Prior, 1953).
Meteor Crater A	55.2 ± 1.1 (53.6 - 56.6)	21.8 ± 1.0 (21.5 - 22.7)	---	
Meteor Crater A	50.6 ± 2.3 (47.1 - 53.6)	17.1 ± 5.4 (11.5 - 22.8) 24.0 ± 0.7 (22.7 - 25.0)	---	Fe content of glass on one side of spherule differs markedly from that on the other.
Meteor Crater B	50.7 ± 0.6 (50.0 - 51.6)	22.8 ± 0.6 (22.2 - 23.5)	17.4 ± 7.2 (0.8 - 23.2)	
Meteor Crater C	61.3 ● 2.0 (57.6 - 64.7)	22.6 ± 0.8 (21.4 - 24.3)	---	
Wabar A	14.1 ± 0.3 (13.5 - 14.7)	7.7 ± 1.0 (6.3 - 8.6)	5.6 ± 2.8 (0.3 - 8.0)	Ni content of parent meteorite is 7.3 wt percent (Spencer, 1933).
Wabar A	12.5 ± 0.2 (12.2 - 12.7)	5.7 ± 1.4 (2.5 - 7.6	5.6 ± 2.8 (0.3 - 8.0)	
Wabar A	14.4 ± 0.3 (14.2 - 14.7)	---	5.6 ± 2.8 (0.3 - 8.0)	
Wabar A	31.8 ± 0.3 (31.2 - 32.1)	9.7 ± 0.4 (9.1 - 10.4)	5.6 ± 2.8 (0.3 - 8.0)	
Wabar B	39.5 ± 0.9 (38.3 - 40.6)	6.3 ± 0.4 (5.8 - 7.0)	4.2 ± 2.4 (1.6 - 6.5)	
Wabar C	11.0 ± 0.7 (9.8 - 13.3)	4.4 ± 0.6 (3.0 - 5.3)	3.3 ± 3.6 (0 - 13.9)	
Wabar C	11.1 ± 0.5 (10.7 - 12.0)	7.2 ± 1.0 (5.5 - 9.7)	3.3 ± 3.6 (0 - 13.9)	
Wabar C	10.0 ± 0.2 (9.9 - 10.2)	6.3 ± 1.3 (4.6 - 10.7)	3.3 ± 3.6 (0 - 13.9)	
Wabar C	10.2 ● 0.4 (9.9 - 10.8)	6.5 ± 1.8 (4.2 - 9.2)	3.3 ± 3.6 (0 - 13.9)	
Wabar C	29.4 ± 0.5 (28.2 - 30.5)	7.6 ± 0.5 (6.3 - 8.6)	3.3 ± 3.6 (0 - 13.9)	
Wabar D	8.4 ± 0.4 (7.9 - 9.0)	8.4 ± 0.6 (6.7 - 9.1)	---	Light-colored glass of Park and Reid (1964). Spherules so abundant that all glass lay within 500 microns of a spherule.
Wabar D	11.5 ± 0.1 (11.3 - 11.7)	7.3 ± 1.3 (4.6 - 9.2)	---	Do.
Wabar D	8.5 ± 0.3 (8.3 - 8.7)	11.5 ± 2.1 (7.8 - 14.2)	---	Do.
Wabar D	8.6	4.2 ± 3.7 (0.1 - 8.8)	---	Light-colored glass, as above. 1 spot analysis of metal only.

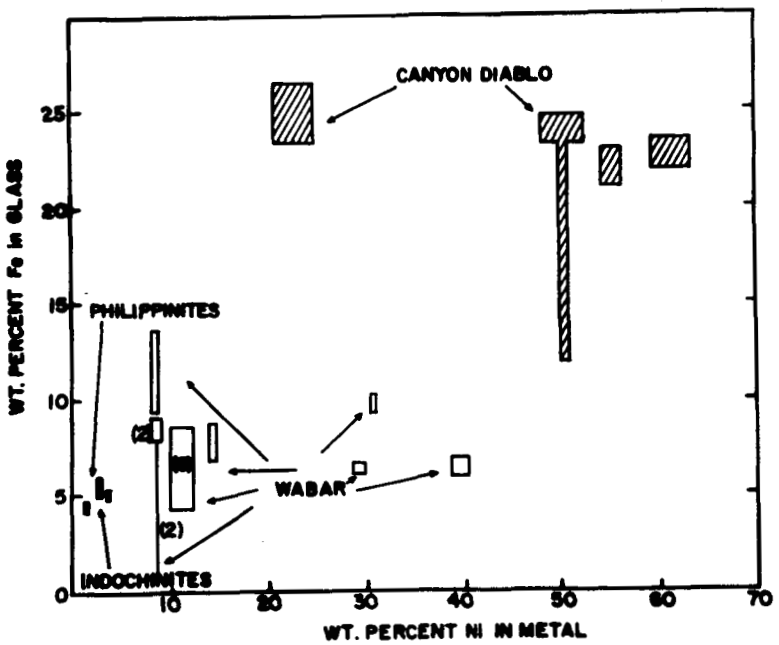

Figure 1.--Plot of Ni in metallic spherules versus Fe content of surrounding glass for indochinite, philippinite, Canyon Diablo (Meteor Crater) impactite, and Wabar impactite specimens. The range of values for any given measurement represents the standard deviation from the mean for the analysis. The figures in parentheses refer to the number of different spherule measurements which plot within the area shown.

Analysis of tektite and impactite glasses showed greater contents of Fe and Ni in glass within 8 microns of the spherule boundaries than in glass farther from the spherule, presumably because of excitation from part of the spherule below the surface. No gradients in Fe content of glass were observed within 100 microns of any spherule. If any gradients exist within 8 microns, they are masked by the excitation effect. Analysis within 8 microns of a spherule are therefore not included in table 3.

Variation ranges of the contents of Ni in metal and Fe in glass in any given impactite bomb are considerably larger than the estimated analytical error. Part of the variation in Ni content of any given spherule may be due to accidental analysis of the tiny troilite and schreibersite particles that occur in these spherules, but most observed analytical differences probably reflect real differences in the Ni content of the metal phase.

The Ni content of tektite glass was no greater than that of a glass standard in which the Ni content is a few parts per million. The Ni content of the impactite glasses was as much as three times greater than that of the standard.

The analytical results can be summarized as follows:

1. In any given tektite, the Fe content of glass is fairly uniform throughout (4-6 wt percent in the philippinites, and 3-4 wt percent in the indochinite specimen). The Fe content of impactite glass in the vicinity of spherules is considerably higher than that of tektite glass. It is fairly constant within 100 microns of any given impactite spherule but diminishes, in some specimens to the limit of detection (0.01 wt percent), at distances 500 microns or more from any spherule. Unfortunately, no continuous profile showing these gradients was obtained.

2. No relation between the size of spherules and their Ni content was found (table 4). Spherules vary widely in their Ni contents within any given impactite bomb, but the amount is fairly constant in any individual spherule.

3. The Ni content of impactite spherules (Meteor Crater, 20-65 wt percent Ni; Wabar, 8-41 wt percent Ni) is considerably higher than that of tektite spherules (philippinites, 1-3 wt percent Ni; indochinites, 4-6 wt percent Ni). The impactite spherules are depleted in Fe with respect to the parent meteorite.

4. The Fe content of Meteor Crater impactite glass in the vicinity of spherules (11-27 wt percent) is higher than that of Wabar glass (0-10 wt percent), even though the Ni contents of the parent meteorites are approximately the same. The Fe content of the glass near spherules in any given bomb is reasonably constant.

5. Neither the spherules in impactites nor tektites showed silicon contents above the silicon background measured for a pure Fe standard.

6. The Ni content of spherules in light-colored Wabar glass reported here is in agreement with the analyses by Park and Reid (1964).

Table 4.--Average Ni content of spherules in Wabar impactite glass arranged in order of increasing spherule diameter

Spherule diameter (microns)	Ni content (wt percent)
8	8.4
10	8.2
10	32.0
12	12.7
15	10.0
20	8.5
20	10.2
25	11.5
28	39.8
30	11.1
36	14.0
57	11.0
105	29.4

THE SYSTEM Fe-Ni-O

To interpret the above results it is necessary to have some understanding of the phase equilibria of the system Fe-Ni-O. Unfortunately, data on the system are insufficent to derive thermochemical conclusions for the present study; in addition, neither the time of heating nor the maximum temperature reached during the formation of impactite and tektite glass has been definitely established. The temperature was above about 1,500°C, as at that temperature Ni-Fe alloys of composition similar to those in impactites and tektites melt (Hansen and Anderko, 1958).

Much has been written on the mechanism of oxidation of Fe-Ni alloys, but Brabers and Birchenall have published (1958) the only phase diagram (1,050°C isotherm) of the Fe-rich portion of the system (fig. 2). Progressive oxidation of Fe-Ni alloys containing less than 55 at. percent Ni results in the formation of wüstite ($Fe_{1-x}O$) in which Ni is virtually absent and in the progressive enrichment of the metal phase in nickel. Continued oxidation causes the formation of a nickel-iron spinel [(Fe, Ni)O.Fe_2O_3] + metal + wüstite and, for alloys with an original Ni content greater than about 24 at. percent Ni, the equilibrium assemblage becomes Ni-rich metal plus Ni-rich spinel.

No details exist on phase equilibria at temperatures other than 1,050°C, but Fechtig and Utech (1964) have shown that molten Fe-Ni alloys become progressively enriched in nickel during oxidation.

In the present study, the metal in the Bogou iron meteorite (total Ni 7.2 wt percent, E. P. Henderson and R. S. Clarke, Jr., oral commun., 1966) within a few microns of the ablation crust caused by oxidation upon entry into the earth's atmosphere was analyzed by the methods described earlier. The Ni content of this metal is consistently high compared with that in the interior of the meteorite, and is locally as high as 65 wt percent where the metal penetrates the oxide at acute angles. The iron oxide contains less than 2 wt percent Ni. Oxidation during ablation therefore depletes Fe in the experimental observations.

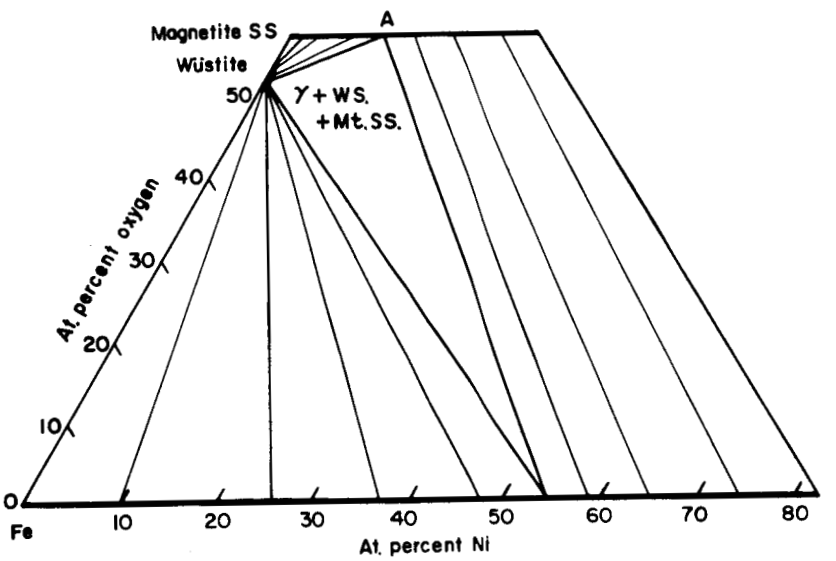

Figure 2.--Phase diagram of the Fe-rich portion of the system Fe-Ni-O at 1,050°C (after Brabers and Birchenall, 1958). Symbols: γ = γ-Fe, Ni; Mt. SS. = magnetite solid solution [$(Fe,Ni)O.Fe_2O_3$], WS. = wüstite (FeO).

EXPERIMENTAL WORK

Some simple heating experiments were made to examine possible mechanixms of Ni enrichment in metallic spherules. Metallic filings of composition approximating that of a coarse octahedrite (92.3 wt percent Fe, 7.0 wt percent Ni, 0.5 wt percent Co, and 0.2 wt percent C) were obtained from Manlabs Inc., Cambridge, Mass. A portion of these filings was partially oxidized by heating in air, another portion was left unoxidized. The two batches of filings were then placed in two silica glass tubes in the narrow space between the tube wall (1.3 mm thick), and a tight-fitting silica glass rod. The tubes were then evacuated and sealed. The part of each tube containing filings was then heated in a hydrogen-oxygen blowtorch flame for approximately 30 seconds. The maximum flame temperature attained in this way is 2,660°C (Lurie and Sherman, 1933); temperatures in the silica glass tubes probably were about 2,000° ± 300°C.

The tube containing metal plus oxide melted more readily than the one containing just metal, and it vesiculated vigorously in places, with rapid diffusion of the oxidized metal through the glass, causing it to become dark in color. There was little or no change in color or appearance of the tube containing unoxidized metal after heating, except for the formation of a few small vesicles. Both runs were cooled in air.

Polished sections were made of both runs, which were then examined microscopically. Spherules had formed by melting of the metal filings. Devitrified glass surrounded the numerous vesicles and the contact of spherules with dark glass in the specimen which had been prepared from partially oxidized filings.

A further run prepared with unoxidized filings and heated for 2 minutes gave results similar to those of the run held at temperature for only 30 seconds. The spherules and glass were then analyzed by the same methods and standards described previously. The Ni

content of the metal in the unoxidized run remained unchanged within the limits of detection, and no Fe was detectable in the silica glass. In the partially oxidized run, the remaining metal was enriched in Ni (Ni = 8-10 wt percent) and the Fe content of the glass ranged from 0 to 14 wt percent.

CONCLUSIONS

Oxidation of Ni-Fe has been shown to enrich Ni in the metal phase. The Ni enrichment in the ablation rim of the Bogou meteorite is caused by this process. Castaing and Frederiksson (1958) proposed oxidation to account for the high Ni contents of some spherles of supposed cosmic origin. It is proposed that the high Ni content of spherules in impactite glass, as compared with that of the parent meteorite, is due to loss of the iron component of the alloy by oxidation. The loss of Fe in the spherules with resultant enrichment in Ni can be accounted for by incorporation of iron in the glass. Spencer (1933) and Taylor and Kolbe (1965) showed that the chemical composition of dark glass of the Wabar and Henbury impactites, respectively, corresponds closely to that of the rock from which the glasses were formed, with the addition of Ni-Fe in meteoritic proportions.

The Ni enrichment cannot be explained by fractionation due to partial vaporization or melting of meteoritic metal, as this demands a very narrow range of impact temperatures, which is highly unlikely.

I have considered four models to explain oxidation of metallic spherules in impactites:

1. Atmospheric oxidation after the spherules were incorporated into the molten silicate bombs. Had this occurred, then oxidation would have taken place progressively from the surface of the glass inwards. The outer portion of each glass bomb would be totally depleted in spherules, and the spherules would be increasingly rich in Fe (less oxidized) toward the center of any given bomb. Observation and electron microprobe analyses in the present study

have shown that spherules are distributed uniformly throughout each bomb and that the Ni content of any spherule is not related to its distance from the surface. The heating experiments reported here have shown that 1.3 mm of silica glass prevents atmospheric oxidation of Ni-Fe for times of at least 2 minutes, even at temperatures in the vicinity of 2,000°C. This model may therefore be rejected.

2. Oxidation of the spherules by CO_2. Any carbonate present in rock from which the impactite bombs formed would decompose at the temperatures which occur during impact, according to the simplified reaction: $CaMg(CO_3)_2+SiO_2=CaMgSi_2O_6+CO$. The diopside melecule which forms would be incorporated into the glass. The Fe in the spherules would simultaneously be oxidized by the reaction: $Fe+CO_2=FeO+CO$. Dolomite (in the Kaibab Limestone) was available for such reaction at Meteor Crater at the time of impact; however, the rock at Wabar is almost pure quartz sand. Hence CO_2 may have contributed to oxidation at Meteor Crater, but not at Wabar.

3. Oxidation by H_2O in the rock from which the impactites were derived. Calculation shows that to oxidize sufficient Fe-Ni by the reation $Fe+H_2O=FeO+H_2$ to enrich the glass by 10 wt percent FeO would require several wt percent H_2O. Geological evidence indicates that at least part of the Coconino Sandstone at Meteor Crater was saturated with water at the time of impact (E. M. Shoemaker, oral commun., 1966). The impactite bombs from Meteor Crater which I examined in the present study consisted partly of fused Coconino Sandstone, so that the above mechanism may have contributed to the oxidation of spherules there. The time of the Wabar impact has not been established, but all available evidence indicates that the crater is of recent origin. The meteorite therefore fell in a desert environment, so that oxidation of the spherules by water at Wabar is dubious.

4. Atmospheric oxidation of spherules prior to their incorporation in impactite bombs. The spherules were partially oxidized in the extremely short period prior to their incorporation in the bombs. Upon incorporation into the bombs, the FeO skin surrounding each spherule diffused into the glass, enriching it in Fe, leaving a clean glass-metal interface. Alternatively, the oxidation may have occurred subsequent to incorporation in the silica melt, while the melt was undergoing turbulent flow. The spherules could have been exposed to the atmosphere during the flowage.

The Fe content in glass on two sides of a spherule from a Meteor Crater impactite may differ because the unoxidized core was not centered with respect to the spherule as a whole. Such asymmetric cores have been reported from spherules of supposed cosmic origin (see Fechtig and Utech, 1964). I consider the fourth model to be dominant in the oxidation of impactite spherules, as only it satisfactorily accounts for oxidation at Meteor Crater and Wabar.

The higher Ni content of metal and accompanying higher Fe content of the surrounding glass from the Meteor Crater impactites with respect to the Wabar impactites indicate that the Meteor Crater material is more oxidized. This suggests that the effective fugacity of oxygen at Meteor Crater was higher than that at Wabar during the meteoritic explosion, or that the molten Meteor Crater spherules were exposed to oxidation longer before they were incorporated into the glass bombs, or, more likely, that CO_2 and H_2O assisted oxidation at Meteor Crater.

An enrichment of Ni in metallic spherules from an original 10 to a final 50 wt percent requires that four-fifths of the original iron in the spherule was oxidized and dissolved in the glass.

Spherules in indochinites, unlike those in impactite glasses, have a lower Ni content than almost any iron meteorite. Spherules from philippinites have a lower Ni content than any reported iron meteorite.

The Ni-Fe ratio of metal in spherules from philippinites may be low because the ratio in the metallic portion of the meteorite which formed them was low. An alternative hypothesis compatible with the above discussion is that the tektites and spherules were formed in a reducing environment such that liquid Fe was exsolved from the silicate melt which formed the tektites, and incorporated into the spherules derived from the parent meteorite, thus diluting their Ni content. Reid, Park, and Cohen (1964) have shown that metallic Fe separates from a tektite melt at high temperatures under reducing conditions.

Unlike the impactite glasses which contain spherules, tektite glasses containing spherules are no richer in Fe than those free of spherules. The above facts suggest that metallic spherules in tektites did not oxidize. The spherules and tektite glass were formed in an environment in which the fugacity of oxygen was so low that the reaction Ni-Fe alloy + oxygen $\rightarrow$ wüstite + Ni-rich alloy was prohibited. This low oxygen fugacity during tektite formation is compatible with the results of Rost (1964), who found a total pressure corresponding to only 35 mm Hg in an undamaged moldavite bubble, and those of Thorpe, Senftle, and Cuttitta (1963), and Walter and Carron (1964), who suggested that tektites may have formed under reducing conditions on the basis of Fe^{+2}/Fe^{+3} ratios in tektite glasses. Suess (1951), O'Keefe, Dunning, and Lowman (1962), and Zähringer (1963) also found low gas pressures inside tektite bubbles. Such low fugacities perhaps occur in the center of an explosion caused by meteoritic impact with the earth (Vand, 1965), but on the basis of present evidence the tektites may equally well have been formed in an extraterrestrial environment in which oxygen fugacities were low. A less likely alternative is that the spherules may have been formed in an environment with high oxygen fugacity but were incorporated into the glass almost instantaneously so that no oxidation could occur. If oxidation of Ni-Fe spherules can be effected by CO_2, H_2O, and air as suggested earlier, then it follows that the material from which tektites were formed contained little carbonate and water.

REFERENCES CITED

Brabers, M. J., and Birchenall, L. E., 1958, High temperature oxidation of iron-nickel alloys: Corrosion, v. 14, p. 179t-182t.

Castaing, R., and Frederiksson, K., 1958, Analyses of cosmic spherules with an X-ray microanalyser: Geochim. et Cosmochim. Acta, v. 14, p. 114-117.

Chao, E. C. T., 1963, The petrographic and chemical characteristics of tektites, chap. 3 of O'Keefe, J. A., ed., Tektites: Chicago, Univ. Chicago Press, p. 51-94.

Chao, E. C. T., Adler, I., Dwornik, E. J., and Littler, J., 1962, Metallic spherules in tektites from Isabela, the Philippine Islands: Science, v. 135, p. 97-98.

Chao, E. C. T., Dwornik, E. J., and Littler, J., 1964, New data on the nickel-iron spherules from southeast Asian tektites and their implications: Geochim. et Cosmochim. Acta, v. 28, p. 971-980.

Chao, E. C. T., Shoemaker, E. M., and Madsen, B. M., 1960, First natural occurrence of coesite: Science, v. 132, p. 220-222.

El Goresey, A., 1966, Metallic spherules in Bosumtwi Crater glasses: Earth and Planetary Sci. Letters, v. 1, p. 23-24.

Fechtig, H., and Utech, K., 1964, On the presence or absence of nickel in dark magnetic cosmic spherules and their mechanics of origin: New York Acad. Sci. Annals, v. 119, p. 234-249.

Goldstein, J. I., and Ogilvie, R. E., 1965, Fe-Ni phase diagram: Am. Inst. Mining Metall. Engineers, v. 233, p. 2083-2087.

Hansen, M., and Anderko, K., 1958, Constitution of binary alloys: New York, McGraw-Hill Inc., 1305 p.

Larson, R. R., Dwornik, E. J., and Adler, I., 1964, Electron probe analysis of "cosmic" spherules: New York Acad. Sci. Annals, v. 119, p. 282-286.

Lurie, H. H., and Sherman, G. W., 1933, Flame temperatures of combustible gas-oxygen mixtures: Indus. and Eng. Chemistry, v. 25, p. 404-409.

Mead, C. A., Chao, E. C. T., and Littler, J., 1965, Metallic spheroids from Meteor Crater, Ariz: Am. Mineralogist, v. 50, p. 667-681.

Nininger, H. H., 1954, Impactite slag at Barringer Crater: Am. Jour. Sci., v. 252, p. 277-290.

_____1956, Arizona's meteorite crater: Sedona, Ariz., Am. Meteorite Mus., 232 p.

O'Keefe, J. A., Dunning, L. A., and Lowman, P. D., Jr., 1962, The composition of gases in a tektite bubble: Science, v. 137, p. 228.

Park, F. R., and Reid, A. M., 1964, A comparative study of some metallic spherules: New York Acad. Sci. Annals, v. 119, p. 250-281.

Prior, G. T., 1963, Catalogue of meteorites: 2nd ed. revised by Hey, M. H., Trustees of British Mus., London, 472 p.

Reid, A. M., Park, F. R., and Cohen, A. J., 1964, Synthetic metallic spherules in a philippine tektite: Geochim. et Cosmochim. Acta, v. 28, p. 1009-1010.

Rost, R., 1964, Surfaces and inclusions in moldavites: Geochim. et Cosmochim. Acta, v. 28, p. 931-936.

Schüller, A., and Ottemann, J., 1963, Vergleichende geochemie und petrographie meteoritische und volkanische gläser (ein beitrag zum briefproblem): Neues Jahrb. Mineralog. Abh., v. 100, 26 p.

Spencer, L. J., 1933, Meteoric iron and silica-glass from the meteorite craters of Henbury (central Australia) and Wabar (Arabia): Mineralog. Mag., v. 23, p. 387-404.

Suess, H. E., 1951, Gas content and age of tektites: Geochim. et Cosmochim. Acta, v. 2, p. 76-79.

Taylor, S. R., and Kolbe, P ., 1965, Geochemistry of Henbury impact glass: Geochim. et Cosmochim. Acta, v. 29, p. 741-745.

Thorpe, A. N., Senftle, F. E., and Cuttitta, F., 1963, Magnetic and chemical investigations of iron in tektites: Nature, v. 197, p. 836-840.

Vand, V., 1965, Astrogeology; Terrestrial meteoritic craters and the origin of tektites: Advances in Geophysics, v. 11, 114 p.

Walter, L. S., 1965, Coesite discovered in tektites: Science, v. 147, p. 1029-1032.

Walter, L. S., and Carron, M. K., 1964, Vapor pressure and vapor fractionation of silicate melts of tektite composition: Geochim. et Cosmochim. Acta, v. 28, p. 937-951.

Zähringer, J., 1963, K-ar measurements of tektites, in Radioactive Dating: Internat. Atomic Energy Agency, Vienna, p. 289-308.

MARTHA'S VINEYARD AND SELECTED GEORGIA TEKTITES: NEW CHEMICAL DATA

By F. Cuttitta,[1] R. S. Clarke Jr.,[2] M. K. Carron,[1] and C. S. Annell[1]

INTRODUCTION

Part I of the systematic investigation of tektites undertaken by the Branch of Astrogeology, U.S. Geological Survey, on behalf of the National Aeronautics and Space Administration is concerned with the 34 million-year-old Texas tektites or bediasites (Chao and others, 1961a, b; Cuttitta and others, 1961, 1962, 1963; Chao, 1963). This report presents results of a study of tektites found in Dodge County, Ga., and Martha's Vineyard, Mass. The study was undertaken in collaboration with the U.S. National Museum. The tektites studied have a potassium-argon age of 34 ± 1 million years (Zähringer, 1963). The age of the Georgia tektites and their occurrence in sand, clayey sand, and gravel of probable Pliocene or Pleistocene age, which unconformably overlie older Tertiary rocks, suggest that they were eroded and transported from older stratigraphic units (King, 1964).

The Martha's Vineyard tektite and seven Georgia tektites were selected for study, the latter to approximately represent the entire range of specific gravities exhibited by the 21 Georgia tektite specimens in the U.S. National Museum. Major element analyses of three randomly selected Georgia tektites and the Martha's Vineyard tektite have been reported by Clarke and Carron (1961) and King (1962, 1964, 1966). However, monitored analytical data for the previously analyzed Georgia tektite USNM-1396 and Martha's Vineyard tektite USNM-2082 (Clarke and Carron, 1961) are pertinent to a comparison with the bediasites and, as a consequence, their major element composition was reanalyzed using a monitored scheme of high-precision semimicro analytical techniques. New major- and

[1]U.S. Geological Survey, Washington, D.C.
[2]U.S. National Museum, Washington, D.C.

minor-element data for the seven selected Georgia and the Martha's Vineyard tektites are presented in tables 1 and 2.

MAJOR ELEMENTS

The Martha's Vineyard and the selected Georgia tektites show physical characteristics and variations in chemical composition similar to those of bediasites. These chemical variations are briefly discussed primarily on the basis of a comparison (table 1 and fig. 1) of the new compositional data with previously presented bediasite analyses (Cuttitta and others, 1962) because the new chemical data strongly suggest a single assemblage for the Texas, Georgia, and Martha's Vineyard tektites. Many investigators have demonstrated the systematic relationship of physical properties of tektites with composition. Precise determinations show that the specific gravities of the Georgia and Martha's Vineyard tektites range from 2.303 to 2.341, which reflects their relatively restricted compositional range as compared with the bediasites whose specific gravity range is 2.336 to 2.416.

Silica analyses for these newly analyzed tektites range from 79.8 to 83.6 wt percent. These values are the highest reported for tektites and are equaled at the lower end of the exhibited range only by a few high-silica bediasites and still fewer moldavites. The combined compositional data (table 1) for the North American tektites show a continuous range of variation for SiO_2 (approx. 71 to 84 wt percent), Al_2O_3 (9.5 to 17.6 wt percent), TiO_2 (0.42 to 1.05 wt percent), and FeO (1.8 to 5.3 wt percent). The continuity in compositional variation shown in table 1 and figure 1 for SiO_2, Al_2O_3, FeO, and TiO_2 coupled with their low MgO, CaO, Na_2O, and K_2O content strongly suggest a common family grouping (single assemblage) for all the North American tektites. Plotted compositional data for the North American family of tektites show that silica has a negative correlation with specific gravity, Al_2O_3, FeO (fig. 2), TiO_2, Fe_2O_3/FeO, Cu, Ga (fig. 4), Cs, Li, Cr, Co (fig. 5),

Ni, V, Sc, Zr, Cr/Ni, and Fe/Ni. A few typical plots are shown in figures 2-5. Silica shows a positive correlation with K_2O, Rb, Sr, K_2O/TiO_2 (fig. 3), and K_2O/Na_2O. A positive correlation also exists between K and Rb and Mg and Li, reflecting either the effects of genetic processes or their chemical coherence.

The significance and quantitative aspects of these correlations reflecting the effects of a closed system are still being studied and evaluated statistically (Miesch and others, 1965). Therefore, any detailed discussion of their implications would be premature and will be held in abeyance until the statistical evaluation has been completed. However, preliminary results of this statistical analysis strongly support differential fractionation as one of the major geologic factors affecting chemical variations in tektites. The characteristics and compositional variations of North American tektites suggest a selective loss of alkalies due to differential volatilization under reducing or nonoxidizing conditions. These conditions are reflected in the low ferric-ferrous ratios characterizing the North American tektites (Cuttitta and others, 1962; Thorpe and others, 1963). In summation, the North American tektites could have been derived from felsic igneous rocks as a result of fusion and loss of alkalies by differential volatilization.

MINOR ELEMENTS

Reliable data on the trace elements in the Georgia and Martha's Vineyard tektites were virtually nonexistant. Twenty-one trace elements (Ag, B, Ba, Be, Co, Cr, Cs, Cu, Ga, La, Li, Mn, Nb, Ni, Pb, Rb, Sc, Sr, V, Y, and Zr) were determined by monitored quantitative spectrographic methods. Au, Bi, Cd, Ge, In, Ir, Mo, Pt, Sb, Sn, Ti, U, W, and Zn were looked for but not found. If present, they were in amounts below the sensitivity limits of the methods used. These new minor-element data combined with previously reported bediasite data (Cuttitta and others, 1962) are presented in table 2. The minor element data of Georgia tektites closely resemble

those of the bediasites: ranges in abundance either overlap and lack discernable trend or show distinct trends in their variation (Cu, Ga, Cs, Rb, Li, Cr, Co, Ni, V, Sc, Cr/Ni, and Fe/Ni).

SIGNIFICANCE

The major and minor element composition of the newly analyzed Georgia and Martha's Vineyard tektites is almost identical with that of silica-rich bediasites. Continuity of the compositional data for the combined North American tektites (table 1, fig. 1), identical potassium-argon ages of 34 ± 1 million years, and their general geographic association strongly suggest (1) that the Georgia and Martha's Vineyard tektites represent the high-silica end-members of the range of compositional variations exhibited by the North American tektite family, and (2), a common origin both by event and parent body for the Texas, Georgia, and Martha's Vineyard tektites. These natural glasses could have resulted from fusion of an unknown target area by meteoritic impact; the glasses may represent crater ejecta distributed in a strewnfield. The grouping of the Texas and Georgia tektites into a single assemblage has also been suggested by King (1966).

The chemical characteristics of the North American family of tektites are:

1. They have a continuous range of variation (in wt percent) for SiO_2 (71.9-83.6), Al_2O_3 (9.5-17.6), FeO (1.8-5.3), and TiO_2 (0.42-1.05); are low in MgO, CaO, and alkalies with K_2O greater than Na_2O and an MgO/CaO ratio approaching unity; and have a very low water content (<0.02 percent).

2. Their compositional data show a positive correlation of K_2O/Na_2O and K_2O/TiO_2 ratios to silica, reflecting the effects of differential volatilization.

3. Virtually all their iron content is in the ferrous state with a characteristic low ferric-ferrous iron ratio ranging from <0.001 to 0.101 and averaging 0.040. These low iron-ratio data suggest that these tektites have been heated to a very high temperature under reducing or nonoxidizing conditions.

4. North American tektites exhibit generally comparable minor element abundances (table 2) which show either restricted unconforming ranges or ranges exhibiting negative correlations to silica (Cu, Ga, Rb, Cs, Li, Cr, Co, Ni, V, Sc, Zr, Cr/Ni, and Fe/Ni) which reflect the effects of formative processes.

5. These new chemical data for the North American tektites are consistent with the previously reported interpretation (Cuttitta and others, 1962; Chao, 1963) that they have been derived from siliceous igneous rocks as a result of fusion and differential volatilization.

REFERENCES CITED

Chao, E. C. T., 1963, The petrographic and chemical characteristics of tektites, in O'Keefe, J. A., ed., Tektites: Chicago, Univ. Chicago Press, p. 51-94.

Chao, E. C. T., Littler, J., and Smysor, B., 1961a, Physical characteristics of bediasites from Lee County, Texas: U.S. Geol. Survey, Astrogeol. Studies Semiann. Prog. Rept., Aug. 25, 1960-Feb. 25, 1961, p. 146-165.

Chao, E. C. T., Smysor, B., and Littler, J., 1961b, Geological occurrences of bediasites: U.S. Geol. Survey, Astrogeol. Studies Semiann. Prog. Rept., Aug. 25, 1960-Feb. 25, 1961, p. 126-245.

Clarke, R. S., Jr., and Carron, M. K., 1961, Comparison of tektite specimens from Empire, Georgia and Martha's Vineyard, Massachusetts: Smithsonian Misc. Colln., v. 143, no. 4, Pub. 4465.

Cuttitta, Frank, Carron, M., and Fletcher, J. D., 1961, Chemical composition of bediasites from Lee County, Texas: U.S. Geol. Survey, Astrogeol. Studies Semiann. Prog. Rept., Aug. 25, 1960-Feb. 25, 1961, p. 166-184.

Cuttitta, Frank, Carron, M. K., Fletcher, J. D., Annell, C. S., and Chao, E. C. T., 1963, The chemical composition of bediasites: U.S. Geol. Survey, Astrogeol. Studies Ann. Prog. Rept., Aug. 25, 1961-Aug. 24, 1962, pt. C, p. 115-148.

Cuttitta, Frank, Carron, M. K., Fletcher, J. D., and Chao, E. C. T., 1962, Chemical composition of bediasites and philippinites: U.S. Geol. Survey, Astrogeol. Studies Semiann. Prog. Rept., Aug. 26, 1961-Feb. 24, 1962, p. 15-47.

King, E. A., Jr., 1962, Field investigation of Georgia tektites and description of new specimen: Georgia Min. Newsletter, v. XV, p. 84-89.

_____ 1964, New data on Georgia tektites: Geochim. et Cosmochim. Acta, v. 28, p. 915-919.

_____ 1966, Major element composition of Georgia tektites: Nature, v. 210, no. 5038, p. 828-829.

Miesch, A. T., Chao, E. C. T., and Cuttitta, F., 1965, Multivariate analysis of geochemical data on Texas tektites (bediasites): U.S. Geol. Survey, Astrogeologic Studies Ann. Prog. Rept., July 1, 1964-July 1, 1965, pt. C, p. 7-45.

Thorpe, A. N., Senftle, F. E., and Cuttitta, Frank, 1963, Magnetic and chemical studies of iron in tektites: Nature, v. 197, p. 836-840.

Zähringer, J., 1963, K-Ar measurements of tektites: unpub. rept. presented at 2d Internat. Symposium on Tektites, Pittsburgh 1963.

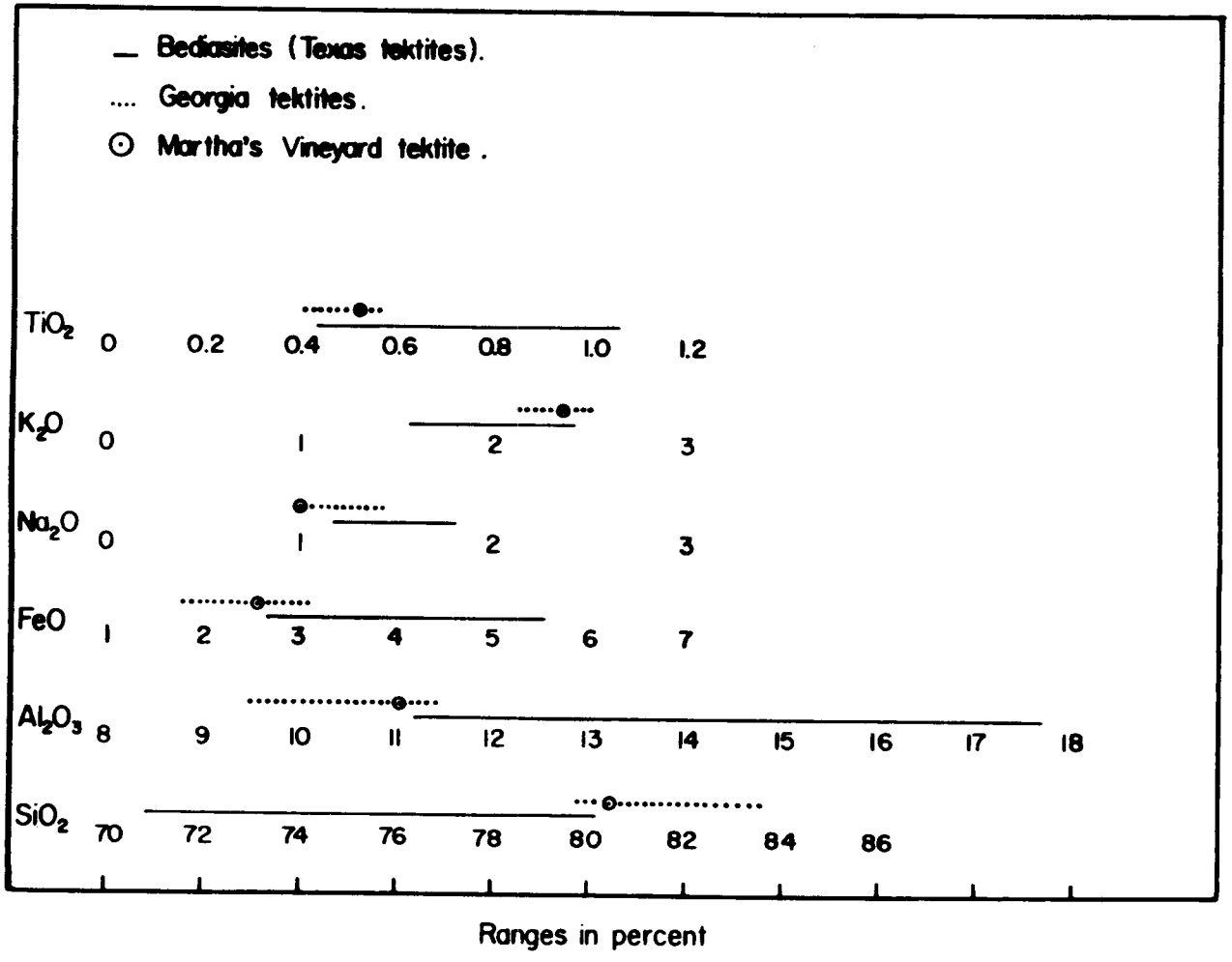

Figure 1.--Comparison of the ranges of SiO_2, Al_2O_3, FeO, Na_2O, K_2O, and TiO_2 in North American tektites.

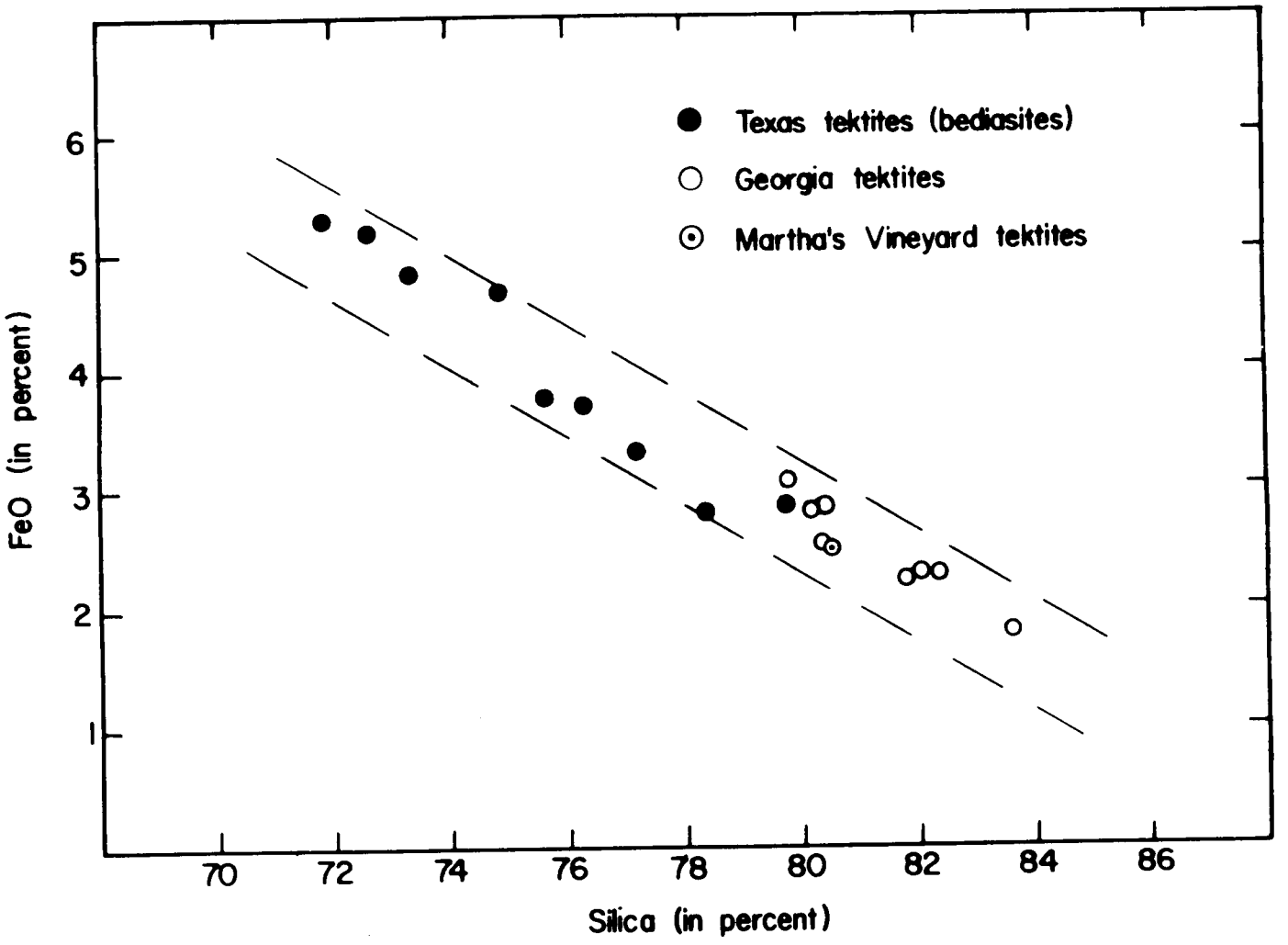

Figure 2.--Variation of FeO as a function of silica in selected North American tektites.

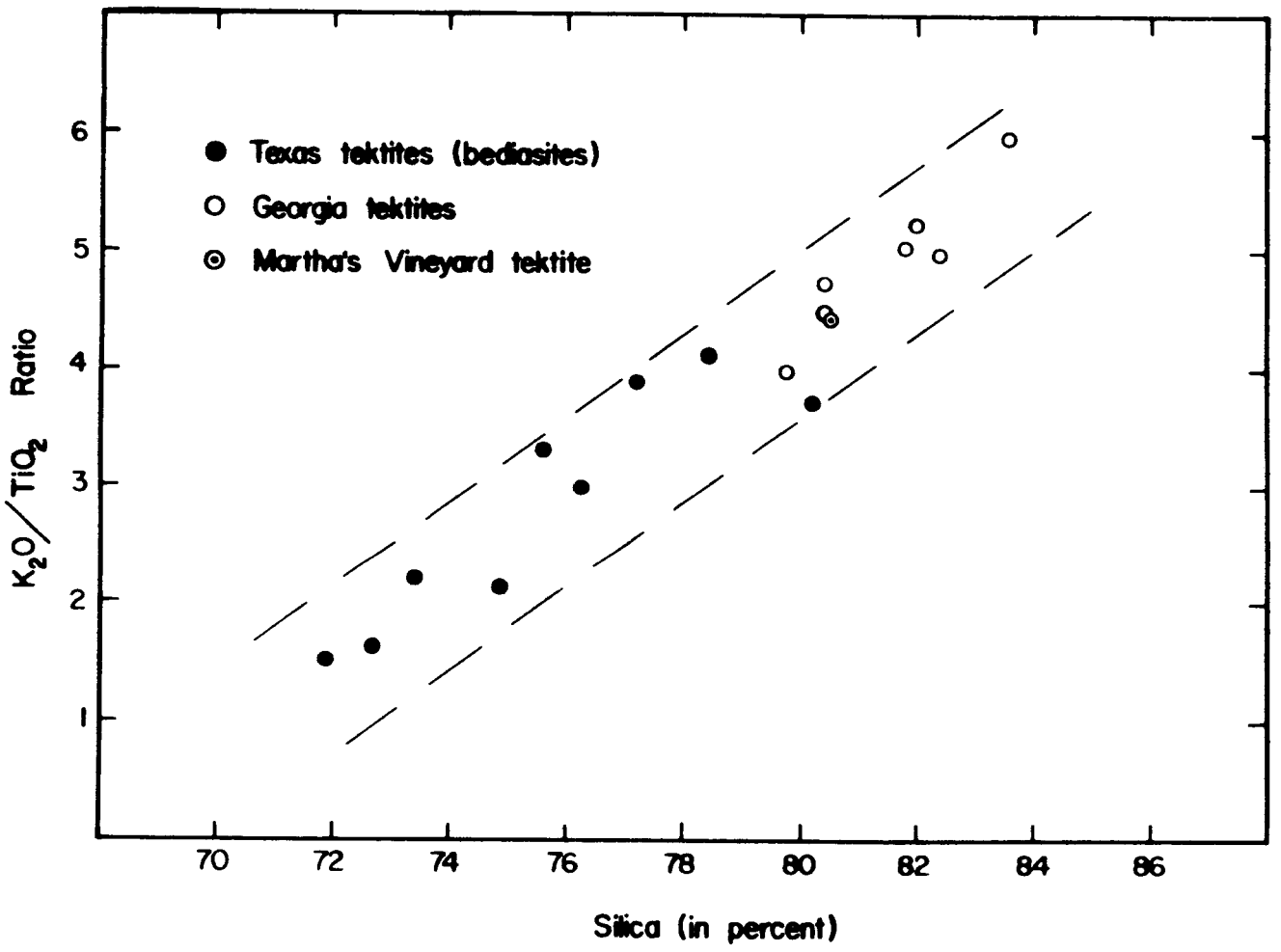

Figure 3.--Variation of K_2O/TiO_2 ratio as a function of silica in selected North American tektites.

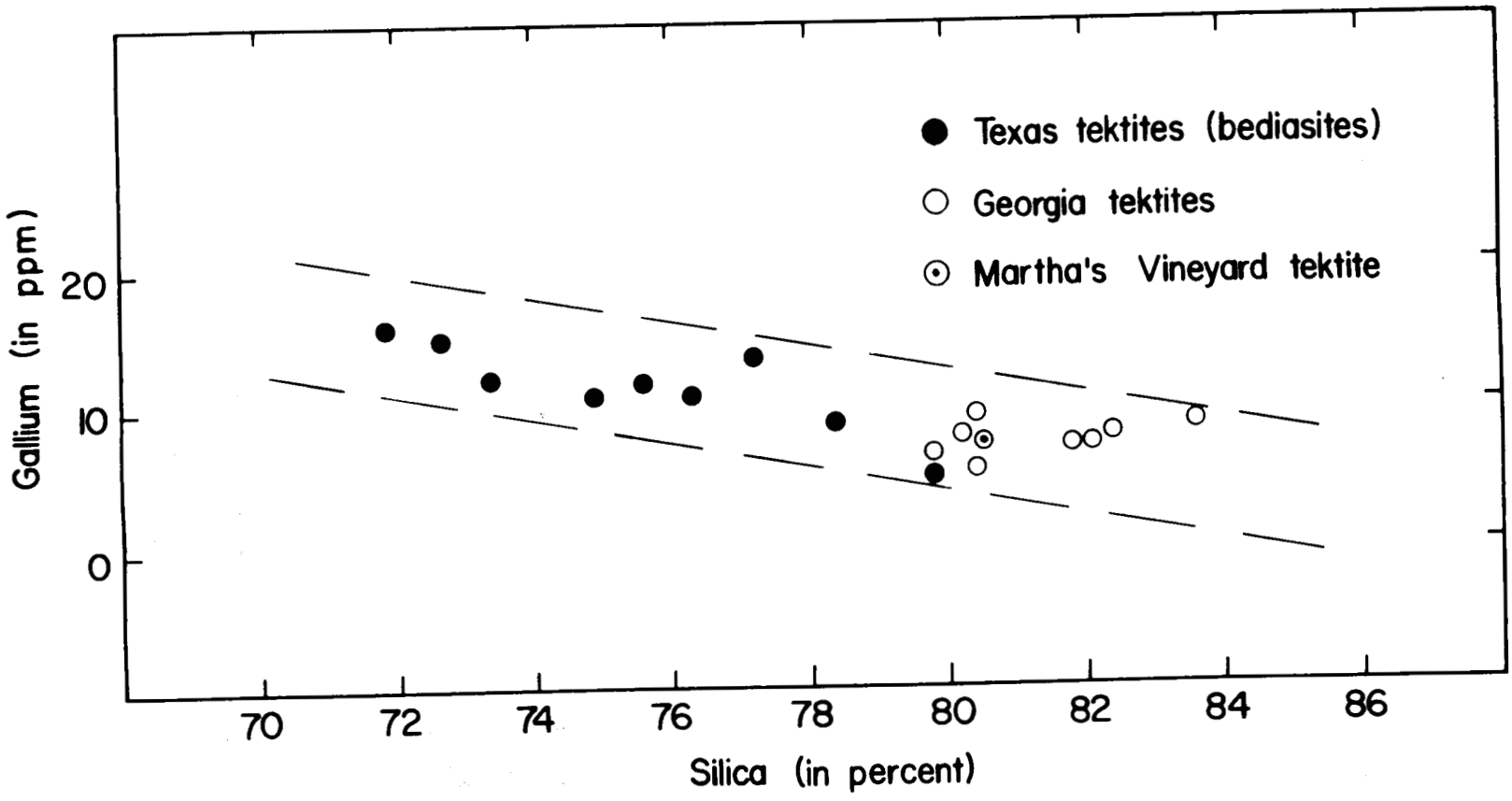

Figure 4.--Variation of Gallium as a function of silica in selected North American tektites.

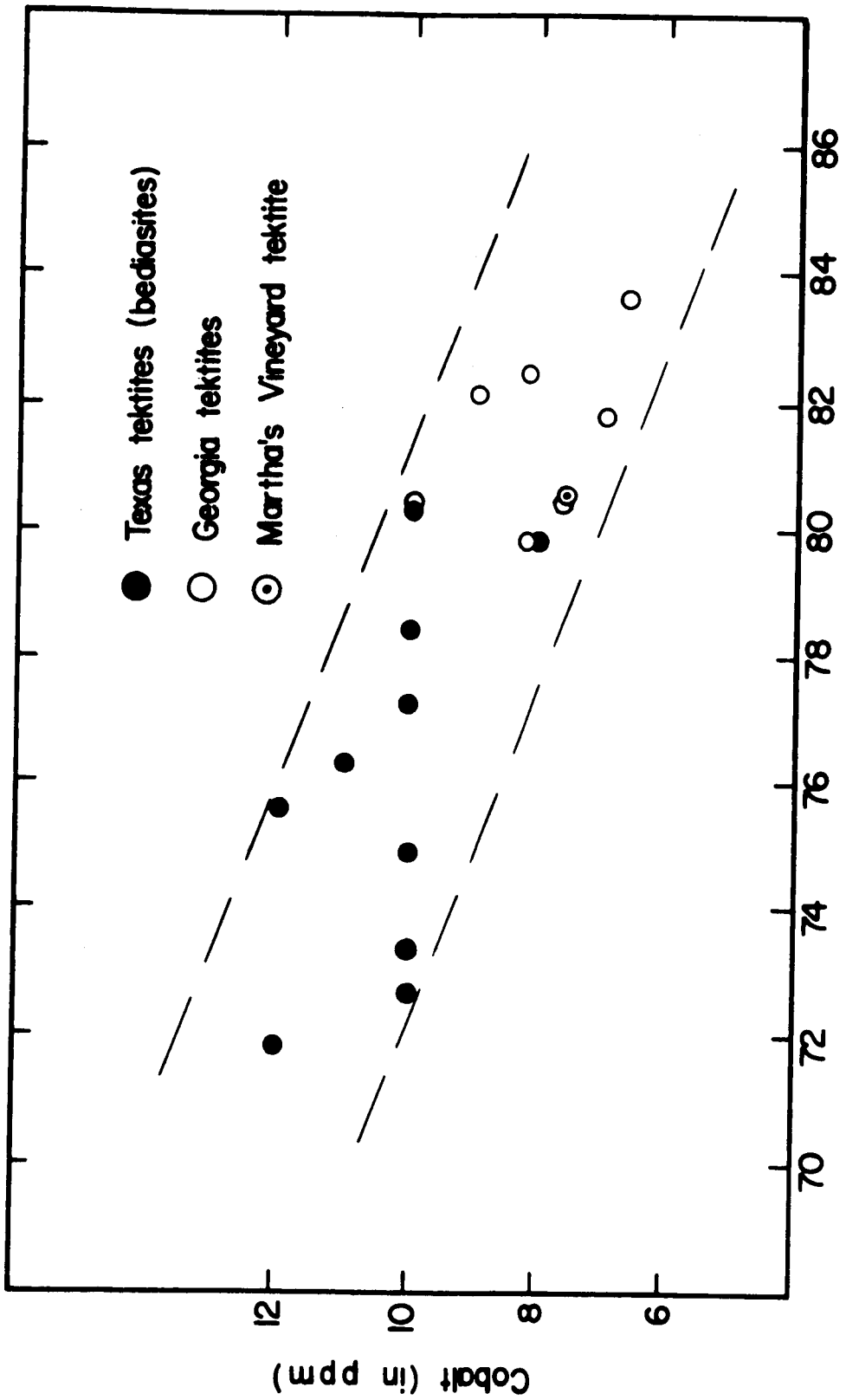

Figure 5.--Variation of cobalt as a function of silica in selected North American tektites.

Table 1.--New major-element analyses of selected Georgia and Martha's Vineyard tektites and analyses of bediasites

[Data are in percent. Samples are arranged in order of increasing silica content. B.D., being determined]

	B-90[1]	30763-10[1]	B-105[1]	B-76[1]	B-84[1]	B-6[1]	B-17[1]	B-20[1]	BM-1[1]	Ga-2339[2]	30775-77[1]	Ga-1396[3]	Ga-2343[4]	MV-2082[5]	Ga-2136[6]	Ga-2345[4]	Ga-2341[2]	Ga-2355[6]
SiO_2	71.89	72.70	73.36	74.94	75.59	76.25	77.21	78.37	79.83	79.80	80.17	80.35	80.35	80.50	81.80	82.03	82.40	83.6
Al_2O_3	17.56	16.53	16.04	14.81	13.54	13.49	12.75	12.21	12.16	11.72	11.19	11.35	11.32	11.20	10.50	10.56	10.03	9.50
Fe_2O_3	.27	.32	.31	.13	.20	.27	.06	.05	.03	.04	.18	.31	.00	.14	.04	.04	.00	.01
FeO	5.26	5.16	4.81	4.68	3.78	3.74	3.31	2.81	2.87	3.09	2.82	2.53	2.88	2.52	2.24	2.30	2.26	1.82
MgO	.78	.70	.75	.43	.66	.74	.50	.70	.46	.68	.37	.61	.62	.69	.54	.57	.44	.42
CaO	.45	.41	.61	.66	.79	.74	.96	.78	.52	.50	.56	.63	.51	.69	.56	.51	.41	.40
Na_2O	1.28	1.43	1.44	1.50	1.72	1.63	1.80	1.84	1.20	1.07	1.53	1.21	1.17	1.00	1.40	1.12	1.19	1.19
K_2O	1.60	1.63	1.93	1.84	2.42	2.22	2.42	2.43	1.86	2.22	2.24	2.34	2.36	2.37	2.41	2.51	2.36	2.51
TiO_2	1.05	.99	.87	.86	.73	.74	.62	.59	.65	.56	.60	.52	.50	.53	.48	.48	.48	.42
P_2O_5	.04	.07	.03	.04	.05	.05	.06	.02	.00	.02	.03	.03	.05	.04	.04	.02	.03	.03
MnO	.02	.04	.03	.02	.05	.05	.05	.05	.02	.07	.04	.05	.04	.05	.03	.04	.03	.03
Total	100.20	99.98	100.18	99.91	99.51	99.94	99.74	99.85	99.60	99.77	99.73	99.94	99.80	99.73	100.04	100.18	99.60	99.93
Total Fe as Fe_2O_3	6.11	6.05	5.65	5.33	4.40	4.42	3.73	3.17	3.22	3.48	3.31	3.11	3.16	2.93	2.53	2.60	2.50	2.03
Nd	1.5076	1.5068	1.5038	1.5000	1.4968	1.4962	1.4914	1.4892	1.4828	B.D.	1.4874	1.485	B.D.	1.485	1.480	B.D.	B.D.	B.D.
Sp gr	2.416	2.411	2.406	2.397	2.387	2.384	2.389	2.368	2.336	2.341	B.D.	2.330	2.332	2.332	B.D.	2.315	2.315	2.303
Fe_2O_3/FeO	.0513	.0620	.0644	.0277	.0529	.0721	.0181	.0177	.0104	.0130	.0638	.1223	<.001	.0555	.0178	<.001	<.001	.0054
K_2O/Na_2O	1.25	1.13	1.34	1.22	1.40	1.36	1.34	1.33	1.55	2.07	1.44	1.93	2.01	2.37	1.72	1.98	1.98	2.10
K_2O/TiO_2	1.52	1.64	2.24	2.13	3.31	3.00	3.90	4.11	2.86	3.96	3.73	4.50	4.72	4.47	5.02	4.92	4.92	5.97

[1] Bediasites from Fayette, Grimes, and Lee Counties, Tex.
[2] Rock Branch Church, Dodge County, Ga. (USNM-2339 and 2341).
[3] Empire, Dodge County, Ga. (USNM-1396).
[4] Jay Bird Springs, Dodge County, Ga. (USNM-2343 and 2345).
[5] Martha's Vineyard, Mass. (USNM-2082).
[6] L. J. Allen Farm, Plainfield, Ga. (USNM-2136 and 2355).

Table 2.--New minor-element analyses of selected Georgia and the Martha's Vineyard tektites and analyses of bediasites

[Data are in parts per million. Samples are arranged in order of increasing silica content. Constituents are arranged in order of decreasing volatility of the oxides in the dc arc. B.D., being determined]

	B-90[1]	30763-10[1]	B-105[1]	B-76[1]	B-84[1]	B-6[1]	B-17[1]	B-20[1]	BM-1[1]	Ga-2339[2]	30775-77[1]	Ga-1396[3]	Ga-2343[4]	MV-2082[5]	Ga-2136[6]	Ga-2345[4]	Ga-2341[2]	Ga-2355[6]
Pb	<10	10	<10	<10	<10	<10	<10	<10	<10	<10	<10	15	<10	18	12	<10	<10	<10
Ag	2	<1	1	<1	<1	<1	<1	<1	<1	<1	<1	<1	<1	<1	<1	<1	<1	<1
Cu	14	18	21	11	12	10	12	10	8	4.7	9	3.3	8.7	3.0	2.2	3.3	4.2	3.2
Ga	15	15	12	11	12	11	14	9	<5	6.7	8	5.7	10	7.2	7.2	7.5	8.3	9.0
Cs	2.3	2.2	2.0	2.2	2.1	1.7	2.0	1.6	1.5	1.9	1.8	2.1	2.0	1.7	1.7	1.4	1.6	1.4
Rb	54	75	67	46	55	72	62	62	54	79	58	70	82	72	74	73	85	80
Li	24	29	27	18	17	22	15	13	9	18	13	B.D.	17	15	15	15	16	14
Mn	170	160	220	210	450	200	360	380	190	559	270	420	271	397	230	328	252	218
Cr	62	61	49	28	28	46	33	29	26	33	28	B.D.	32	B.D.	B.D.	29	31	18
B	30	30	20	10	20	<10	<10	<10	<10	<10	<10	<10	<10	<10	<10	<10	<10	<10
Co	12	10	10	10	12	11	10	10	8	8.2	10	7.6	10	7.6	7.0	9.0	8.2	6.7
Ni	14	18	12	10	14	16	16	13	6	8.4	13	B.D.	13	B.D.	B.D.	13	14	9.5
Ba	420	380	540	800	1100	440	370	650	600	705	500	340	580	390	370	600	650	715
Sr	60	70	80	72	100	85	70	130	70	186	110	140	150	180	140	116	164	153
V	100	150	89	92	74	120	83	60	95	45	68	44	41	52	42	52	39	37
Be	5	2	2	4	3	2	2	2	2	1.7	<2	1.0	2.0	1.0	1.2	1.6	1.9	1.9
Nb	22	19	16	13	13	18	14	15	22	<10	14	18	<10	20	22	<10	<10	<10
Sc	16	12	13	25	25	10	10	10	9	13	9	10	11	10	10	7.5	9.3	7.8
La	40	70	40	40	40	50	30	30	30	<50	<30	<50	<50	<50	<50	<50	<50	<50
Y	30	20	20	20	20	20	20	20	20	26	20	17	26	20	17	20	22	20
Zr	260	250	200	200	180	220	160	180	220	211	220	170	218	190	180	177	195	180
Cr/Ni	4.42	3.38	4.08	2.8	2.00	2.87	2.06	2.23	4.33	3.92	2.15	--	2.46	--	--	2.23	2.21	1.89
Fe/Ni	3055	2353	3296	3731	2200	1934	1631	1707	3757	2900	1782	--	1702	--	--	1400	1250	1496

[1] Bediasites from Fayette, Grimes, and Lee Counties, Tex.
[2] Rock Branch Church, Dodge County, Ga. (USNM-2339 and 2341).
[3] Empire, Dodge County, Ga. (USNM-1396).
[4] Jay Bird Springs, Dodge County, Ga. (USNM-2343 and 2345).
[5] Martha's Vineyard, Mass. (USNM-2082).
[6] L. J. Allen Farm, Plainfield, Ga. (USNM-2136 and 2355).

THE OCCURRENCE AND ORIGIN OF LAMELLAR TROILITE IN IRON METEORITES

By Robin Brett[1] and E. P. Henderson[2]

INTRODUCTION

Oriented lamellae of troilite (FeS) in iron meteorites were first described by von Reichenback (1861a, b) and were named after him by Brezina (1882). Since their discovery, lamellae described as Reichenback lamellae have been noted in at least 33 meteorites.

Reichenback lamellae were defined by Brezina as troilite plates oriented parallel to the cube planes of iron. With time, the usage has broadened to the extent that some authors have termed all elongated troilite bodies in iron meteorites Reichenbach lamellae, while others have used the term to describe oriented bodies other than troilite.

The purpose of the present study is to examine the occurrence of troilite lamellae and to speculate on their origin.

PREVIOUS WORK

Although there have been many descriptions of Reichenbach lamellae in the literature, identification has been visual without supporting chemical or X-ray diffraction methods. The definition of Reichenbach lamellae has broadened over the years, so that it has become virtually meaningless. For example, in describing schreibersite [$(Fe, Ni)_3P$] lamellae in the Gibeon meteorite, Cohen (1900) incorrectly stated, "This is perhaps one of the so-called Reichenback lamellae; that is to say, it lies possibly parallel to a cube face."

[1]U.S. Geological Survey.

[2]U.S. National Museum.

According to most descriptions, Reichenbach lamellae are longer than they are wide (2 cm χ 0.1 mm are typical dimensions). Recently, however, some authors (e.g., Spencer, 1951) have reported Reichenbach lamellae up to several millimeters wide and about a centimeter long.

Many accounts state that the lamellae are crystallographically oriented on planes comprising either the {010} or {011} forms with respect to the orientation of taenite (γ-Fe, Ni) in the Widmanstätten texture. Spencer (1951) pointed out that troilite lamellae in meteorites are oriented on {011} and possibly {010} and {211}. It is noteworthy that schreibersite lamellae occur on all the above planes, and more (Spencer, 1951).

In view of the confusion in the literature over the definition of Reichenbach lamellae, and the lack of rigor in the identification, we regarded previous identifications with suspicion.

METHODS

Specimens of most iron meteorites in the U.S. National Museum collection were examined for troilite lamellae. Particular attention was paid to those meteorites in which previous workers reported these lamellae. Polished faces of meteorites were first examined under a binocular microscope, then lamellar structures resembling troilite were examined by reflected-light microscopy, by treating the powdered material with a magnet, and by determining if the powder effervesced in 1:1 HCl. Troilite, unlike cohenite [$(Fe, Ni)_3C$] and schreibersite, with which it may possibly be confused, is nonmagnetic and is readily attacked by HCl. The above methods were sufficient to identify the lamellar material in most of the meteorites examined. If any doubt remained after such examination, the material was examined by X-ray powder diffraction using Fe Kα radiation.

The iron meteorites listed in table 1 have previously been reported to contain Reichenbach lamellae. Of the meteorites listed in table 1, only Ilimaes, Moorumbunna, and Juncal were unavailable for study. Of the meteorites studied, those in table 2 were found to contain lamellar troilite bodies that resemble Reichenbach lamellae photographed and described by previous workers. It must not be assumed that the meteorites listed in table 1 in which we failed to find this habit of troilite necessarily contain no lamellae.

Table 1.--Meteorites previously reported to contain "Reichenbach" lamellae

Bartlett	Duel Hill (1854)	Moorumbunna[1]
Bear Creek[2]	Gibeon	Prambana
Breece[2]	Henbury	Ruff's Mt.
Bristol[3]	Ilimaes[1]	Staunton
Cabin Creek[3]	Joe Wright	Thule
Cape York	Juncal[1]	Thunda
Carlton[3]	Kyancutta	Tocopilla
Charlotte[3]	La Caille[3]	Trenton[2]
Cleveland	Lenarto	Victoria West[3]
Coahuila	Maria Elena	Walker Co.
Drum Mts.	Merceditas[3]	Yanhuitlan

[1]Not available for study.

[2]No troilite seen in present study; narrow schreibersite lamellae present.

[3]No troilite seen in present study.

Table 2.--Meteorites found to contain lamellar troilite inclusions

[Data on average Ni content of the class were obtained from Short and Anderson (1965). Bulk Ni content and type were obtained from Prior (1953), with the exception of the data for Bartlett and Wiley, which were determined in the present study]

Meteorite	Inclusions: Type 1 (narrow)	Inclusions: Type 2 (wide)	Oriented	Swathing kamacite	Type	Bulk Ni (wt percent)	Avg Ni content of class
Bartlett	X			X			8.9
Bacubirito	X			X	Off	13.0	9.4
Cape York	X			X	Om	8.3	8.0
Cleveland	X			X	Om	8.3	8.1
Coahuila		X			H	5.6	5.6
Drum Mts.	X				Om	8.3	8.6
Duel Hill (1854)	X		X	X	Of	9.1	9.8
Gibeon		X			Of	9.1	8.0
Henbury		X			Om	8.3	7.3
Joe Wright	X				Om	8.3	7.5
Kyancutta	X			X	Om	8.3	7.3
Lenarto	X			X	Om	8.3	8.6
Maria Elena		X			Of	9.1	7.7
Monohans	X			X	Atax		10.9
Nordheim	X			X	Atax		11.7
Staunton	X		X	X	Om	8.3	8.0
Thule	X				Og	6.8	8.1
Thunda	X				Om	8.3	8.5
Tlacotepec		X			Atax		16.2
Tocopilla		X	X		H	5.6	5.4
Walker Co.	X			X	H	5.3	5.6
Wiley	X			X	Atax	11.7	
Yanhuitlan		X		X	Of	7.4	9.1

Off = very fine octahedrite. Og = coarse octahedrite.
Of = fine octahedrite. H = hexahedrite.
Om = medium octahedrite. Atax = ataxite.

RESULTS

Two main types of troilite bodies which may be called lamellae[1] were seen in an examination of the specimens.

Type 1 Lamellae

The first group consists of hairline cracks in the metal, filled with troilite, as much as 6 cm long and 0.1 to 0.2 mm wide (figs. 1, 2). Most of the lamellae are about 2 cm long. Few of the lamellae are straight, even to the naked eye; some curve and branch (e.g., Drum Mts., Cleveland). Table 2 lists the meteorites which contain narrow lamellae of this type. These bodies were found in Bacubirito, Monahans, Nordheim, and Wiley, although they were not reported by previous investigators.

The boundaries of the lamellae are commonly irregular, and in some instances opposite sides match one another. In Drum Mts. and Staunton some fractures filled with troilite connect a series of nearly spherical troilite bodies, with a diameter up to 4 mm in such a way that the structure resembles a string of beads. Some of the filled fractures terminate in similar troilite blebs (fig. 1). In Thule the lamellae are frequently discontinuous and pinch and swell and occur en echelon.

In Staunton the lamellae are strongly oriented in two directions, probably on {011}. Lamellae in Duel Hill also show pronounced orientation. In Drum Mts. and in some other meteorites containing such bodies, little orientation was evident (fig. 1), and commonly too few troilite bodies were present to determine orientation. Spencer (1951) listed some examples of oriented troilite bodies in iron meteorites but stated that they are very uncommon.

Most meteorites containing such narrow troilite bodies have narrow kamacite (α-Fe, Ni) rims (swathing kamacite) surrounding the

[1] In this work, "lamella" refers to any body shaped like a thin plate; the definition contains no connotations of orientation, or regularity of the walls.

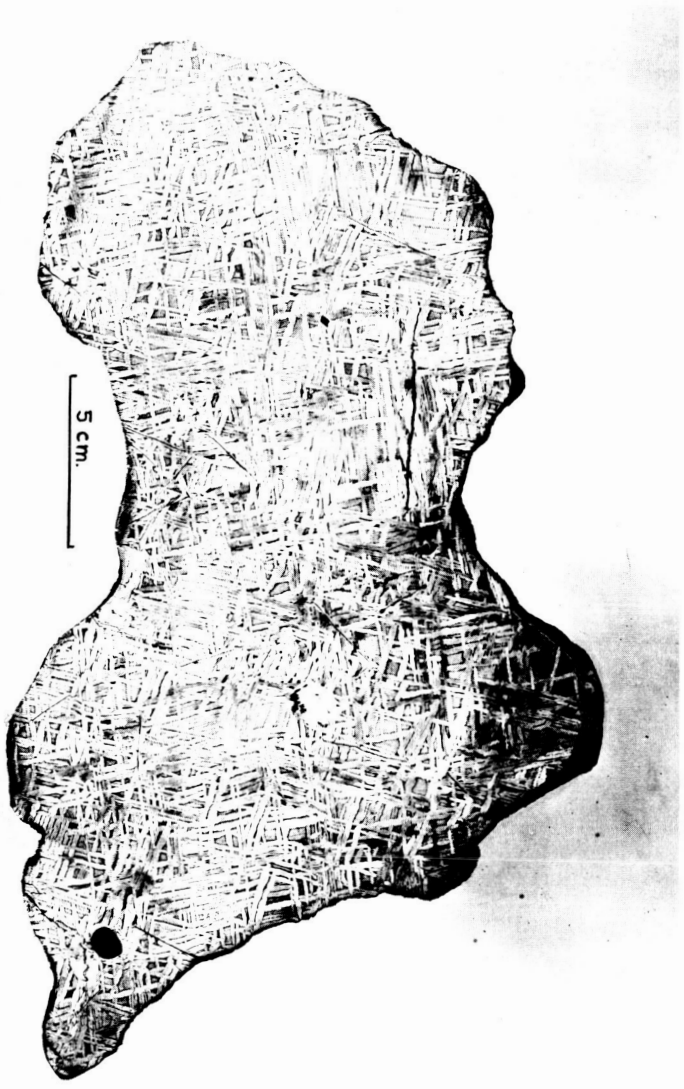

Figure 1.--Section of Drum Mts., showing narrow, irregular type 1 troilite lamellae (dark hairlike lines), largely oxidized to magnetite. Note that some lamellae terminate in troilite blebs. The dark inclusions are troilite nodules. The wide irregular black veins may have been troilite that was oxidized to magnetite and hydrous iron oxides, or may be oxidation fractures formed by ablation (Henderson and Perry, 1948).

Figure 2.--Type 1 troilite lamella in Wiley. Note swathing kamacite. Nital etch. Photograph by John Tennant, U.S. National Museum.

troilite. The Widmanstätten texture commonly is not continuous across the troilite; thus, growth of kamacite took place independently on both sides of the fractures. In many examples, the orientation of the Widmanstätten lamellae is locally displaced a few degrees across the lamellae (fig. 1).

The lamellae are dominantly troilite with uniform crystallographic orientation, as shown by the uniform orientation of twin lamellae within the troilite. Daubreelite ($FeCr_2S_4$), both in oriented lamellae and as rare irregular masses, commonly occurs within the troilite. The textures are highly suggestive of exsolution of daubreelite from troilite. The identification of daubreelite from the Cape York specimen was checked both by electron microprobe analysis (K. Fredriksson, oral commun.) and by X-ray diffraction methods.

In the Cape York iron, many troilite bodies terminate so that the daubreelite lamellae project into the kamacite, as shown by El Goresy (1965, fig. 25). El Goresy suggested that the daubreelite projections are due to selective replacement of troilite by kamacite; nowever they may equally well represent nucleation of daubreelite in irregularities within a fracture. One apparent exsolution lamella of troilite was seen in daubreelite.

Schreibersite commonly occurs as noncontinuous bodies along the contact between kamacite and troilite. These bodies occur both parallel to the fracture walls and as irregular masses within kamacite, abutting on the troilite. Fractures containing troilite commonly terminate in irregular schreibersite bodies up to several millimeters in diameter.

Type 1 troilite lamellae oxidize very readily to magnetite and limonite. Unoxidized lamellae are hard to find. Schreibersite in the lamellae appears to be most resistant to oxidation, followed by daubreelite, then troilite. The troilite in the lamellae oxidizes much faster than troilite in the more common sulfide nodules found in iron meteorites. We suspected that this rapid

oxidation could be caused by lawrencite ($FeCl_2$) along the lamellae, but semiquantitative electron microprobe analysis failed to disclose significant chlorine (K. Fredriksson, oral commun.). Another possibility is that the large surface area between troilite and metal in the type 1 lamellae greatly aids oxidation.

Type 2 Lamellae

Members of the second group of elongated troilite bodies (type 2, table 2) are wider than those described above. They occur in elongated masses ranging from 2 cm long and 3 mm wide to 5 mm long and 2 mm wide. These lamellae were found in Tlacotepec in addition to those meteorites in which they have been described. In several of the meteorites which contain them there is a gradation in shape from round blebs to ellipsoids to the platelike masses described above. Boundaries of these bodies are commonly ragged and irregular on a microscale, and no preferred orientation is evident. The Widmanstätten texture is continous across the lamellae.

The mineralogy of type 2 lamellae is similar to that of type 1, namely troilite with oriented lamellae of daubreelite (see Heide and others, 1932, fig. 2). Additional minerals are graphite and rare silicate grains, with chromite in Tocopilla. Schreibersite masses at troilite borders are commonly absent, as is swathing kamacite. Small kamacite grains intermixed with the troilite are common around the borders, expecially in Tocopilla, Maria Elena, Henbury, and Gibeon. Heide and others (1932) described an extremely fine grained eutecticlike texture between kamacite and troilite at the boundaries of the troilite inclusions in Tocopilla. Type 2 lamellae are much more resistant to oxidation than type 1.

Table 2 indicates that type 1 and type 2 lamellae are mutually exclusive. This may be a sampling difficulty rather than representing a real relationship.

ORIGIN OF TROILITE LAMELLAE IN METEORITES

Previous Work

Several origins have been proposed for Reichenbach lamellae. Rinne (1910) stated that the elongated inclusions in Gibeon are melt formed. Perry (1944) suggested that Reichenbach lamellae crystallized from a melt along crystallographic planes in δ-Fe. The δ phase does not occur in Fe-Ni alloys containing more than 5.2 at. percent Ni (Hellawell and Hume-Rothery, 1957), and small amounts of P, S, or C do not significantly stabilize the phase (Hansen and Anderko, 1958). Therefore, the δ phase could only have existed in a very few meteorites with extremely low Ni contents.

Edwards (1946) proposed that the troilite of Reichenbach lamellae separated from the nickel-iron in the solid state. Vogel (1945) was unable to exsolve troilite from iron and stated, accordingly, that all troilite in iron meteorites formed by crystallization from the melt. He explained the formation of Reichenbach lamellae by crystallization of the residual eutectic liquid in oriented interstices in the nickel iron. Goldstein and Ogilvie (1963) stated that Reichenbach lamellae and other troilite inclusions "of the same general sizes as the phosphides" form in the solid state owing to decrease of troilite solubility in the metal during cooling.

Solubility of FeS in Fe, Ni

Isothermal sections (fig. 3) have been drawn, using the existing data on the systems Fe-Ni (Goldstein and Ogilvie, 1965a), Fe-S (Hansen and Anderko, 1958; Ainslie and Seybolt, 1960), Ni-S (Elliott, 1965), and Fe-Ni-S (Kullerud, 1963). Phase boundaries are assumed to be linear, following the thermodynamic reasoning of Meijering (1959) for ferrite-austenite-type equilibria.

The solubility of S in Fe-Ni alloys of composition resembling those of most iron meteorites (5-20 wt percent Ni) in equilibrium

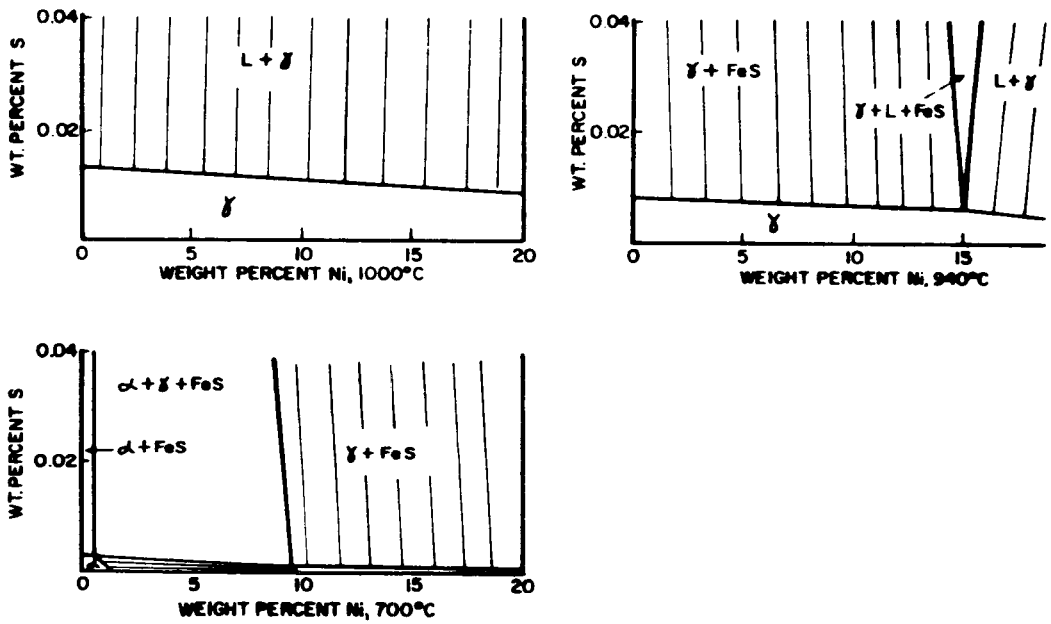

Figure 3.--Isothermal phase diagrams of the Fe-rich part of the system Fe-Ni-S. Symbols: L = Fe-Ni-S liquid; γ = γ-Fe, Ni; α = α-Fe, Ni; FeS = troilite.

with sulfide liquid is approximately 0.01 wt percent at 1,000°C (fig. 3). This solubility decreases with temperature, so that sulfide liquid exsolves from metal. Interpolating from Kullerud (1963), sulfide liquid in equilibrium with Fe-Ni alloys ranging in composition from 5 to 25 wt percent Ni solidifies within the approximate temperature range 940° $\pm$ 20°C. At 940°C, the solubility of S in Fe-Ni of the above composition range is approximately 0.008 $\pm$ 0.001 wt percent. Other elements are not present in sufficient amounts to significantly change this figure. Below the solidification temperature, solid FeS exsolves from the metal. Kamacite begins to separate from taenite at approximately 770°C for alloys of meteoritic composition. Figure 3 shows that at 700°C the solubility of sulfur in alloys of the above composition is negligible (below 0.002 wt percent). Hence, the temperature at which the bulk of the solid FeS exsolves from metal in meteorites is between 840° and 700°C.

The solubility of S in kamacite is greater than in taenite, so that some FeS is redissolved in metal during the formation of kamacite and is then reprecipitated at lower temperatures. The solubility is so low, however, that the effect is of little importance quantitatively, especially if kamacite forms in meteorites at temperatures as much as 100°C lower than the equilibrium Fe-Ni diagram predicts, because of supersaturation effects (Wood, 1964; Goldstein and Ogilvie, 1965b; Short and Anderson, 1965) or stabilization of taenite by C (Brett, 1966).

Calculation shows that 0.008 wt percent S, if totally exsolved from metal, corresponds to 0.04 volume percent troilite or a 2-cm length of exsolved troilite, 0.2 mm wide, in any random 10 $\times$ 10 cm slab of meteorite. Point-count analysis of the slab of Gibeon and the slab of Drum Mts. (fig. 1), which contain type 2 and type 1 troilite bodies, respectively, indicates that they contain 1.3 volume percent and 0.7 volume percent troilite in lamellar form respectively. The amount of lamellar troilite in these slabs is not unusually high compared with that in other meteorites. Therefore

the amount of troilite is too large to be explained by an exsolution origin.

The lack of continuity of the Widmanstätten texture across the type 1 troilite bodies and the presence of swathing kamacite commonly surrounding them are indications that the troilite formed prior to the formation of the Widmanstätten texture. Similarly, the lack of continuity of schreibersite masses across the troilite bodies suggests that the schreibersite formed after the troilite and nucleated at the troilite-metal interfaces. These phosphide masses formed from the solid state (Goldstein and Ogilvie, 1963).

The troilite bodies are very similar mineralogically to the large rounded troilite nodules which occur so commonly in iron meteorites. These large bodies formed by crystallization of a sulfide melt (Vogel, 1945) according to the phase equilibria shown in figure 3. The fact that both nodules and type 1 lamellae formed prior to the formation of schreibersite and Widmanstätten texture, and that neither show characteristics of exsolution texture and could not have formed by exsolution, suggests that the elongated troilite bodies also formed from a melt.

Swathing Kamacite

Perry (1944) stated that swathing kamacite, which commonly surrounds meteoritic troilite bodies, was formed by rejection of metal that crystallized with troilite from the residual melt, with further exsolution from the solid. He also stated that some of the swathing kamacite surrounding Reichenbach lamellae was formed by nucleation of kamacite on earlier kamacite of the above origin during the formation of the Widmanstätten texture. Buchwald (1966) also stated that swathing kamacite is formed by rejection of Ni-poor metal from troilite on solidification.

It has been shown above that Ni-Fe alloys corresponding to the composition of the majority of iron meteorites (Ni 5-25 wt percent) become totally crystalline at 940° $\pm$ 20°C. For such compositions

the Widmanstätten texture begins to form at approximately 760°C for Ni_5Fe_{95} and 520°C for $Ni_{25}Fe_{75}$ (Goldstein and Ogilvie, 1965a). Meteorites must therefore cool more than 100°C from the temperature at which the remnant sulfide liquid solidifies to the temperature at which kamacite begins to appear. Assuming cooling rates of 1°-10°C per million years for iron meteorites (Wood, 1964; Short and Anderson, 1965; Goldstein and Ogilvie, 1965b), this 100°C minimum temperature difference corresponds to a cooling time of more than 10 million years, which from the diffusion results of Goldstein and others (1965) is ample time for inhomogeneities in Fe-Ni surrounding the sulfide inclusions to be annealed out. In addition, Kullerud's (1963) work has shown that the metal crystallizing from the residual melt in the Fe-rich part of the system Fe-Ni-S does not differ greatly from the bulk metal composition. Metal surrounding sulfide inclusions would therefore not be Fe rich as implied by Perry. There is little, if any, solubility of Fe in FeS (Hansen and Anderko, 1958) so that swathing kamacite cannot form by exsolution. Therefore, in contradiction to Perry's conclusions, swathing kamacite surrounding troilite bodies in iron meteorites is not formed from the metal crystallizing from the residual sulfide melt or by exsolution, but is due to nucleation of kamacite at the troilite-metal interface during the formation of the Widmanstätten texture. Our inability to find swathing kamacite about type 2 lamellae is therefore puzzling.

Cooling Rates

Sims (1959) has shown by heating experiments on an alloy closely resembling the composition of the Grant meteorite that the size of troilite nodules is proportional to the cooling time during the solidification interval. The meteorites Gibeon, Maria Elena, Henbury, Yanuitlan, Tocopilla, Tlacotepec, and Coahuila consistently contain type 2 (wide) troilite inclusions, with few of the larger troilite nodules commonly found in iron meteorites. The lack of large nodules may be due to sampling difficulties rather than any real relationship. From the results of Sims, it would appear that these meteorites cooled faster, at least during solidification, than most iron meteorites.

It is noteworthy that the octahedrites in the above group are exceptionally low in nickel compared with other meteorites in their class (table 2). This is especially true of the three fine octahedrites whose nickel contents are closer to those of coarse octahedrites than fine octahedrites. The work of Wood (1964), Short and Anderson (1965), Goldstein and Ogilvie (1965b), and Reed (1965) suggests that for a given nickel content, the width of the kamacite lamellae is proportional to the cooling rate. The above octahedrites have exceptionally narrow kamacite lamellae compared with other meteorites of similar composition, which suggests that they cooled more rapidly during the interval in which the Widmanstätten texture formed than the majority of iron meteorites. This additional evidence suggests that the above meteorites may have cooled more rapidly over the entire cooling range, at least from the temperature at which sulfide began to solidify. These meteorites therefore cooled in a body smaller than that from which most meteorites originated, or near the surface of a large body.

The fine-grained kamacite-troilite intergrowths observed at the troilite-kamacite contact in Tocopilla, Maria Elena, Gibeon, and Henbury are indicative of rapid cooling. Had these meteorites cooled slowly, the troilite and kamacite would have separated into coarser grained masses. Gibeon has apparently been reheated (El Goresy, 1965), as has Henburg (Spencer, 1933; Perry, 1944; Wood, 1964), so it is likely that the fine-grained texture represents partial melting and rapid cooling at some time subsequent to the formation of the Widmanstätten texture. The source of heat may have been shock, which causes maximum heating at grain boundaries, which would explain why the troilite-kamacite intergrowths are observed only at the boundaries between these two phases. The fine-grained kamacite may have been swathing kamacite prior to the reheating, which explains the lack of swathing kamacite about these type 2 troilite lamellae.

The amount of nickel in meteorites containing type 1 lamellae corresponds closely to the average nickel content of the class (table 2). These meteorites also generally contain large troilite nodules, so that it is unlikely that they cooled unusually rapidly. The narrow troilite lamellae may be fractures formed by minor settling movements in the meteorite parent body or by shock while part of the sulfide fraction was still molten. The rough orientation of the narrow troilite bodies in some meteorites is suggestive of a fracture pattern. Doubtless many other fractures formed at the time, but only those that were filled with troilite persisted; the rest rehealed during the long cooling period which iron meteorites have undergone.

The lamellae with near-perfect orientation (Duel Hill and Staunton) may have resulted from entrapment of sulfide liquid remnants between two growing metal crystal faces at a slight angle to one another. The common slight difference in orientation of the Widmanstätten lamellae across the lamellae tends to support this origin.

CONCLUSIONS

The following conclusions can be drawn from the present study:

1) Use of the term Reichenbach lamellae is so confused in the literature that we suggest that it be dropped, or, if used, a complete description should be given of the body so designated.

2) All troilite bodies in meteorites were formed from a sulfide melt, with extremely minor contribution from troilite exsolved in the solid state.

3) The type 1 lamellae in iron meteorites appear to have formed by filling of fractures. The well-oriented bodies may have formed by crystallization of the residual sulfide liquid in oriented interstices in the nickel-iron. The type 2 lamellae appear to have formed in iron meteorites which cooled more rapidly than most iron meteorites. Such rapid cooling is suggestive of origin

in a small parent body, compared with the size of the parent body of other iron meteorites, or of cooling near the surface of a large body.

4) Swathing kamacite surrounding troilite in iron meteorites was formed by nucleation at the troilite-metal interface during the formation of the Widmanstätten texture.

REFERENCES CITED

Ainslie, N. G., and Seybolt, A. U., 1960, Diffusion and solubility of sulfur in iron and iron-silicon alloys: Iron and Steel Inst. Jour., v. 194, p. 341-350.

Brett, R., 1966, Cohenite in meteorites: a proposed origin: Science, v. 153, p. 60-62.

Brezina, A., 1882, Über die Reichenbach'schen Lamellen in Meteoreisen: Denkschr. der k. Akad. der Wiss., Math. -Naturw. Kl. 43, pt. 2, p. 13-16.

Buchwald, V. F., 1966, The iron-nickel-phosphorous system and the structure of iron meteorites: Acta Polytech. Scand. (Chem. ind. Metall. Ser.) no. 51, 46 p.

Cohen, E., 1900, The meteoritic iron from Bethany, Great Namaqualand: South African Mus. Ann., v. 2, pt. 2, p. 21-29.

Edwards, A. B., 1946, The Moorumbunna meteorite: Royal Soc. South Australia Trans., v. 70, p. 348-353.

El Goresy, A., 1965, Mineralbestand und Strukturen der Graphit - und Sulfideinschlüsse in Eisenmeteoriten: Geochim. et Cosmochim. Acta, v. 29, p. 1131-1151.

Elliott, R. P., 1965, Constitution of binary alloys: 1st supp., New York, McGraw-Hill, 877 p.

Goldstein, J. I., Hannemann, R. E., and Ogilvie, R. E., 1965, Diffusion in the Fe- Ni system at 1 atm. and 40 kbar pressure: Trans. Metall. Soc. America Inst. Mining Metall. Eng., v. 233, p. 812-819.

Goldstein, J. I., and Ogilvie, R. E., 1963, Phosphides and sulfides, pt. 1 of Electron microanalysis of metallic meteorites: Geochim. et Cosmochim. Acta, v. 27, p. 623-637.

_____1965a, A re-evaluation of the iron-rich portion of the Fe-Ni system: Trans. Metall. Soc. America Inst. Mining Metall. Eng., v. 233, p. 2083-2086.

_____1965b, The growth of the Widmanstätten pattern in metallic meteorites: Geochim. et Cosmochim. Acta, v. 29, p. 893-920.

Hansen, M., and Anderko, K., 1958, Constitution of binary alloys: 2d ed., New York, McGraw-Hill, 1305 p.

Heide, F., Herschkowitsche, E., and Preuss, E., 1932, Ein neuer Hexaedrit von Cerros del Buen Huerto, Chile: Chem. Erde, v. 7, p. 483-502.

Hellawell, A., and Hume-Rothery, W., 1957, The constitution of alloys of iron and manganese with transition elements of the first long period: Roy. Soc. [London] Philos. Trans., v. A249, p. 417-459.

Henderson, E. P., and Perry, S. H., 1948, The Drum Mountains, Utah meteorite: Smithsonian Misc. Colln. 110, no. 12, p. 1-7.

Kullerud, G., 1963, The Fe-Ni-S system: Carnegie Inst. Washington Yearbook 62, p. 175-189.

Meijering, J. L., 1959, Thermodynamical calculation of phase diagrams: Natl. Phys. Lab. Symposium 9, v. 2, Paper 5A, p. 2-20.

Perry, S. H., 1944, The metallography of meteoritic iron: U.S. Natl. Mus. Bull. 184, 206 p.

_____1942-53, Photomicrographs of meteoritic irons: 9 v. Circulated privately by the author.

Prior, G. T., 1953, Catalogue of meteorites: 2d ed., revised by Hey, M. H., London, Trustees British Mus., 472 p.

Reed, S. J. B., 1965, Electron-probe microanalysis of the metallic phases in iron meteorites: Geochim. et Cosmochim. Acta, v. 29, p. 535-549.

Reichenbach, K. L. von, 1861a, Uber das innere Geffüge der näheren Bestandtheile des Meteoreisens: Annalen Phys. u. Chem., 4th ser., v. 21, p. 99-132.

_____1861b, Uber die näheren Bestandtheile des Meteoreisens. Das Bandeisen: Annalen Phys. u. Chem., 4th ser., v. 21, p. 477-491.

Rinne, E., 1910, Ein Meteoreisen mit Oktaeder und Wüfelbau (Tessera-Oktaedrit): Neues Jahrb. Min., v. 1, p. 115-117.

Short, J. M., and Anderson, C. A., 1965, Electron microprobe analyses of the Widmanstätten structure of nine iron meteorites: Jour. Geophys. Research, v. 70, p. 3745-3759.

Sims, C. E., 1959, The non-metallic constituents of steel: Am. Inst. Mining Metall. Engineers Trans., v. 215, p. 367-393.

Spencer, L. J., 1933, Meteoric iron and silica-glass from the meteorite craters of Henbury (Central Australia) and Wabar (Arabia): Mineralog. Mag., v. 23, p. 387-404.

_____1951, "Reichenbach" and "Brezina" lamellae in meteoritic irons: Mineralog. Mag., v. 29, p. 545-556.

Vogel, R., 1945, Über Troilit: Chem. Erde, v. 15, p. 371-387.

Wood, J. A., 1964, The cooling rates and parent planets of several iron meteorites: Icarus, v. 3, p. 429-459.

ELECTRON MICROSCOPY OF MICROMETEORITES COLLECTED ON THE 1965 LUSTER EXPERIMENT

By M. H. Carr and H. J. Gabe

INTRODUCTION

A sounding rocket payload, designed to recover micrometeorites from the upper reaches of the earth's atmosphere, was successfully launched and recovered by Ames Research Center on November 16, 1965. The purpose of the shot, a part of the Luster program, was to collect extraterrestrial material and return it to earth for analysis (Farlow and Gault, 1964). A group from the Geological Survey participated in the shot as guest experimenters by designing and examining collectors placed in one of the 12 collection pans flown. This report is a summary of the results of examining material on collectors specifically designed for use in the electron microscope. The results are surprising in that far less material than anticipated was collected. Only six particles of possible extraterrestrial origin were found in the 2×10^{-1} sq cm of collection surface scanned. No evidence of high velocity impact was found.

The Luster payload and details of the November flight have been described in other reports (Farlow and Blanchard, 1966; Farlow, Blanchard, and Ferry, 1966) and are only summarized in this one. The payload consists of a central column and three deployable arms. Four pans, in which the collectors are mounted, are attached to each arm; the pan covers are fixed to the central column (fig. 1). The collection pans, in a vacuum-sealed condition, are attached to the payload before launch. After launch, when the payload reaches collection altitude, the arms are deployed so that the pans are approximately at right angles to the line of flight. The pan covers remain attached to the central column. At the end of the collection period the arms are retracted, and the pans are

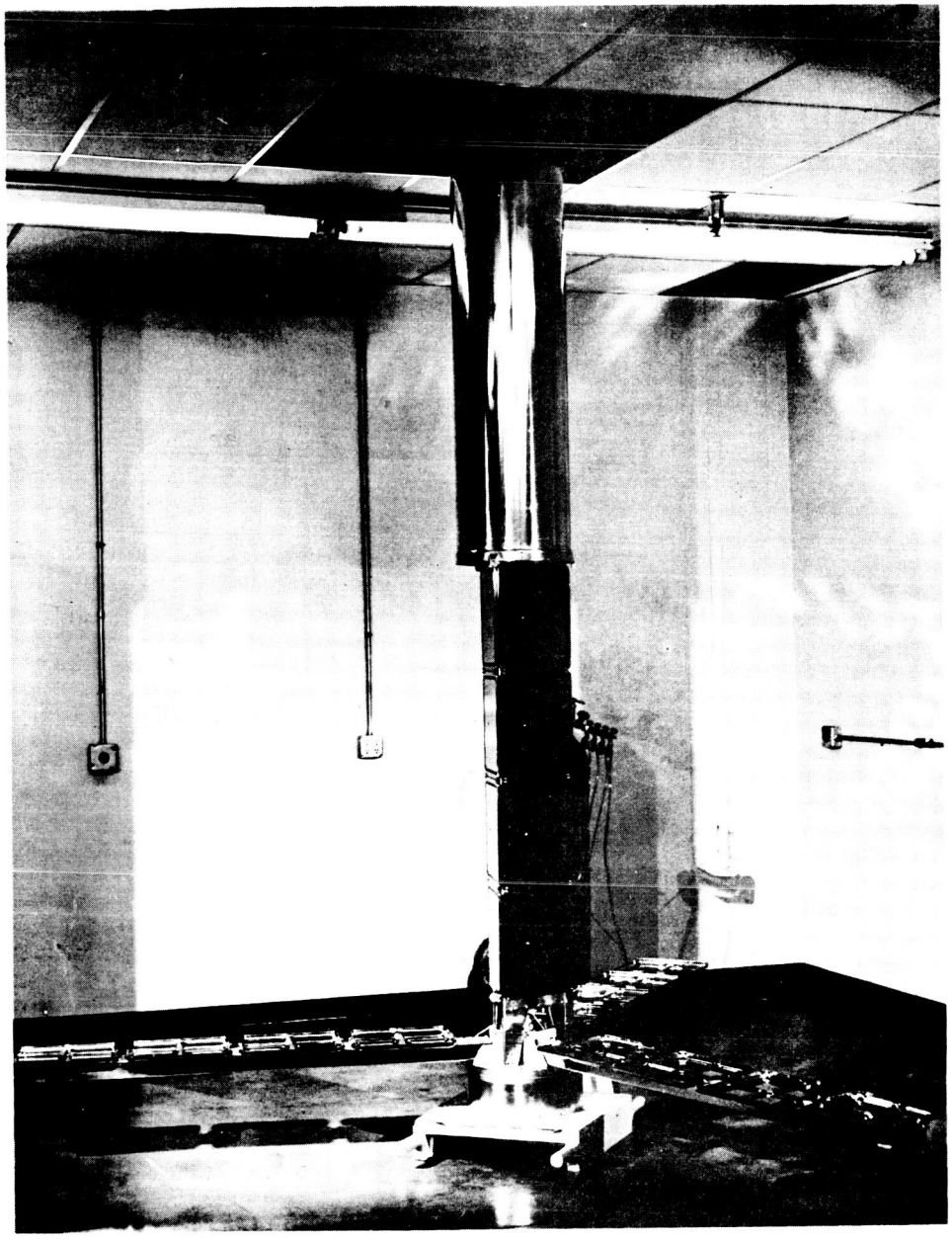

Figure 1.--Luster sampling instrument fully open (reproduced by permission of NASA, Ames Research Center).

mated with their covers and vacuum sealed.

Sampling of the Leonid meteor shower was intended in the November 1965 experiment. The Luster payload was carried on an Aerobee 150 sounding rocket and launched from White Sands Missile Range at 1600 hours (U.T.) November 16, within a few hours of the estimated peak of the Leonid meteor shower. The payload opened during ascent at an altitude of 64 km, reached a maximum altitude of 145 km, and closed on descent at 116 km. The sampler remained open for a period of 200 seconds. After recovery, the pans, still vacuum sealed, were detached from the payload and returned to the experimenters.

SAMPLE PREPARATION AND CONTAMINATION CONTROL

The electron microscope mounts were intensively studied first because a shadowing technique was available for clearly discriminating between contaminants and noncontaminants. Only a small proportion of the total area available in the collection pan was set aside for electron microscopy. The rest of the area was reserved for collecting material to be examined optically or in the electron microprobe. The results from examining the electron microscope mounts are critical for interpreting future data from the optical and microprobe mounts since only in the electron microscope mounts can the contaminants be clearly recognized.

Surfaces designed for the collection and examination of submicron particles in the electron microscope included copper mesh covered with 200-400 A thick films of formvar and collodian that were shadowed with aluminum. Extreme precautions were taken to prevent contamination during the preparation of the mounts. All work was conducted on a laminar flow clean bench in a clean room. Cleanliness on the laminar flow bench exceeded the Class IV requirements in Air Force T.O. 00-25-203, 1 March 1962. Chemicals and cleaning fluids were filtered before use to eliminate particles greater than 0.05 μ in diameter. All solid parts

were cleaned ultrasonically as well as rinsed in filtered cleaning solutions. Separate vacuum chambers were used for shadowing with aluminum and for sealing the collection pans. Each chamber opened up onto the clean bench so that between shadowing and vacuum sealing in the collection pan the mounts never left the clean environment of the laminar flow bench. As an additional precaution, filters were placed across the air inlet valves of the vacuum chambers to eliminate particles larger than 0.05 μ. The only time that the collection pans were opened between leaving the clean bench before flight and returning to the clean bench after flight was during the flight itself.

The double shadowing technique was used to discriminate between contaminants and noncontaminants. The copper mesh was shadowed immediately prior to sealing in the collection pan and immediately after removing from the pan subsequent to flight. Particles having one shadow must have landed on the collection surface either (1) in the short time between shadowing and sealing in the pans, while the mounts were exposed only to filtered air, (2) during shipment of the vacuum-sealed pans, as a result of contaminants falling off the inside walls of the pans or, (3) while the payload was deployed in flight. All particles with two shadows or no shadows must be contaminants; only particles with one shadow can be noncontaminants.

A preliminary examination of the collectors showed that the principal contaminant was Cu or CuO from the copper mesh: submicron particles were found along the edges of some of the screen openings but not in the center. Where contamination occurred, the copper was slightly discolored. To avoid interference from the copper, areas of copper mesh were selected for examination from those areas of copper mesh that still appeared fresh and uncorroded.

RESULTS

The grids were far cleaner than anticipated. An area of 2 x 10^{-1} sq cm, 2,000 grid openings, was examined systematically at magnifications of 16,000 to 20,000. At these magnifications, particles larger than 0.07 μ in diameter are seen with ease. Only 6 single-shadowed particles were found; 116 double-shadowed particles were present. No holes or flaps, indicative of penetration of the organic support films by particles, were observed. Several of the grids flown were shielded from the micrometeorite flux by lucite. No single-shadowed particles were found on these grids, but this is not surprising since many of the unshielded grids also yielded no single-shadowed particles.

Although extremely low levels of contamination were achieved, the contaminant to noncontaminant ratio remained high, approximately 20:1, because of the low number of noncontaminants found. This high ratio is consistant with the preliminary results of Farlow, Blanchard, and Ferry (1966), who found no significant difference in the number of particles on unshielded and shielded grids, and on flight samples and samples not flown. The total number of particles found per unit area is comparable with the total number of particles, single and double shadowed, found here (610 per sq cm), indicating similar levels of contamination.

The number of single-shadowed particles per unit area is almost two orders of magnitude less than found on the Venus Fly Trap experiment (Hemenway and Soberman, 1962) for which flight conditions were very similar. Even the total number of particles per unit area for Luster, including contaminants, is less than the number of single-shadowed particles for the Venus Fly Trap experiment. Three man-months of work produced only six particles; because of this, electron microscope work was curtailed. Photographs of two of the single-shadowed particles are shown in figure 2. Four of the single-shadowed particles are crystalline and give diffraction patterns. The patterns are not complete enough for identification, but definitely do not represent Ni-Fe, Fe, or Ni.

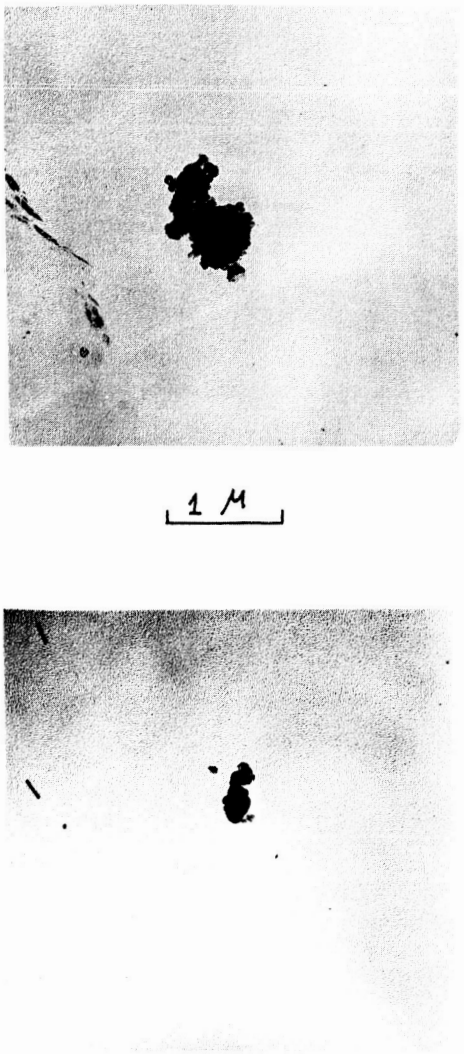

Figure 2.--Two typical single-shadowed particles.

INTERPRETATION

From the few particles collected, an estimate was made of the particle flux during flight using a method similar to that of Soberman and Hemenway (1965). The particles were assumed to be falling at their terminal velocities, Vp, which was computed from

$$Vp = \frac{2\pi \rho_p g d}{3 \alpha c \rho_a}$$

where ρ_p and ρ_a are, respectively, the particle density, taken as 3 gm per cc, and the ambient air density. d is the diameter of the particle, g is the acceleration due to gravity, c is the ambient mean molecular speed, and α is a constant, taken as $\frac{4\pi}{3}$. Vp was calculated for various altitudes from values of ρ_a, c, and g published in U.S. Standard Atmosphere (1962).

From the flight data furnished by Ames Research Center and the values of Vp at various altitudes, the velocity of the particle with respect to the collector, Vpc, was calculated for various times, t, after deployment of the collector. If the number of particles per unit volume sampled is Dp, then the total number of particles collected, N, is given by

$$N = \int_{t_1}^{t_2} Vpc \; Dp \; dt$$

where t is the time the collector was deployed and t_2 is the time the collector was retracted. If the flux of particles is assumed constant, then

$$N = f \int_{t_1}^{t_2} \frac{Vpc}{Vp} \; dt$$

where f is the flux. The integral gives the effective open time of the collector and was solved graphically for different particle sizes. The effective open time as a function of particle size is given in figure 3. For most of the flight, the ratio $\frac{Vpc}{Vp}$ is close

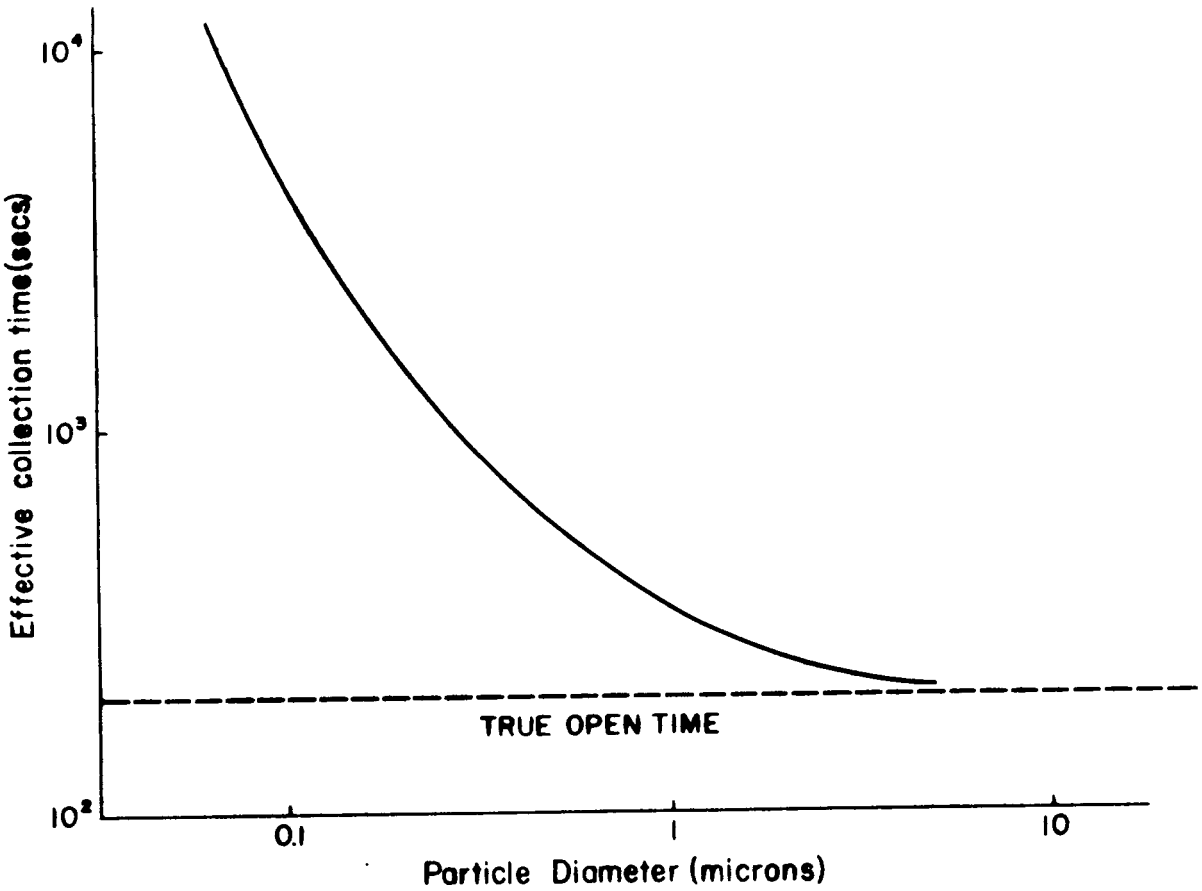

Figure 3.--Effective collection time as a function of particle size.

to 1. In the first few seconds of flight, however, the collector is at an altitude where a 0.1 μ particle falls at a velocity of only a few centimeters per second, compared with a velocity of over 1 km per sec for the collector, and the ratio $\frac{Vpc}{Vp}$ is greater than 10^2. This implies that for 0.1 μ size particles, most of the collection took place in the first few seconds after deployment of the collector. This effect is far less pronounced for 1 μ particles, as their terminal velocities at deployment altitude are still high.

The flux calculated is a maximum since the number of single-shadowed particles represents the maximum possible number of extraterrestrial particles collected. Some of the single-shadowed particles are probably contaminants that fell on the collector during shipment or from the vehicle during deployment. Films of the Pegasus satellite show large amounts of debris falling off the satellite during deployment of its arms, and the Luster payload may similarly be a source of contamination. Even this maximum flux is less than the flux determined from satellite data and from the Venus Fly Trap experiment (fig. 4).

Most of the space available in the collection pans was reserved for collectors designed for optical examination and examination in the electron microprobe. Only very preliminary work has been done on these mounts. The electron microscopy results are disturbing in that they indicate a high contaminant to non-contaminant ratio and a very low number of single-shadowed particles. For the optical and microprobe mounts there is no clear way of distinguishing contaminants, and so results from these mounts are suspect. Furthermore, only an extremely small number of particles will be found. If we assume a particle-size distribution similar to the Venus Fly Trap collection, then the electron microscope results can be extrapolated to larger sizes. This extrapolation indicates that in the total effective sampling area in the USGS module only 10 particles larger than 4 μ will be found. Distinguishing

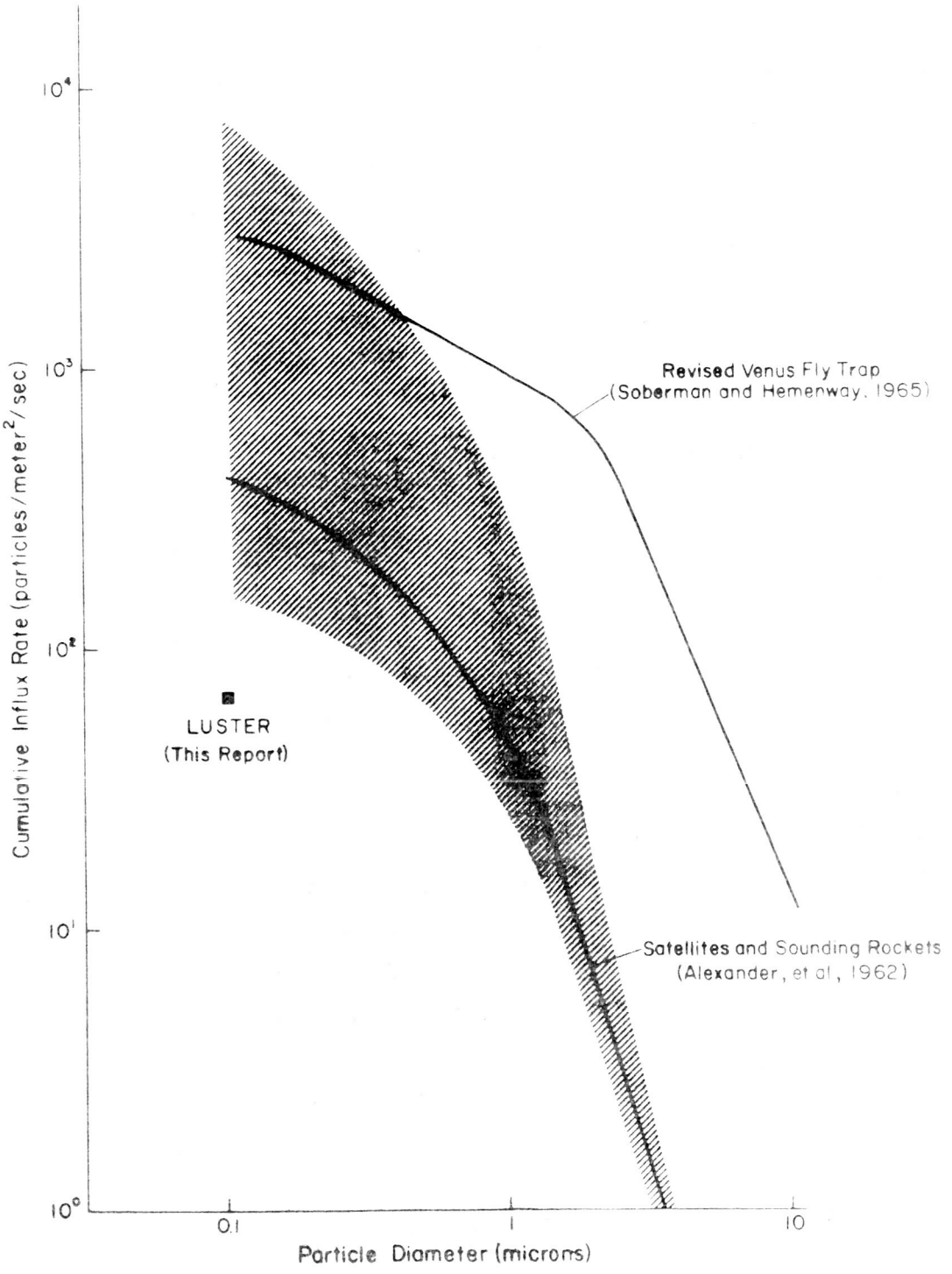

Figure 4.--Comparison of estimates of the flux of interplanetary dust near the earth based on satellite data and data from the Venus Fly Trap and Luster collections. Shaded area indicates the uncertainty in the satellite data.

these particles from all the contaminants present will be exceedingly difficult, if not impossible.

ACKNOWLEDGMENTS

The authors wish to thank Ames Research Center for inviting us to participate in the Luster experiment. Special thanks go to Neil Farlow of Ames for his ever helpful comments and suggestions.

REFERENCES CITED

Alexander, W. M., McCracken, C. W., Secretan, L., Berg, O. E., 1962, Rockets, satellites, and space-probe measurements of interplanetary dust: Am. Geophys. Union Trans., v. 43, no. 3, p. 351-360.

Farlow, N. H., and Blanchard, M. B., 1966, A preliminary microscopic survey of four sampling slides exposed during the November 1965 Luster flight: Prelim. Rept., Ames Research Center, Moffett Field, Calif.

Farlow, N. H., Blanchard, M. B., and Ferry, G. V., 1966, Sampling the Leonid Meteor stream with a Luster sounding rocket: Prelim. Rept., Ames Research Center, Moffett Field, Calif.

Farlow, N. H., and Gault, D. E., 1964, Luster: A sounding rocket experiment to sample lunar dust near the earth: Ames Research Center, Moffett Field, Calif.

Hemenway, C. L., and Soberman, R. K., 1962, Studies of micrometeorites obtained from a recoverable sounding rocket: Astronom. Jour., v. 67, p. 256-266.

Soberman, R. K., and Hemenway, C. L., 1965, Meteoric dust in the upper atmosphere: Jour. Geophys. Research, v. 70, p. 4943-4949.

U.S. Standard Atmosphere, 1962: Washington, U.S. Govt. Printing Office.

NEW TECHNIQUES IN GEOCHEMICAL ANALYSIS

By Irving May and Frank Cuttitta

INTRODUCTION

The field of geochemical analysis has been experiencing an explosive development of new techniques in recent years. Chemical analysis of naturally occurring substances was a major activity of chemists as early as the 18th centry. Consequently, systematic methods of analysis of rocks and minerals were developed relatively early. Such methods underwent gradual refinement and also enlargement to accommodate new elements as they were discovered. Fundamentally, however, techniques remained relatively static for many years.

As recently as the late thirties the situation hadn't changed much. However, there were already signs of the impending instrumental revolution. Spectrographic analyses were being applied increasingly to analytical problems. Heyrovsky's polarograph was on the market, although little used in this country. Recording spectrophotometers had already been described although none were as yet being produced commercially.

Things changed rapidly in the 1940's. Wartime industry required analyses that were increasingly complex and sophisticated. Spurred on by these requirements of industry and assisted by generous support from the government, a tremendous expansion in the electronic and optical instrument industries occurred. The impact on analytical chemistry was revolutionary.

In this report, some of the modern trends in geochemical analysis will be discussed. What are some of the trends in geochemical analysis? First of all, geochemical studies are growing in size and scope. There are reciprocating stimuli acting between the field and the laboratory. As the capability of the laboratory for making

rapid and complex analyses increases, it becomes feasible to tackle field problems requiring what would have been formerly a prohibitive number of samples or determinations. Similarly, the need for many analyses forces the analyst to adopt new analytical techniques and to develop new methods.

We see also a growing demand for the analysis of small samples and of trace constituents of large samples. A large proportion of mineral analysis is performed on the semimicro and micro levels. Samples of minute metallic spherules and of dust particles collected at high altitudes require micro and ultramicro techniques. In preparing for the analysis of returned lunar samples, a premium is being placed on the ability to extract a maximum of information from the smallest size sample.

CHROMATOGRAPHY

Chromatographic methods have provided new and comparatively simple techniques for performing separations of complex materials previously considered almost impossible to achieve. The techniques of column, paper, thin-layer, and gas chromatography generally utilize one or more of the four principal chromatographic phenomena of adsorption, partition, ion-exchange, and electrochromatography. Only the two techniques which recently have shown the greatest analytical development, i.e., thin-layer chromatography and gas chromatography, will be discussed here.

The discovery of chromatography is attributed to Mikhail Tswett, a botanist. In 1906, he published his first paper on resolving plant pigments by absorbing them on columns of calcium carbonate and separating them into colored bands by eluting with petroleum ether. Because of the bright color of some of the bands, he named the process the chromatographic method.

It is of particular interest to geochemists that David Talbot Day, a distinguished chemist and geologist at the U.S. Geological Survey, starting in 1898 performed similar chromatographic separations in connection with his studies of Pennsylvania oils. Day fractionated crude petroleum into a series of oils differing in color and specific gravity by diffusing the oil through columns of fuller's earth. He found that Texas oils contain considerable amounts of constituents readily removable by absorption, and he speculated on a common source for petroleum from Texas, Ohio, and Pennsylvania. The differences in their composition were explained as due to the greater distance of Ohio and Pennsylvania oils from the source and their consequent passage through greater lengths of absorbing media (Day, 1903). Day's studies were continued by J. E. Gilpin and his associates, who found that fuller's earth tends to retain unsaturated hydrocarbons, sulfur compounds, and nitrogen compounds. Paraffinic hydrocarbons move through the earth most rapidly, the fractions of lower specific gravities penetrating first (Gilpin and others, 1908, 1911, 1913).

Despite the remarkable accomplishments of the pioneering investigators of chromatography, little was done with the method for some thirty years, after which column separations began to be used widely. Interest in chromatography expanded phenomenally with the development of paper chromatography by Martin and Synge in 1951 and the introduction of gas chromatography in 1952 by James and Martin.

Chromatography is fundamentally a separation process. The separation takes place on a porous stationary medium when a sample is passed through the medium. The sample may be a liquid, a solid dissolved in a liquid, or a gas. A convenient tabulation of chromatographic systems is given in table 1.

Table 1.--Systems, techniques, and principles of chromatography (from Maier and Mangold, 1964)

Stationary phase	Mobile phase	Techniques	Physical principles
Solid	Liquid	Column, thin-layer, and paper chromatography	Absorption, ion exchange, gel filtration, and others.
Liquid	--do--	--do--	Partition, reversed-phase partition.
Solid	Gaseous	Gas-solid chromatography	Absorption.
Liquid	--do--	Gas-liquid chromatography	Partition, reversed-phase partition.

A comprehensive discussion of the theory and techniques of chromatography has been presented by Lederer (1957; see also Rosenthal and others, 1961). A review of recent developments and literature has been published (Heftmann, 1966). Applications of column and paper chromatography in geology have been discussed by Ritchie (1964).

The various chromatographic methods have several common features that make them appealing to analysts. Foremost, chromatographic separations can be made of mixtures that are not readily separated by other techniques. Chromatographic separations can be conducted rapidly, within as short a time as a few minutes. Separations can be made with small samples; in fact, for some of the techniques--paper, thin-layer, or gas chromatography--micro samples are best. Column-absorption chromatography, the oldest of the chromatographic procedures, has been largely superseded by the newer chromatographic techniques. Its first application, the fractionation of petroleum components, is now performed more readily and more effectively by gas chromatography. Paper methods are generally faster than column methods, permit two-dimensional analysis, and are more amenable to development of colors or

fluorescence by reaction with reagents after development. They are particularly useful in the separation of amino acids and for the identification of metallic elements in field studies. The relatively older techniques of column and paper chromatography will not be discussed further here.

Gas Chromatography

Gas chromatography is a technique for separating gases or vapors from one another by passing them over a stationary solid or liquid phase having a large surface area. Separations occur because of differential volatility of the components, differential solubility of the gas mixture in a liquid phase, or differential adsorbability on a solid phase. The technique has been discussed comprehensively by Dal Nogare and Juvett (1962, 1966) and by Littlewood (1962).

Gas chromatographic methods are of two types: 1) gas-solid chromatography, in which a gas, such as helium, argon, hydrogen, or nitrogen, carrying a gaseous mixture to be resolved, passes over a porous absorbing solid, and 2) gas-liquid chromatography, in which the stationary phase is a nonvolatile liquid coated on a porous solid support. Gas-solid chromatography is particularly applicable to the analysis of gases and of volatile nonpolar liquids. These are generally separated in the order of their volatility, the more volatile gas coming through first. Gas-liquid chromatography is the more generally applicable method as there are a large number of stationary liquid media available that differ in their chemical and solvent behavior. Proper selection of the liquid facilitates many otherwise difficult separations.

Three procedures may be used in gas chromatography: elution, frontal, or displacement analysis. Elution analysis, the most widely used of the three, is performed by sweeping the sample through the column with an inert carrier gas. Components which are resolvable have different retention times in the column and

appear at the detector at times characteristic for each component with a given column and set of operating conditions. The response of the detector is plotted as a function of time, so that a component arriving at the detector will be represented by a peak above a base line. The height, or more generally the area, of the peak is proportional to the concentration of the component. Components separated by gas chromatography cannot be identified without the use of independent identification techniques or without prior knowledge of the composition of a sample and the performance of the column with a given set of conditions.

Two parameters of gas chromatographic separations are the efficiency and resolution of a column. The efficiency of a column is the measure of its ability to produce sharp peaks. It depends on such factors as carrier-gas flow rate, sample size, temperature, and packing material. The number of theoretical plates, which is a measure of the efficiency, is defined as $r = 16 (x/y)^2$ where x and y are defined in figure 1. The resolution of a column refers to its efficiency in separating two solutes from one another. From analysis of the degree of overlap of the curves of two solutes, the number of theoretical plates required to effect complete separation can be calculated. Columns can be readily made that provide efficiencies of up to hundreds of thousands of theoretical plates. Increased resolution can be obtained by lengthening the column, decreasing its diameter, using a packing with more favorable partition characteristics, and decreasing the rate of carrier-gas flow.

As an analytical tool, gas chromatography is increasingly popular for several reasons. Foremost is its applicability on a micro scale--less than 20 ml for liquid samples and less than 5 ml for gases. Nevertheless, columns with much greater capacity also may be used for the preparation of ultrapure compounds. Many of the detection methods are nondestructive, and the separated effluent vapors can be collected and then subsequently studied by other analytical methods such as ultraviolet, infrared, X-ray, mass

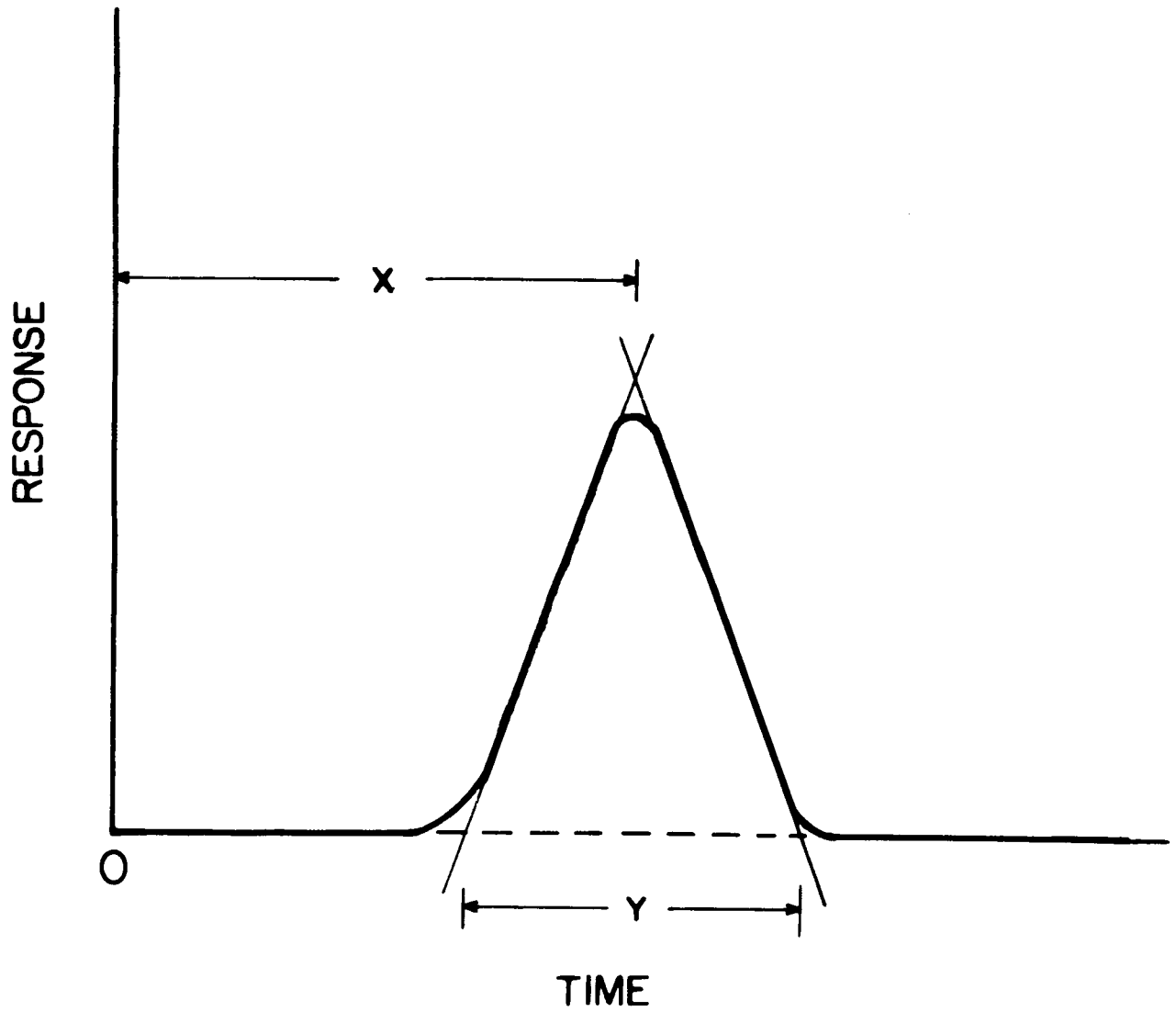

Figure 1.--Measurements for calculating column efficiency.

spectrometric, and optical spectrographic analysis. Gas chromatographic separations can be performed rapidly, often in well under an hour per run.

Columns are often only a few feet in length; 3- to 6-foot lengths are common. For separations with maximum efficiency, capillary columns several hundred feet long are used. In gas-solid chromatography, commonly used adsorbents are activated charcoal, molecular sieves, alumina, and silica gel. With gas-liquid chromatography, stationary solvents selected for their high transition temperatures are deposited on an inert solid substrate such as powdered Teflon, diatomaceous earth, and steel or glass helices or spheres. Hundreds of such liquids are available; among the most popular are glycols, natural oils and waxes, and silicones.

Any detecting device sensitive to small changes in the physical or chemical properties of the effluent gas or vapor can be used. Most commonly used are thermal-conductivity, ionization, flame-ionization, and electron-capture detectors. Quantitative data are obtained by relating recorded peak heights or areas of the chromatographic curve to concentrations.

Applications

Gas chromatography is an important method for analyzing atmospheric pollutants and has also been used for the analysis of volcanic gases. Gas-liquid chromatography is being used to great advantage in organic geochemical studies. The hydrocarbon constituents of shales of various ages ranging up to 2.5×10^9 years (Soudan formation) were studied by gas-liquid chromatographic separation followed by mass spectrometric measurements to determine the relative distribution of the normal alkanes and of isoprenoids (Belsky and others, 1965). The isoprenoids indicate biogenic processes. Biogenic steranes and pentacyclic triterpanes were similarly isolated and identified in the Soudan shale (Burlingame and others, 1965).

Although most applications of gas chromatography have been to

the analysis of organic and biochemical samples, gas-liquid chromatography of metals has been investigated and shows great promise. Chromatographic separations of volatile halides of tin, titanium, niobium, tantalum, and uranium have been made. Many of the other volatile halides have been studied. Systematic studies are being made of the separation from one another of the volatile metal chelates (Moshier and Sievers, 1965), particularly of the metal β-diketones. Microgram quantities of such hard to separate combinations as beryllium, aluminum, and scandium give completely resolved, well-defined peaks. The 1965 and 1966 Annual Review issues of Analytical Chemistry cite hundreds of references to applications of gas chromatography.

Thin-Layer Chromatography

Thin-layer chromatography (TLC) is a chromatographic technique wherein the adsorbent is prepared as a uniformly thin deposit on rigid supporting plates such as glass, plastic sheets, or metallic foils and plates. It is more suitable than column methods as a micro technique and is particularly useful for the analysis of complex mixtures, resembling paper chromatography in the simplicity of analysis. Unlike paper techniques, which generally are partition procedures and are used best with polar developers and solutes, thin-layer chromatography is essentially a form of adsorption chromatography. With the proper choice of chromatographic medium and solvent mixtures, it can be used also for partition or exchange chromatography.

Essentials of TLC have been known for almost 30 years, and it has been used intermittently by various investigators. Thin-layer operating techniques were perfected and applied successfully to many problems particularly through the efforts 15 years ago by Kirchner and co-workers (1951), and more recently by Stahl and co-workers (1958, 1965). Maier and Mangold (1964) have reported on general techniques, apparatus, and applications and have discussed the advantages of TLC over other chromatographic techniques.

The technique is now being used extensively, particularly in biochemical analysis.

A large number of adsorbents are available, although those most frequently used are very fine (minus 200 mesh) silica gel, alumina, diatomaceous earth, cellulose, and carbon. Alumina is best used for adsorption chromatography, whereas diatomaceous earth and cellulose are most useful for partition chromatography of polar melecules. Silica gel can be used for either type of separation, depending on the solvent systems used.

The adsorbent is generally mixed with a binder such as plaster of Paris or starch, and modifiers are often added to change the properties of the adsorbent. Adsorptive properties of cellulose and of diatomaceous earth may be suppressed to favor partition effects by impregnating cellulose using an acetone solution of formamide, and diatomaceous earth with an aqueous solution of propylene glycol. Reagents giving characteristic reactions with separated species also can be incorporated into the adsorbant.

In reversed-phase partition chromatography, a stationary nonpolar liquid phase is used with a moving polar liquid. Hydrophobic adsorbents, such as acetylated cellulose and powdered polyethylene, are used. Normally, hydrophylic adsorbents are impregnated with hydrophobic additives such as paraffin, silicones, or tetradecane.

Plates are best used fresh and are, therefore, prepared by the researcher. A slurry of the adsorbent and binder is used to coat the plate, which is generally 5 $\times$ 20 cm or 20 $\times$ 20 cm. Mechanical spreading devices providing variable thicknesses from 50μ to 3,000μ are usually used to ensure a uniform coating; layers about 250μ thick are used most often. The coating is then dried.

Sample application can be in the form of solutions or as effluents from gas chromatographs collected directly on TLC plates. Small drops of the solutions to be analyzed are deposited near the edge of the plate and then dried. Development is carried out by placing the plate in a covered chamber for about 20 to 60 minutes,

the time for a travel of about 10 cm. Ascending vertical development is most often used, although descending development as well as horizontal ring and streak techniques are not uncommon. Complex mixtures can be further separated by two-dimensional chromatography.

Highly colored or fluorescent materials can be detected directly. More often colors or fluorescence are produced by the addition of appropriate reagents by spraying or, occasionally, by dipping. Organic compounds are often detected by charring with a carbonizing acid such as sulfuric acid or sulfuric-chromic acid. Alternative detection methods include the use of radioactively labeled compounds or dilution with a radioisotope. An autoradiograph is made of the developed plate, or the separated spots are eluted or removed by scraping and then are counted with a scintillation counter. Quantitative results are obtained by densitometric methods, by measuring the areas of the spots, or in the case of radioelements by counting the activity of the spots.

As in paper chromatography, in a given medium and solvent system, the rate of movement of a substance is an intrinsic property of the substance, and the R_f value is defined as the ratio of the distance traveled by the center of the spot to the distance traveled by the solvent front.

Thin-layer chromatography has several advantages over column and paper chromatography. It has substantially greater sensitivity, sharpness of separation, and speed. As a consequence, separations formerly requiring many hours are possible with shorter lengths and in faster times. The method can be used with corrosive solutions that would destroy paper. It is more flexible than paper chromatography in that one of a large number of possible adsorbants can be selected which would be most effective, depending on the chemical properties of the substance being separated.

Applications

Generally, the evaluation and separation techniques for TLC are those already developed for paper chromatography. TLC has been applied to many inorganic problems such as the separation of As, Sb, Bi, and the noble metals by chelation. The technique has also been applied to the systematic analysis of all the common cations and anions.

Thin-layer chromatography is especially useful for the analysis of liquids. There are also numerous applications to the determination of amino acids and peptides. Elemental sulfur, lipids, and hydrocarbons were isolated from extracts of the Orgueil carbonaceous meteorite by Murphy and others (1965). They used silica gel-magnesium silicate adsorbents with and without impregnation with silver nitrate and developed the chromatograms with hexane.

The separation of sterols from corresponding stanols can be accomplished by thin-layer chromatography. β-sitosterol and β-sitostanol occur in various peats. The separation of one from another has been accomplished by two techniques. In one, the mixture is brominated, the stanol remaining unchanged. The stanol is then separated from the brominated sterol on plates covered with silica gel or alumina (Ikan and others, 1964). In another technique, β-sitosterol is separated from β-sitostanol directly on thin layers of silica gel impregnated with silver nitrate (Ikan and Cudzinovski, 1965). This latter medium also gives good separations of tetracyclic triterpenes occurring in peat (Ikan, 1965).

ACTIVATION ANALYSIS

The installation at many research centers during the past few years of commercially available, relatively low-cost accelerators and nuclear reactors has resulted in a marked increase in the use of activation analysis. Only recent developments concerned chiefly with the automation of activation analysis systems and with the

improvement of the sensitivity, precision, and selectivity of geochemical analyses by activation techniques can be briefly presented here. Bowen and Gibbons (1963) comprehensively discussed activation analysis, including geochemical applications, and Lyon, Ricci, and Ross (1966) reviewed recent literature on the subject.

Separation Techniques

Although there is a definite trend toward limiting radiochemical separations to the minimum required for instrumental discrimination, in order to achieve the sensitivity required (table 2) radiochemical separations often are still necessary. Volatilization techniques have been used for some separations. Heating in a stream of nitrosyl chloride or bromine trifluoride volatilizes W, Ta, Nb, and Fe. Relatively volatile materials such as mercury sulfide or mercury metal can easily be vacuum-distilled. Low-temperature ashing of geochemical samples high in organic matter can be accomplished with atomic oxygen.

Table 2.--Sensitivities for elements using activation analysis (from Lyon, 1966)

[Based on a thermal neutron flux of 10^{12} and irradiation time of 0.5 $T_{\frac{1}{2}}$ or 1 week, whichever is shorter]

<0.002 μg	0.02-0.002 μg	0.2-0.02 μg	2-0.2 μg	>2 μg
Ag	Al	Ce	Ba	Ca
Au	Ar	Cl	Bi	F
As	Cd	Ge	Mg	Fe
Br	Cu	Hg	Ni	O
Co	Cr	In	S	Sn
Dy	Cs	K	Tl	Zr
Eu	Er	Mo	Zn	
Ho	Ga	P		
Ir	Gd	Pt		
La	Hg			
Lu	I			
Mn	Na	Rb		
Pa	Nb	Ru		
Pr	Nd	Se		
Re	Os	Si		
Rh	Pd	Sr		
Sc	Sb	Ta		
Sm	Tb	Te		
Tm	Th	Ti		
V	U	Y		
W	Yb			

Quantitative, essentially carrier-free separation techniques which have gained much popularity in recent years include ion exchange, partition chromatography, solvent extraction, distillation (Hg, Cr, Os, As, Sb, Ge, Se, Ru, and Mn), and controlled-potential electrolysis. Ion exchange with organic resins or inorganic exchangers are often employed advantageously in sequential separation such as the rapid separation of neutron-activated rare earths. Liquid ion exchangers combine the advantages of solvent extraction with ion exchange or, chromatographic separations when used as the stationary liquid phase (Cerrai, 1964).

Measurement of Radioactivity

Recent improvements in the measurement of radioactivity are generally refinements in existing techniques rather than new instrumentation. A survey of commercially available detectors and preamplifiers was published recently (Nucleonics, 1964, vol. 22, p.5, 22). Although not substantially improved lately, the thallium-activated 3 χ 3 inch sodium iodide crystal is still the most used gamma-ray scintillation detector. Pure and europium-activated calcium iodide detectors have been reported to provide a higher light-output signal and therefore, a higher resolution as compared with the sodium iodide (Tl) detector. The thickness of calcium iodide detectors produced up to now is limited to about 6 mm.

In recent years, neutron counting has been used in certain activation analysis problems. Neutrons produced by the (γ, n) reaction of O^{18} and the (γ, n) reaction of F^{19} are useful for the determination of oxygen and fluorine.

Recently, semiconductor detectors (such as silicon and germanium lithium-drifted detectors) have entered the field of nuclear detection with very promising results. Their most interesting use in activation analysis is gamma-ray spectroscopy where the lithium-drifted germanium detector has a much higher resolving

power than the NaI (Tl) scintillator. Presently, resolutions of 7 Kev for 2.75 Mev gamma-rays are obtainable compared with 100-120 Kev for a 3 $\times$ 3 inch NaI (Tl) detector. However, there are drawbacks. They must be operated in vacuum at liquid-nitrogen temperatures, and their efficiency for high-energy gamma-rays is low because of their small size. Gallium arsenide, which has shown some promise as a semiconductor at room temperature, may obviate one difficulty. Commercially available digital spectrum stabilizers provide stabilization in high resolution experiments of long duration. These form high-performance systems when used together with large multiparameter analysis units (4,096 channels) and high-resolution lithium-drifted germanium detectors.

Automation of Activation Analysis

The modular aspects of activation analysis (activation, radiochemical separations, gamma spectroscopy, and computer data processing) provide the means of automating the entire activation analysis sequence. Completely automated systems have been applied to process-stream monitoring of coals and ores (i.e., copper) and should find application in geochemical prospecting and exploration where low cost, rapid, and accurate elemental analyses of large number of samples are required. In recent years, the use of electronic computers in nuclear and radiochemistry has grown spectacularly. They are used for determining photopeak areas, analyzing complex spectra resulting from mixtures by fitting a set of library spectra to unknown spectra or by spectrum stripping, and for the analysis of multicomponent radioactive decay curves. New developments in sealed-tube fast neutron generators with outputs in the range of 10^{10} to 10^{11} neutrons per second and pneumatic transfer systems have made many techniques, such as the analysis of oxygen, fast, reliable, and accurate.

Some Geochemical Applications

Because of its exceptionally high sensitivity for many elements, radioactivation analysis is particularly valuable in the determination of geochemical trace-element distributions. Such efforts are exemplified by studies of the distribution of about 18 trace elements in sea water by neutron-activation analysis after irradiating the salt residues obtained by freeze-drying in vacuum, and performing some radiochemical separations prior to measurement by gamma-ray spectrometry.

Neutron-activation analysis has been applied particularly to studies of meteorites. Copper and zinc abundances were determined in one study in chondritic meteorites. The fluorine content of chondrites, determined by the (γ, n) reaction of F^{19} was suggested as a means of classifying chondrites. Following ion exchange and radiochemical separations, the rubidium and cesium contents of chondrites determined by neutron activation have provided the means of studying possible fractionation mechanisms based on volatility and the leaching action of water. The tantalum content of chondrites was found to be 0.021 ppm by Ehmann and 0.023 ppm by Atkins and Smales. Abundances of Au, Ir, and Pt have been determined in a wide range of meteoritic and terrestrial materials. Neutron-activation determination of gold in a variety of rock samples gave a spread of 1 to 10 ppb for two-thirds of the samples. Compared to previous estimates of 4-5 ppb, the crustal abundance of gold from these new data is estimated as 2.5 ppb. The zinc contents of geochemical standard samples (G-1, W-1, NBS samples) were determined by gamma-ray spectrometry.

FISSION TRACK ANALYSIS

The passage of a heavy charged particle through an insulating solid produces radiation damage along a submicroscopic track. Such tracks were discovered first in mica as a result of irradiation with fission fragments from uranium-235 (Silk and Barnes, 1959). Similar

natural particle tracks or fossil tracks were discovered in mica (Price and Walker, 1962). These are produced by heavy particle fragments resulting from spontaneous fission of uranium mineral inclusions present in the mica or of uranium mineral particles located nearby. Such tracks have since been found to occur in a large number of insulating materials, including many minerals, glasses, and certain plastics. It is postulated that they are caused by the removal of electrons by the bombarding particles. The resulting positive ions are mutually repelled into interstitial positions leaving high concentrations of voids and interstitials along the path of the particle. Some materials, such as metals which are good conductors of electrons and semiconductors which are good conductors of holes, do not form tracks.

The damage trails, which are only 50 A or less in diameter, are stable indefinitely at temperatures below a critical value, depending on the material. If a freshly exposed surface of the material is etched by appropriate chemical attack then preferential attack takes place along the tracks. The etch figures produced can be seen with an optical or an electron microscope.

Applications

Solid-state track detectors can be made sensitive not only to heavy fission particles but also to neutron and alpha particles (they are sometimes used as dosimeters for the latter). They have been applied to measuring spontaneous-fission lifetimes ranging from 10^{-16} seconds to 10^{16} years, and to determining low concentrations of elements which emit alpha or fission particles either spontaneously or after bombardment (Fleischer, and others, 1965b).

Exceedingly low concentrations of uranium can be determined in minerals in which tracks can form and be developed. Concentrations of uranium as low as an atom fraction of 10^{-12} have been determined in crystals of quartz, mica, and olivine. The atom fraction of uranium, C_V, is given by the relationship,

$$C_V = \rho_i / \varphi t \sigma N_o K f$$

where ρ_i is the number of tracks per square centimeter, φ is the flux of thermal neutron irradiation, t is the time irradiated, σ is the cross section for thermal neutron-induced fission, N_o is the number of atoms of the material per cubic centimeter, K is a factor approximately equal to the etchable range of a track in the material, and f is the known fraction of uranium atoms undergoing fission as a result of the irradiation.

In practice, fossil tracks are first etched and counted, or sometimes removed by annealing, and then the sample is irradiated, etched, and recounted. The increase in track concentration is a measure of the uranium concentration. This technique also enables study of the distribution of uranium in the sample. Inclusions of uranium minerals produce clusters of tracks. Furthermore, the uranium content of individual mineral separates can be determined from small samples.

Determinations can be made even when the material itself does not form stable or developable tracks. Samples of such material are irradiated between sheets of mica of low uranium content. The mica is then etched, and the track densities, obtained in the regions of the grains, are used to calculate the uranium content. In this manner, Fleischer and others (1965a) studied minerals separated from the Vaca Muerta mesosiderite and measured uranium concentrations ranging from 4,000 ppm in zircon down to less than 1 ppb in hypersthene and anorthite.

The fission track technique has also proved very useful for dating terrestrial and extraterrestrial materials. The dates obtained are those since the material had cooled below the track erasing temperatures. The relationship between age, T, and track density ρ_s per square centimeter of surface is

$$\rho_s = [\exp.\ (\eta_d T) - 1]\ \eta_f N R C_{238} / \eta_d$$

where η_d and η_f are the total and spontaneous fission decay constants for U^{238}, N is the number of atoms per cubic centimeter, C_{238} is the U^{238} atomic fraction, and R is the range of fission tracks. Where T is less than 10^9 years, the equation is simplified

$$\rho_s \simeq \eta_f T N R C_{238}$$

If the sample is exposed to a quantity of $\underline{n}$ thermal neutrons and the density ρ_I of new tracks which result from fission of U^{235} is measured then,

$$T = (\rho_s/\rho_I)\underline{n}\sigma/\eta_f$$

where $I = C_{235}/C_{238}$ and σ is the cross section for thermal fission of U^{235}.

These techniques have been used for dating numerous materials, particularly micas, tektites, and meteorites. By incorporating uranium into various glasses, the track method may be used as a dosimeter for neutrons. A tremendous range can be measured with the further advantage that the materials are not sensitive to other types of radiation. Plastic materials which produce alpha tracks have also been made. Such materials can be used to monitor alpha irradiations and also to measure low concentrations of boron or lithium which emit alpha particles on bombardment with neutrons.

MÖSSBAUER SPECTROMETRY

Rudolph Mössbauer discovered in 1958 that nuclei bound in a crystalline lattice could, under certain conditions, emit or absorb gamma rays without undergoing significant recoil. If the energy of the gamma ray does not exceed about 150 Kev, then the energy is not sufficient to break chemical bonds, and the recoil energy is absorbed and dissipated by vibrational waves within the crystal lattice. As a result, the emitted gamma ray has an extraordinarily sharp line width, on the order of 10^{-8} ev or about 10^{-12} of the total energy of the gamma ray. Such a sharply tuned gamma ray can be absorbed resonantly by a nucleus similar to

the emitting one which is suitably bound in a crystalline lattice.

The Mössbauer resonance effect is so sensitive that changes in energy levels of the emitting or absorbing nucleus as low as 1 part in 10^{12} can be readily detected. The Doppler effect change in the energy of a gamma ray resulting from relative movement of the order of 0.01 mm per sec between the source and detector can also be determined.

Use is made of this Doppler shift to obtain Mössbauer absorption spectra. As the motion of the source relative to an absorber is changed, the energy of the gamma ray is changed. A Mössbauer spectrum (fig. 2) is obtained when the radiation transmittance of the sample measured by counting with a detector is plotted as a function of velocity.

The Mössbauer effect can resolve the hyperfine nuclear structure resulting from the interaction of magnetic and electric fields surrounding the nucleus. If the absorber is in a different state of chemical combination than the source atoms, an isomeric or chemical shift in energy is obtained, and the source must be moved toward or away from the absorber to restore resonance. This shift is a linear function of the density of s-electrons around the nucleus. Effects produced by changes in inner electron shells such as in the lanthanides and actinides also produce shifts. Therefore, analysis of Mössbauer spectra can yield information about electronic and magnetic configurations around the nucleus as well as valence states of atoms and charge distributions in a crystal lattice. A complete discussion of the Mössbauer effect is given by Wertheim (1964) and a review of the recent literature by Devoe and Spijkerman (1966).

Instrumentation

Recently, research-oriented Mössbauer effect analyzers have become commercially available. Typical spectrometers employ a mechanical or electromechanical means for imparting a relative

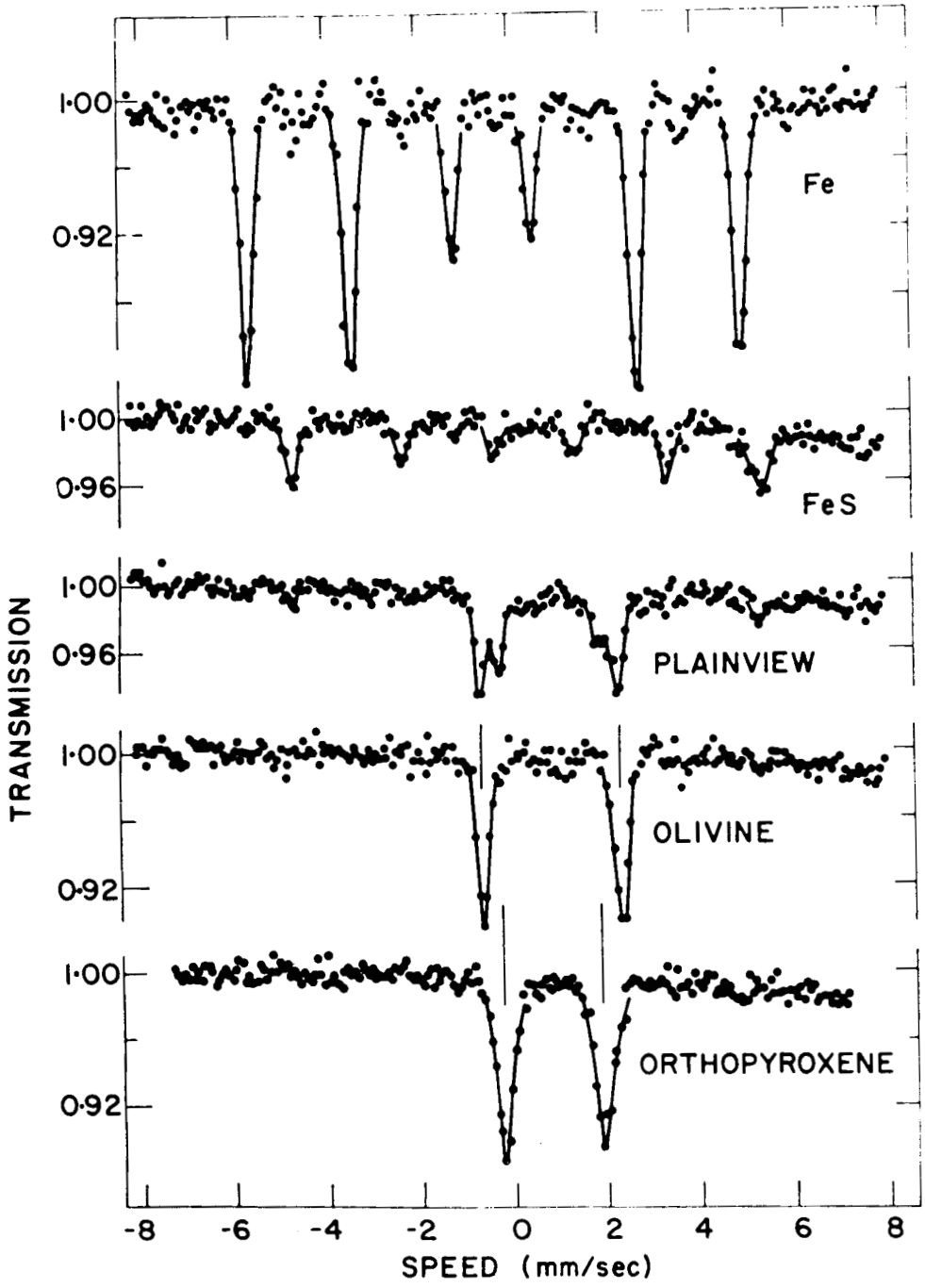

Figure 2.--Mössbauer absorption spectra of the Plainview meteorite and reference minerals present in most stone meteorites. (Positive velocity indicates a motion of the source toward the absorber.) From Sprenkel-Segel and Hanna (1964).

velocity between the source and absorber, thereby changing the energy of the gama rays.

The radionuclide source for the study of the Fe^{57} nucleus is 267-day Co^{57} diffused into copper or platinum. In the process of radioactive decay, Co^{57} generates an isomeric state of the decay product Fe^{57}, the decay scheme being $Co^{57} \rightarrow Fe^{57m} \rightarrow Fe^{57}$.

If metallic, the absorber is used as a thin sheet. Crystalline materials are mounted in plastic. The rays passing through the absorber are fed into a single-channel pulse-height analyzer and counted with a multichannel analyzer after being modulated in proportion to the instantaneous velocity of the source.

Applications

Mössbauer effect provides a valuable supplement to more traditional methods of analysis. Of the elements which have nuclides suitable for observing Mössbauer effects, only a few have been studied extensively. Most work has been done with iron, tin, the rare-earth elements, gold, and the platinum group. Isotopes of other elements in which the effect has been observed include nickel, zinc, tellurium, krypton, iodine, xenon, tantalum, hafnium, tungsten, and rhenium.

Structural studies have been made of a number of iron compounds and minerals, including prussian and turnbull's blue, potassium ferrate (III and VI), spinel oxides, and amosite. Of particular interest is a study of the iron in the Plainview, Holbrook, and Johnstown stone meteorites by Sprenkel-Segel and Hanna (1964). By comparison with absorption patterns of known materials, they were able to identify the iron-bearing minerals present, the relative proportion of the minerals, and the oxidation state of the iron ions. Spectra obtained for the Plainview meteorite and reference minerals are shown in figure 2.

ATOMIC ABSORPTION SPECTROMETRY

Atomic absorption spectrometry is one of the most significant analytical developments of the last decade. The first observation of the absorption of spectral energy by certain elements was recognized by W. H. Wollaston in 1802. Although observations of atomic absorption have long been employed in astrophysics and atomic physics, it was not until about 1955 that the analytical applicability of this technique was suggested by the Australian chemist, A. Walsh (1955). Reviews (Zettner, 1964; Kahn, 1966) and comprehensive discussions of the theoretical basis (Elwell and Gidley, 1962) have appeared in the literature.

The basic principle of atomic absorption is simple. Free atoms absorb light on narrow resonance lines, about 0.001 A wide, which are characteristic and specific for each element. In a flame, only a very small fraction of the atomic population (generally <1 percent) is excited to high energy states, whereas the majority remains as unexcited free atoms still available to absorb light within the flame. It is this large unbound population which accounts for the high sensitivity of atomic absorption methods. Thus, while flame photometric methods measure emission of spectral radiation from a sample solution passing through a flame, atomic absorption measures absorption of characteristic radiation from an external source such as a hollow cathode lamp by the unexcited atoms in the flame. Atomic absorption is applicable to more elements than flame emission techniques because, in atomic absorption, compounds are dissociated only into free ground-state atoms rather than into excited atoms.

The method is less subject to interference from foreign elements than flame emission photometry and is capable of yielding greater precision. These considerations, coupled with the simplicity of the technique and the availability of excellent instruments, account for the phenomenal increase in its use by analysts.

Flames and Burners

Flame temperatures ranging from 1,700 to 2,200°C can be obtained by burning coal gas, propane, hydrogen, or acetylene with air; temperatures ranging from 2,700 to 3,100°C are obtained with these gases burned in oxygen. The acetylene-nitrous oxide flame gives a temperature of 2,955°C. Using the standard air/acetylene flame, Fe, Mg, Ca, Na, K, Mn, Li, Cr, Ni, Cu, Zn, Rb, Sr, Cd, Pb, Bi, Ag, and Au can be reliably determined in geologic materials.

The tendency of some elements to form refractory compounds rather than atoms when they burn has limited the use of atomic absorption for the analysis of such elements. In general, this effect can be ascribed to too low a flame temperature. Massive burners using a mixture of nitrous oxide and acetylene as a fuel rather than the conventional air-acetylene or air-propane mixtures enable determination of elements such as aluminum, some lanthanides, and silicon as well as boron, germanium, hafnium, titanium, tungsten, and vanadium. On the other hand, if flame temperature is too high, a loss of sensitivity can result because of significant ionization. Ionization of barium in a nitrous oxide-acetylene flame can approach 90 percent.

A sheathed oxygen-acetylene or oxygen-hydrogen burner is now available commercially, and reports on the use of oxygen-acetylene atomizer-burners indicate a gain of at least an order of magnitude in detection limits by both emission and absorption methods. Atomic absorption spectroscopy is generally limited to the analysis of liquids. A finer degree of dispersion and a higher concentration of the aerosol has been obtained by the use of continuous ultrasonic nebulizers. Special techniques are being developed to aspirate suspensions and to sputter solid samples for atomic absorption measurement.

Sources

The most commonly used light source is a hollow-cathode lamp which has a cathode made of the element sought and a low-pressure filling of neon or argon. The light emitted by such a lamp is rich in the resonance lines of the element. Until recently, only one element could be determined at a time; each element required the installation in the instrument of a special source lamp. Multi-element hollow-cathode lamps such as Ca-Zn, Cr-Mn, or Ca-Mg-Al made from alloys, intermetallic compounds, or mixtures of powders sintered together are now being manufactured. However, complicated emission spectra and poorer detection limits because of reduced energy limit the utility of some of these lamps. A recent improvement in lamp technology is the high-intensity lamp. It produces 10 to 100 times more intense resonance lines than conventional hollow-cathode lamps without significant increase in the intensity of the spectrum of the rare-gas filler. Such lamps also suppress the ion lines of the cathode element. A further advantage is that low photomultiplier voltages are adequate, thereby resulting in greatly increased signal-to-noise ratios. High-intensity lamps are of particular value where the signal produced by conventional hollow cathodes at the resonance wavelength is weak (As, Bi, Pb, Sb, or Se) or where the element sought is at concentrations close to the sensitivity limit (<5 percent absorption). In addition, they have been applied to elements with complex spectra (Ni, Fe, Co, and Sn). Improvements can be expected also for the determination of the "refractory" elements.

Fassel and co-workers (1966) have presented the results of a critical evaluation of the feasibility of employing, as primary sources, spectral continua from the tungsten lamp, the hydrogen arc, and the xenon arc. Using such spectral continuum primary sources, the sensitivities observed for 32 elements were either comparable to or exceeded those obtained with sharp-line primary sources. The stable high-pressure xenon-mercury lamp permits use of the sensitive lines of many elements (Na, Sr, and Ca) in the ultraviolet region where tungsten lamps emit little or no ultraviolet light.

Instrumentation

Currently used instruments employ either the basic principle of atomic absorption or one of two modifications in their construction. In the simplest (single-beam d-c system), light from a lamp source is passed through the flame and the resonance wavelength absorption measured electronically after isolation by a monochromator or filter and d-c amplification. In order to minimize interference from flame emission such as radiation continuum of other constituents around the resonance line of the element sought, most instruments modulate the source light by mechanical or electronic chopping, leaving the flame light unchopped. The unmodulated flame emission is filtered out electronically. Such instruments may be either single- or double-beam ac systems. In instruments employing double-beam systems, a rotating sector mirror is used as the chopper. It passes the source light alternately through and around the burner flame, and the ratio of the recombined sample and reference beams is measured electronically. Double-beam a-c instrumentation compensates for drifts in detector sensitivity and changes in source intensity, reportedly eliminating the need for prolonged source warmup.

Sensitivity Enhancement and Elimination of Interferences

As in flame emission, the limit of sensitivity (table 3) for atomic absorption is customarily defined as that concentration of an element in solution which results in an absorption producing a signal 1 percent above background. One method of improving the sensitivity of an atomic absorption analysis is by increasing the absorption path length by multiple passes of the beam through the flame using mirrors. Using 12 traversals of the beam, sensitivity increases of almost an order of magnitude have been reported. However, the merits of multiple-passing are debatable.

Table 3.--Detection limits by atomic absorption

(concentration ranges in micrograms per liter)

0.001-0.01	0.01-0.1		0.1-1		1-10	
Cu	Ag	Fe	Al	Pb	As	Si
K	Be	Mn	Au	Pt	Ba	Sn
Li	Ca	Ni	Bi	Rh	Ga	Ta
Mg	Cd	Rb	Co	Sb	Ge	Ti
Na	Cr	Sr	Hg	Te	Pd	V
Rb	Cs		In	Tl	Se	W
Zn			Mo			

Of general applicability in atomic absorption spectrometry is the use of organic chelating agents and solvent extraction, thereby effectively screening the metal atom sought from deleterious ions and yet being readily released in the flame during chelate decomposition. An example of this technique is the protective chelation of magnesium with 8-hydroxyquinoline to overcome the interference of sulfate, phosphate, aluminum, and silicon. Only one magnesium line (2,852 A) is suitable for absorption measurements, and serious interferences occur in the presence of other elements capable of forming high-temperature stable acidic oxides. Such interferences may also be eliminated by the use of competing cations or releasing agents such as lanthanum or strontium. Organic additives (i.e., glycerol, methanol, or EDTA) to increase the effectiveness of inorganic releasing agents such as lanthanum also help suppress interferences of Al, Ti, Zr, Fe, S, and P in the determination of the alkaline earths in silicates.

Solvent extraction of heavy metals (Cd, Co, Ni, Zn) or chelation-extraction permit not only the separation and preconcentration of elements sought from large samples but also their direct aspiration for atomic absorption measurement. The technique is typified by the chelation of heavy metals with sodium diethyldithiocarbamate followed by extraction into methylisobutyl ketone (MIBK); the extraction of zinc, thallium, and cadmium bromides into MIBK;

or the extraction of cesium with a solution of sodium tetraphenylboron in hexone-cyclohexane which is then aspirated.

The preferred resonance lines of some elements lie below 2,100 A (Se at 1,960 A and As at 1,937 and 1,972 A), making it mandatory, for these determinations, to use fused silica optics capable of being purged with nitrogen or helium. Multichannel atomic absorption quantometers are now commercially available. One, a direct-reading instrument employing a fixed grating with photomultiplier tubes mounted behind fixed slits and a meter readout system, has found practical application.

Atomic Fluorescence

Atomic fluorescence spectrometry, which embodies principles of both emission and absorption spectroscopy, has recently been introduced as a means of chemical analysis. As in absorption spectroscopy, the sample solution is aspirated by a total consumption atomizer-burner into an oxygen-hydrogen or oxygen-acetylene flame to produce ground state atoms. The radiation from an appropriate metal-vapor lamp is used at right angles to the optical axis of the monochromator to excite the atoms to fluorescence. The fluorescence intensity is a measure of the concentration of the element being determined. Fluorescence techniques are reportedly as sensitive or more so than absorption and emission methods and are especially useful in the analysis of elements which have resonance lines in the ultraviolet, such as Zn (2,139 A), Cd (2,288 A), Hg (2,537 A) and Tl (3,776 A). Combining a xenon-arc continuous source, a total-consumption atomizer-burner, and a low resolution monochromator, sensitivities usable in trace analysis for 13 elements of geochemical interest (Ag, Au, Ba, Bi, Ca, Cd, Cu, Ga, Mg, Ni, Pb, Tl, and Zn) were obtained by flame fluorescence spectroscopy--for example: Zn (0.0001 ppm), Ti (0.04 ppm), In (10 ppm), Hg (0.1 ppm), and Ga (10 ppm).

Geochemical Applications

Atomic absorption spectroscopy is being used increasingly in geochemical prospecting for ore deposits; routine mineral assays for Cd, Cu, Pb, Ag, and rapid analysis of silicate and carbonate rocks. It has also been incorporated by one of the authors into a system of high precision methods for the analysis of materials of astrogeologic interest such as tektites, stony meteorites, impactites, and crater materials. Atomic absorption is being used for the determination of Ca, Mg, Na, K, Mn in a rapid rock analysis scheme at the U.S. Geological Survey. Largely because of the speed of atomic absorption determinations and their relative freedom from interferences, a complete rock analysis for 12 elements is made in about 3 hours. Determinations by atomic absorption of elemental concentrations in sea waters without prior chemical separation have provided concentration-depth profiles for both the North Atlantic and Gulf of Mexico.

OPTICAL EMISSION SPECTROMETRY

When atoms are heated to high temperatures, such as in arc, spark, or gaseous discharges, they emit light of definite wavelengths characteristic of the element or molecule. Spectroscopy is a convenient, relatively simple, multielement technique amenable to trace-element analysis as well as microanalysis. Some 70-odd elements at levels down to 10 nanograms are detectable or determinable simultaneously when covering a practical spectral range from 1,650 to 9,000 A. Principles, practices, and analytical applications of optical emission spectrometry have been presented or reviewed by Scribner and Margoshes (1965), Burakov and Yankovskii (1964), and Ahrens and Taylor (1961).

Sample preparation techniques often include preliminary separation and enrichment procedures. Space limitations do not permit a general description of the various enrichment methods used in spectrographic analysis, but an illustrative listing would include evaporation, ashing, volatilization, precipitation, solvent extraction,

chromatography, ion exchange, electrolysis, controlled potential electrolysis, amalgamation, fire assay, magnetic separation, and zone refining.

Steps have been taken to automate emission spectroscopy using modern computer technology. Photographic plates have been replaced by photomultiplier detectors placed behind slits, each slit isolating a desired spectral line. Precision readout systems have been developed for spectrometers which use capacitors or analog computer-type integrators to integrate current signals from the phototubes. One such instrument can be programed to determine quantitatively 11 elements at the same time. Another instrument has been designed for routine six-step semiquantitative determination of 40 elements simultaneously. It is fully automatic from time of arcing to the final typing of the report.

High-speed electronic computers developed especially for spectroscopic applications are now commercially available. Some of the computations being handled are calibration of photographic emulsion, transformation of microphotometer readings to relative intensities including background corrections, and statistical analysis of data such as least-square fitting of linear functions to data points.

Sources

A selected number of recent developments will be briefly discussed here, namely, excitation in controlled atomosphere, laser microprobe, the microspark, and the plasma jet.

Controlled Atmosphere Arc Excitation

In emission spectroscopy, the normal practice of sample excitation by an electrical discharge in air results in cyanogen band formation from the reaction of the graphite electrode with nitrogen in the air. These bands obscure the most sensitive lines of several elements. The use of controlled-atmosphere excitation (Ar or He) either in an electrode-chamber or as an arc sheath not only eliminates the cyanogen bands but also reduces the electrode temperature,

the latter being especially advantageous in selectively vaporizing volatile constituents while leaving refractory elements behind. Use of the arc sheath also stabilizes the discharge position, probably by overcoming convection currents.

Inert Atmosphere Spark Excitation

Quantitative emission spectroscopy is a comparative method based on the relation between element concentration and intensity using spectra of similar reference standard processed in the same manner. Rapid analysis of metallic materials such as meteorites for Fe, Ni, Co, and Cu can be undertaken by point-to-plane spark excitation in controlled atmospheres (N_2 or Ar) using closely matching reference standards and plotting calibration curves in terms of concentration ratios (i.e., Ni I / Fe I, and Ni I / Fe II). Unlike excitation in air, inert atmosphere spark excitation provides nearly constant background intensity with line intensities nearly proportional to concentration and does not require presparking of samples because line intensities reach a steady value almost as soon as the spark is started.

Laser Microprobe Excitation

Direct spark microanalysis of nonconducting specimens was not possible until the recent advent of the laser microprobe, which provides a high-intensity, pulsed laser beam. Laser probe excitation looks promising for the qualitiative and quantitative analysis of samples as small as 35μ in diameter (sample weight as small as 10^{-7} g). Q-switched ruby laser can provide the energy for immediately vaporizing a target area. The laser light is focused onto the specimen by a metallurigcal microscope, which is also used for specimen viewing and sample area selection. Additional energy for exciting the sample vapor is provided by a spark circuit. The technique has high absolute sensitivity (amounts as small as 10 pg) and has been applied to the analysis of naturally occuring metallic microspherules, schlieren bands in tektites, and sulfide minerals.

Microspark Excitation

Another recent development, the microspark excitation system, can pinpoint a 5μ inclusion in a heterogeneous sample and analyze selected areas of heterocrystalline geologic meterials and intermetallics of meteorites. The device is a chemically pointed rod of tungsten, placed on the stage of a modified microscope, in close opposition to a sample. A sample alinement within 2μ of the section to be analyzed can be achieved through a micromanipulating system and a Filar eyepiece.

Plasma Jet

The plasma jet is a technique permitting the determination of elements in solution with exceptionally high precision. The technique employs the aspiration of the sample solution mixed with an inert gas under pressure through a small orifice into a d-c arc (temperatures rising as high as 10,000°C) producing predominately spectra of ionized lines characteristic of the d-c arc. Some advantages of the plasma jet are universality of liquids analyzed, high sensitivity, extreme stability, capability of continuous analysis, and the reduction in matrix effects. Addition of organic solvents (ethylene glycol-dimethyl ether) to the solutions has extended sensitivity limits as much as six-fold. Using silica-free solutions, this technique has proven very useful in major-element analysis of very small amounts of geologic materials.

Selected Geochemical Applications

Optical emission spectroscopy is an indispensable instrument in the modern geochemical laboratory. Abundances of 20 trace and minor elements in dolostones and dolomites have been obtained spectrographically using an air-jet to stabilize the arc column and to suppress selective volatilization. Statistical analysis of these data yield separate populations of the two major lithologic varieties of dolomitic carbonate rocks for certain trace elemnts.

The contents of many trace elements (B, Co, Cr, Cu, Mn, Mo, Ni, P, Pb, Sn, Ti, V, Y, and Zr) have also been determined spectrographically using an air-jet and indium as an internal standard in geologic reference materials (limestones, dolomites, shales, granites, clays). Geochemical behavior of trace elements during bauxite and kaolinite formation by the weathering of andesite lava under humid tropical conditions in Malaysia was studied by obtaining analytical data for Cr, Co, Ga, Mn, and Ni spectrographically. The problem of the geochemical behavior of boron during the metamorphism of carbonate rocks required analytical data. These were obtained using a d-c arc emission spectrochemical technique.

Analytical separation and enrichment operations involving ion exchange and solvent extraction have been integrated with spectrochemical techniques into systems of complete analysis of naturally occurring silicates such as basalt, ultramafics, syenite, shale, soil, and stony meteorites for the following elements: Ag, Al, Au, Ba, Ca, Cd, Ce, Cs, Cu, Fe, Ga, In, La, Li, Mn, Mn, Mo, Na, Nd, Ni, Pb, platinum group, Rb, Sc, Si, Sn, Sr, Ti, Tl, V. Y, Zn, and Zr.

Spectrographic determination of rhenium in molybdenite with d-c arc excitation requires its preconcentration by solvent extraction from basic solution as the quaternary amine (tetrabutyl ammonium bromide) with 4-methyl-2-pentanone. A measured protion of an HCl solution of the residue remaining after wet-ashing (with $CoCl_2$ added as an internal standard) is placed on a previously prepared electrode, dried, and spectrographed.

Solution techniques have been applied to direct-reading emission spectroscopy for the partial analysis (Al_2O_3, CaO, Fe_2O_3, TiO_2, MgO, and Mn_2O_3) of high-silica materials such as quartzite, flint, sand, silica refractories, impactites, and tektites.

Zinc can be used as an indicator of the thermal history experienced by tektites and was determined spectrographically with the argon d-c arc down to 2 ppm in a 20 mg sample. Analysis of over 65 carefully selected tektite specimens representative of every known strewnfield showed zinc concentrations ranging from 5 to 50 ppm.

X-RAY FLUORESCENCE SPECTROSCOPY

In recent years, X-ray fluorescence spectroscopy has been applied to many analytical problems, often yielding results with higher precision and at greater speed than would be possible by other methods. It has been particularly useful where the size of the sample as well as the complexity of the materials make determinations by wet chemical methods difficult.

X-ray fluorescence spectroscopy is concerned with the analysis of characteristic electromagnetic radiation (2,000-8,000 A) emitted by the elements as a result of excitation by irradiation with primary X-rays, generally from an X-ray tube. Excitation by primary X-ray radiation leads to secondary X-ray emission by all elements of atomic number three or higher. The frequency of the emitted X-ray lines depends on the atomic number. For almost all elements with $Z>12$, several series of X-ray lines (K, L, M---) are emitted within a frequency range measurable with standard equipment. For any given atom, the wavelengths of the spectral series increase--the K lines have the shortest wavelengths and the M spectrum the longest wavelengths. K and L spectra are used predominantly in X-ray spectroscopy, but recent improvements in detectors and crystals have made the long wavelength M spectra useful analytically.

An XRF unit basically comprises a power source and voltage regulator, an X-ray tube (primary excitation source--Pt, Cr, W, Mo, etc.), a beam collimating system, an analyzing crystal of known d-spacings, a detector-counting system, and a goniometer for precise measurement of the reflected angles. The use of controlled-atmosphere paths, helium or a vacuum, permits transmission of the longer wavelengths. Emergent X-rays are detected by means of scintillation counters or various types of gas-filled proportional counters. The X-ray quanta are converted into electrical pulses which are registered on electronic consoles containing scalers, ratemeters, automatic read-out systems, and strip chart recorder.

The method is nondestructive and can be applied to liquid or solid samples. Quantitative analysis is realized because of the proportionality of fluorescent intensities to concentration. Recorded intensities depend, however, not only on the concentration of the element being analyzed but on the composition of the total sample as well. Deviations from linearity may be positive (enhancement) or negative (absorption), and the effect is commonly referred to as the "matrix effect" or "interelement effect." The effect is usually minimized by dilution, by addition of a heavily absorbing element, or by corrections based on weight fractions and mass absorption coefficients. Assuming controlled instrumental conditions and uniform sample preparation, accuracy and reproducibility of results will depend upon attaining optimum signal-to-noise ratios and reasonably brief counting times.

Analyzing Crystals for X-ray Spectroscopy

In analyzing crystals used for X-ray spectroscopy, the following data are sought: Interplanar spacing, degree of crystal perfection, minimal fluorescence of crystal, coefficient of reflection for first-order reflection, and coefficient of reflection for higher order reflections. Crystals commercially available for X-ray analysis and the crystal ranges for the K and L lines of the elements are shown in figure 3A and table 4. Analyzing crystals such as alkali-acid malonates, sucrose, and pentaerythritol (PET) have been employed in the X-ray fluorescence analysis of silicon, aluminum, and other low atomic number elements. Of these crystals, PET gives the highest count rate for silicon and aluminum.

Reflectivities of analyzing crystals vary with individual crystals and wavelengths; different crystals of the same type vary by as much as a factor of two. Crystal surface generally affects performance. Etched surfaces are more highly reflecting at shorter wavelengths and polished surfaces more efficient at longer wavelengths (ADP and PET) because rough-surfaced crystals tend to absorb the diffracted longer wavelengths. The deliberate introduction of elastic or plastic strain

in a given crystal can increase the diffraction intensity without excessively broadening the diffracted line.

Table 4.--Analyzing crystals for X-ray spectroscopy

(from Adler and Rose, 1965)

Crystal	Reflecting planes	2d, A	Reflectivity
SiO_2 (quartz)	5052	1.624	Low
Topaz[1]	303	2.712	Variable
SiO_2 (quartz)	1012	2.750	Low
LiF	200	4.026	High
NaCl	200	5.641	Do.
Si[2]	111	6.271	Do.
Fluorite	111	6.32	Do.
Ge[2]	111	6.54	Do.
SiO_2 (quartz)	1011	6.686	Do.
SiO_2 (quartz)	1010	8.510	Medium
PET (pentaerythritol)	002	8.74	Do.
EDDT (ethylene diamine ditartrate)	020	8.803	Do.
ADP (ammonium dihydrogen phosphate)	110	10.64	Do.
Gypsum	020	15.12	Do.
Mica[3]	002	19.92	Do.
KAP (potassium acid phthalate)	1010	26.4	Do.

[1]Topaz is used to minimize spectral interference (high spectral resolution crystal).

[2]Primarily, silicon is used with intermediate and heavy atomic numbered elements whereas germanium is used with light atomic numbered elements, in cases where 2d order interferences occur (both suppressing 2d order reflections).

[3]Mica is used as curved crystal (microprobe).

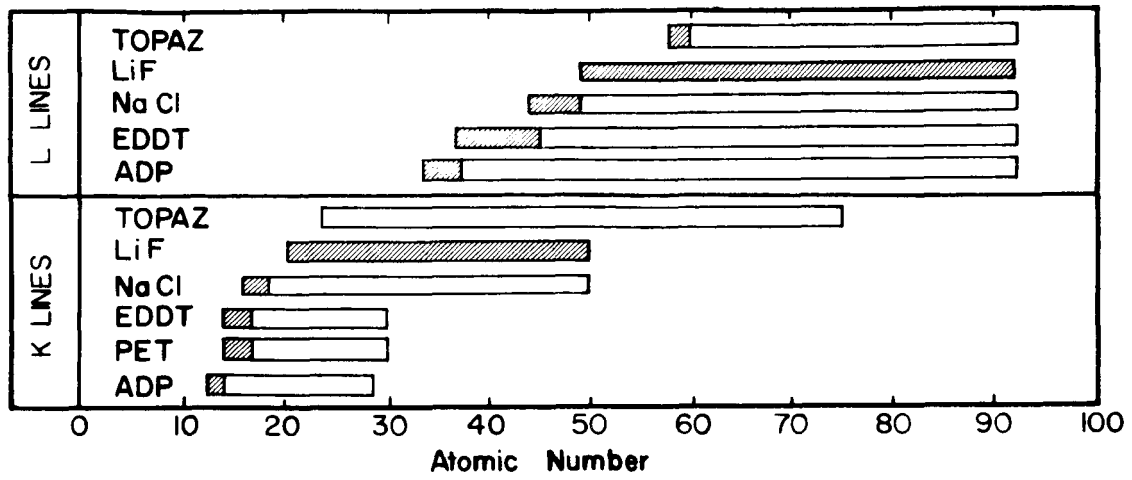

Figure 3A.--Crystal ranges for K and L lines of the elements. Shaded areas indicate optimum range of the crystal.

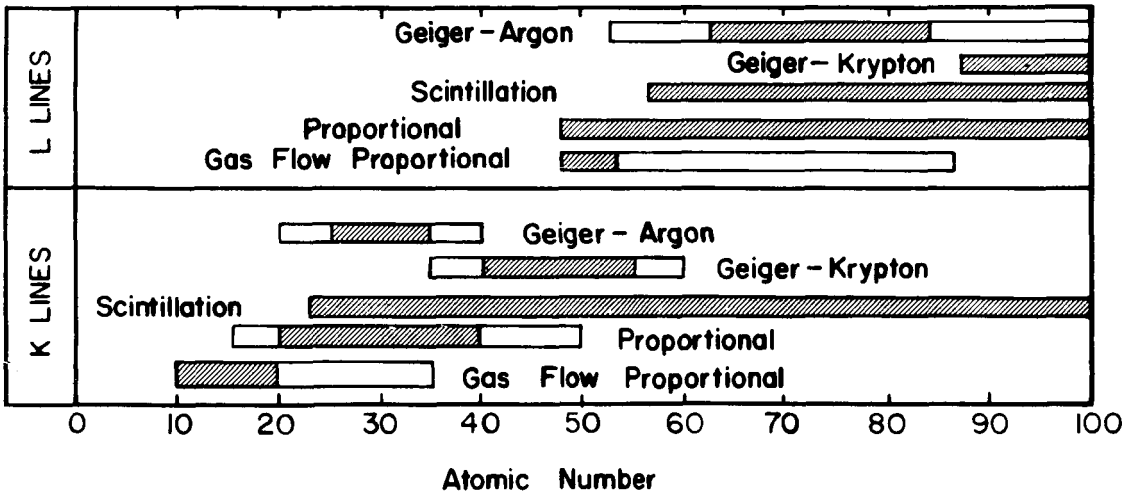

Figure 3B.--Detector ranges for K and L lines of the elements. Shaded areas indicate optimum range of the counter.

Spectrometers with focusing curved crystals are used increasingly for microanalysis as well as macroanalysis. A wide variety of analyzing crystals is available. The most commonly used are LiF, EDDT, PET, ADP, KAP, NaCl, quartz, gypsum, topaz, and Langmuir-Blodgett soap films (for very long wavelengths). A lead lignocerate multilayer soap-film structure has been used to disperse the K emission lines of boron and beryllium resulting from both electron and X-ray excitation. Curved analyzing crystals of KAP and lead stearate-decanoate have been used to measure intensities of oxygen and fluorine K emission lines from oxides and fluorine compounds.

X-ray fluorescence analysis is often complicated by interferences of higher order reflections, as in the case of the Nb-Ta and Zr-Hf systems. The use of crystals (silicon or germanium) whose second order reflections are missing or weak is one method of overcoming or minimizing these interferences. For mica, odd orders are very strong and even orders weak. This phenomenon produces a crowding of the spectrum in the light element region.

Detectors

Detectors used in X-ray emission spectroscopy may be either gas-filled Geiger and proportional detectors, photomultipliers, scintillation counters, or high-resolution semiconductor devices. Because of its very high efficiency for the most useful analytical region from 3 A down, the scintillation counter consisting of a thallium-activated NaI phosphor is currently the most widely used X-ray detector. The optimum elemental range for some of the commercially available detectors is presented in figure 3B.

High-resolution semiconductor detectors--in particular, semiconductor diodes of silicon and germanium developed primarily for nuclear gamma-ray spectrometry--have many potential uses in X-ray analysis. Data indicate that silicon diodes 3 mm thick can serve as good detectors of K X-rays of lighter elements (up to barium, Z=56) and also for the measurement of L X-rays of the

heavier elements. For the heavier elements (high-energy K X-rays up to 120 Kev), lithium-drifted germanium is the favored counter material. Rugged miniaturized instruments for rapid nondestructive qualitative analysis of geologic materials both in the field and in the laboratory are being developed.

X-ray Tubes

A modern X-ray spectrometer is built around an X-ray tube having high-energy output, spectral purity, and long-term stability. Until recently, W and Mo target tubes were the only ones commonly obtainable. However, a number of new tubes (Pt, Cr, Ti, Al, Rh, Ag, Cu, and a dual target Cr-W tube) suitable for optimum excitation of specific wavelengths have become commercially available. They have also provided increased line intensities as well as improved signal-to-noise ratios. With the development by Henke of a demountable tube with changeable targets, replaceable filaments, and a continuously pumped ultrasoft X-ray source, quantitative analysis by X-ray spectrometry has been extended into the very light element range (magnesium through boron). Use of a vacuum isolation gate permits the convenient utilization of extremely thin detector windows (e.g., 1μ polypropylene film) which can be changed without disturbing tube vaccum. Various modifications of the Henke tube have been reported in the literature. Recently, the analysis of C, O, F, Na, and Mg has been greatly improved by the application of multilayer analyzers to ultrasoft X-ray spectroscopy (Langmuir-Blodgett type such as stearate and lignocerate systems with 2d spacings equal to 100 and 130 A, respectively).

Some Instrumental Developments

Analysis with vacuum X-ray quantometers (also known as polychromators or multichannel analyzers) is rapid and compatible with computer technology. Programed scanning spectrometers have also been incorporated, permitting either slow or rapid scanning over a predetermined wavelength range and the integration of spectral

intensities at specific wavelengths. Programed analysis systems with as many as 22 channels are available. Also available commercially now are single goniometers with sequential programing capability.

Associated Chemical Techniques

Quantitative X-ray fluorescence analysis may involve preconcentration or isolation. Such concentration extends the applicability of X-ray fluorescence analysis to the determination of microgram quantities, thereby providing improved sensitivity and minimized absorption and enhancement effects. A further advantage is that standards covering the anticipated analytical composition can be prepared from solutions. These techniques have been applied to the determination of microgram quantitites of zirconium (precipitated as the para-bromomandelate) and to the determination of trace amounts of chlorides. Silver chloride, for example, is precipitated and filtered into a Millipore filter which is exposed to the X-ray beam as a thin film, producing a linear relationship between intensity and concentration.

Measurement of X-ray intensities of preconcentrated elements requires some sort of support medium. Commonly used media include cellulose powder, borax, lithium borate, ion exchange resins, Millipore filters, filter paper, alumina, glass-fiber filters, and plastic films. To reduce matrix effects, an internal standard or a heavy metal "buffer" can be incorporated into the support media. Systematic studies have shown that high-precision trace analyses are possible using ion exchange materials not only to separate and collect elements but also as support media. Using an X-ray microprobe with fully focused curved crystal optics, as little as 0.01 μg of metals taken up on very small ion exchange discs has been determined. Combined ion exchange–X-ray spectroscopic techniques should find wide applicability in geochemical prospecting, the study of stream pollution, and mineral and rock analysis.

Selected Geochemical Applications

Comprehensive treatments of the principles of quantitative X-ray analysis have been presented by Liebhafsky and colleqgues (1960). Adler and Rose (1965) and Campbell and co-workers (1962, 1966) have reviewed the fundamentals and recent literature of micro- and trace-element analysis.

Accurate determinations of Zr and Hf are of importance not only with respect to Hf/Zr ratios and possible Earth-meteorite fractionation but also for testing models of nucleosynthesis and their related cosmic abundance curves. X-ray fluorescence techniques have provided meaningful data. X-ray fluorescence analysis of niobate-tantalate ore concentrates has brought speed and accuracy to determinations that are difficult to do chemically. Fluorescent X-ray spectrometry, using strontium as an internal standard, has yielded results comparable to those obtained by gamma-ray spectrometry in the determination of thorium in monazite and other rare-earth ores.

An X-ray fluorescence method has been developed that enables quantitative determination of major constituents in very small amounts (0.2-5 mg) of rocks, minerals, impactites, tektites, and meteorites (Rose and others, 1965). In this technique, the sample solution is absorbed onto powdered chromatographic paper, which is dried and pelleted and then exposed to the X-ray beam.

X-ray milliprobes have been developed for mineralogical analysis of small samples or inclusions from about 0.1 to 1.5 mm in diameter. Concentration profiles in polished, flat sections of rocks are rapidly determined by collimating the primary X-ray beam at the sample and accurately moving the sample across the X-ray beam with a motor driven micrometer.

The use of soft X-ray sources (CuL for B, C, N, and O; Alk for O, F, Na, and Mg; AgL for Al, Si, P, S, Cl; and CrK for K, Ca, and Ti) according to the wavelength region of interest, coupled with stearate, KAP, or PET analyzing crystals in vacuum system, holds

great promise for the analysis of these elements.

Computer programs (such as Fortran II) have been devised to detect and correct for instrumental drift, to compute and statistically evaluate calibrations, to test standards for contamination, and to test replicates of unknowns for precision. Using curved crystals, modified instruments permit the examination of very small areas (about 0.5 mm in diameter) for identification of single-grain inclusions or the study of the distribution of selected elements along a chosen traverse. Rapid semiquantitative determinations providing elemental ratios can be obtained from recorded X-ray spectra.

REFERENCES CITED

Adler, I., and Rose, H. J., Jr., 1965, X-ray emission spectrography, chap. 8 of Morrison, G. H., ed., Trace analysis--physical methods: New York, Interscience Pub., p. 271-324.

Ahrens, L. H., and Taylor, R. S., 1961, Spectrochemical analysis: 2d ed., Reading, Mass., Addison-Wesley Pub. Co., 454 p.

Belsky, T., Johns, R. B., McCarthy, E. D., Burlingame, A. L., Richter, W., and Calvin, M., 1965, Evidence of life processes in a sediment two and a half billion years old: Nature, v. 206, p. 446-447.

Bowen, H. J. M., and Gibbons, D., 1963, Radioactivation: Oxford, Oxford Univ. Press, 295 p.

Burakov, V. S., and Yankovskii, A. A., 1964, Practical handbook on spectrochemical analysis: London, Pergamon Press.

Burlingame, A. L., Haug, P., Belsky, T., and Calvin, M., 1965, Occurrence of biogenic steranes and pentacyclic triterpenes in an eocene shale (52 million years) and in an early precambrian shale (2.7 billion years): a preliminary report: Natl. Acad. Sci. Proc., v. 54, p. 1406-1412.

Campbell, W. J., and Thatcher, J. W., 1962, Fluorescent X-ray spectrography: determination of trace elements: U.S. Bur. Mines Rept. Inv. 5966.

Campbell, W. J., Brown, J. D., and Thatcher, J. W., 1966, X-ray absorption and emission: Anal. Chemistry, v. 38, p. 417R-439R.

Cerrai, E., 1964, Chromatographic reviews: 6, 129, Amsterdam, Elsevier Pub. Co.

Dal Nogare, S., and Juvet, R. S., Jr., 1962, Gas-liquid chromatography--theory and practice: New York, Interscience Pub.

_____1966, Gas chromatography: Anal. Chemistry, v. 38, p. 61R-79R.

Day, D. T., 1903, Experiments on the diffusion of crude petroleum through fuller's earth [abs.]: Science, v. 17, p. 1007-1008.

DeVoe, J. R., and Spijkerman, J. J., 1966, Mössbauer spectrometry: Anal. Chemistry, v. 38, p. 382R-393R.

Elwell, W. T., and Gidley, J. A. F., 1962, Atomic absorption spectrophotometry: New York, Macmillan, 102 p.

Fassel, V. A., Mossotti, V. G., Grossman, W. E. L., and Kniseley, R. N., 1966, Spectrochim. Acta, v. 22, p. 347-357.

Fleischer, R. L., Naeser, C. W., Price, P. B., and Walker, R. M., 1965a, Fossil particle tracks and uranium distributions in minerals of the Vaca Muerta Meteorite: Science, v. 148, p. 629.

Fleischer, R. L., Price, P. B., and Walker, R. M., 1965b, Solid-state track detectors: applications to nuclear science and geophysics: Ann. Rev. of Nuclear Sci., v. 15, p. 1-28.

Gilpin, J. E., and Bransky, O. E., 1911, The diffusion of crude petroleum through fuller's earth: U.S. Geol. Survey Bull. 475, 50 p.

Gilpin, J. E., and Cram, M. P., 1908, The fractionation of crude petroleum by capillary diffusion: Am. Chem Soc. Jour., v. 40, p. 495.

Gilpin, J. E., and Schneeberger, P., 1913, Fractionation of California petroleum by diffusion through fuller's earth: Am. Chem. Jour., v. 50, p. 59.

Heftmann, E., 1966, Chromatography: Anal. Chemistry, v. 38, p. 31R-61R.

Ikan, R., 1965, Thin-layer chromatography of tetracyclic triterpenes on silica impregnated with silver nitrate: Jour. Chromatography v. 17, p. 591-593.

Ikan, R., and Cudzinovski, M., 1965, Separation of sterols and corresponding stanols on thin layers of silica impregnated with silver nitrate: Jour. Chromatography, v. 18, p. 422-423.

Ikan, R., Harel, S., Kashman, J., and Bergmann, E. D., 1964, The separation of sterols and corresponding stanols by thin-layer chromatography: Jour. Chromatography, v. 14, p. 504-506.

Kahn, H. L., 1966, Instrumentation for atomic absorption, pts. 1, 2: Jour. Chem. Education, v. 43, p. A7-A42, A103-A132.

Kirchner, J. G., Miller, J. M., and Keller, G. J., 1951, Separation and identification of some terpenes by a new chromatographic technique: Anal. Chemistry, v. 23, p. 420-425.

Lederer, E., and Lederer, M., 1957, Chromatography: New York, Elsevier Pub. Co., 711 p.

Liebhafsky, H. A., Pfeiffer, H. G., Winslow, E. H., and Zemany, P. D., 1960, X-ray absorption and emission in analytical chemistry: New York, John Wiley & Sons, 357 p.

Littlewood, A. B., 1962, Gas chromatography: New York, Academic Press.

Lyon, W. S., 1966, Radioactivation analysis as an analytical tool: New York Acad. Sci. Annals, v. 137, p. 311-322.

Lyon, W. S., Ricci, E., and Ross, H. H. 1966, Nucleonics: Anal. Chemistry, v. 38, p. 251R-260R.

Maier, R., and Mangold, H. K., 1964, Thin-layer chromatography in Reilly, C. N., ed., Advances in analytical chemistry and instrumentation: v. 3, New York, Interscience Pub., p. 375-477. 477.

Moshier, R. W., and Sievers, R. E., 1965, Gas chromatography of metal chelates: Oxford, Pergamon Press, 163 p.

Murphy, M. T. J., Bartholomew, N., Rouser, G., and Kritchevsky, G., 1965, Identification of sulfur in lipid extracts by TLC: Am. Oil Chemists Soc. Jour., v. 42, p. 475-480.

Price, P. B., and Walker, R. M., 1962, Observations of fossil particle tracks in natural micas: Nature, v. 196, p. 732.

Ritchie, A. S., 1964, Chromatography in geology: New York, Elsevier Pub. Co., 185 p.

Rose, H. J. Jr., Cuttitta, F., and Larson, R. R., 1965, Use of X-ray fluorescence in determination of selected major constituents in silicates: U.S. Geol. Survey Prof. Paper 525-B, B155-B159.

Rosenthal, I., and others, 1961, chaps. 33-37, in Kolthoff and Elving, eds., Treatise on analytical chemistry: pt. I, v. 3, New York, Interscience, p. 1411-1723.

Scribner, B. F., and Margoshes, M., 1965, Emission spectroscopy in Kolthoff and Elving, eds., Treatise on analytical chemistry: pt. I, v. 6, New York, Interscience Pub., p. 3347-3461.

Silk, E. C. H., and Barnes, R. S., 1959, Examination of fission fragment tracks with an electron microscope: Philos. Mag., v. 4, p. 970.

Sprenkel-Segel, E. L., and Hanna, S. S., 1964, Mössbauer analysis of iron in stone meteorites: Geochim. et Cosmochim. Acta, v. 28, p. 1913-1932.

Stahl, E., 1958, Dunn schichtchromatographie. II. Standard. Isierung sichtbarmachung, dokmention und anwendung: Chemiker-Ztg., v. 82, p. 323-328.

Stahl, E., ed., 1965, Thin-layer chromatography--a laboratory handbook: New York, Academic Press.

Walsh, A., 1955, The application of atomic absorption spectra to chemical analysis: Spectrochim. Acta, v. 7, p. 108-117.

Wertheim, G. K., 1964, The Mössbauer effect-principles and applications: New York, Academic Press.

Zettner, A., 1964, Principles and application of atomic absorption spectroscopy, in Sobotka and Stewart, eds., Advances in clinical chemistry: p. 2-62, New York, Academic Press.

THE SIMULTANEOUS DETERMINATION OF Cs, Hf, AND Ta BY NEUTRON ACTIVATION

By Paul Greenland

One of the major difficulties in identifying the parent material of tektites stems from uncertainty of the importance to be attributed to chemical fractionation due to selective volatilization during the fusion process. One approach to this problem is the study of volatile/involatile element ratios in tektites and comparison of these results with similar ratios found for crater materials of known meteoritic impact origin. As a first step in this program, a procedure for the simultaneous determination of Cs (a volatile element) and Hf and Ta (involatile elements) by a neutron activation technique has been developed.

SUMMARY OF PROCEDURE

Samples of about 100 mg were irradiated for 8 hours in a thermal neutron flux of 10^{13} neutrons cm^{-2} sec^{-1} using the Naval Research Laboratory reactor. After a delay of at least 10 days to permit decay of short-lived activities, the sample was fused with Na_2O_2 in the presence of carriers for Ta and Hf. The fusion cake was leached with water containing 10 mg Cs_2CO_3 as carrier for the Cs activity and was filtered. The precipitate was washed carefully to ensure that Cs would appear quantitatively in the filtrate. The filtrate was counted on a 3 $\times$ 5 inch NaI (Tl) scintillation crystal coupled to a 256-channel analyzer. The precipitate was dissolved in a dilute HF-HCl mixture, and the rare earths were precipitated using La as a carrier. The filtrate from this was passed through an anion-exchange column which retained the fluorocomplexes of Hf and Ta while most other elements were washed through. Hf was then eluted with dilute HF-HCl, scavenged for rare earths as above, precipitated with NH_4OH, and dissolved in dilute HF for counting. After further washing, Ta was eluted from the column using a dilute

mixture of $HF \cdot NH_4Cl$ as the solvent, precipitated with NH_4OH, and dissolved in dilute HF for counting. After counting, the chemical yield of the procedure for Hf and Ta was determined by irradiating the solutions and comparing the induced activity with standard solutions; the chemical yield of Cs was assumed to be 100 percent.

DISCUSSION OF PROCEDURE

Using this procedure, only Ta appears in a reasonably radiochemically pure state. In the Cs fraction, peaks due to Cr^{51} and Mn^{54} (from an n, p reaction on Fe^{54}) are routinely observed while Fe^{59} and Sc^{46} are also frequently present. In the Hf fraction, Pa^{233} (from β-decay of Th^{233}), Sc^{46}, and Fe^{59} are usual contaminants. The gamma spectrometric counting system in use here easily resolves these interferences; thus, this procedure may be considered a semiinstrumental one since only limited radiochemical separations are employed.

The useful sensitivity limit of this procedure is about 0.01 ppm Cs, Hf, Ta. Although this is entirely satisfactory for most samples, it could be greatly lowered by increasing sample size and (or) irradiation time. The accuracy and precision of this method is presently being evaluated by analyzing a number of rocks, including several that have been previously analyzed by other techniques. Analyses of tektites and crater materials will immediately follow the demonstration of acceptable accuracy and precision of the procedure.

SPECTROGRAPHIC DETERMINATION OF ZINC AND SILVER IN SILICATES USING AN ARGON-D-C ARC

By Charles Annell

INTRODUCTION

The volatile elements zinc and silver can act as indicators providing information on the thermal history of tektites and other naturally occurring silicates and also on the extent and effects of differential volatilization processes occurring during their formation. Schnetzler and Pinson (1963) have reported a range of approximately 1 to 20 ppm zinc for 42 tektites from various strewnfields. They also presented data obtained by other investigators for the concentrations of zinc in various terrestrial silicates which averaged from 16 ppm in sandstones to 95 ppm in shales. The spectrographic procedure (Bastron and others, 1960) generally employed in the Geological Survey laboratory has a detection limit of 300 ppm Zn, which precludes its use for the determination of zinc in tektites and other silicates.

Self-absorption and scattering of the emitted light occur when high concentrations of atoms of the same species are present in the arc. The volatility of zinc at relatively low temperature (bp 907°C) suggests that the most efficient excitation can be effected by using a relatively cool arc. Vallee and Baker (1956) have reported that prolonged periods of volatilization and enhancement of line intensities can be achieved by using an inert gas such as argon as the arcing atmosphere. They also reported that the use of an alkali metal salt has little apparent effect on the line intensities of volatile elements arced in argon--an observation substantiated in the course of this study.

The use of helium as the arcing atmosphere for zinc determinations was disappointing. The higher anode temperature engendered by use of helium resulted in greatly suppressed Zn line intensities, in agreement with earlier reports (Vallee and others, 1950; Vallee and Peattie, 1952). A spectrochemical procedure for determining a number of elements in transistor-grade silicon carbide by an argon–d-c arc has been reported (Morrison and others, 1960). In this case, the level of impurities is in the parts per billion to low parts per million range. The samples were mixed with 10 ppm GeO_2, which acted as an internal standard for more volatile elements. The spectrochemical determination of trace elements in silicon dioxide using an argon–a-c arc has been described by Vecsernyes (1961). A method is presented here for the determination of trace concentrations of zinc and silver in silicates.

ANALYTICAL CONDITIONS

In the Geological Survey laboratory, controlled atmospheres have been effectively employed using an open-top gas jet with the controlling gas sweeping around the sample anode (Helz, 1964). An argon gas flow of 6.6 liters per minute coupled with a d-c arc of 25 amperes produced a very steady arc. A "jumping plate" of 10 second exposures indicated complete volatilization of zinc from a variety of silicates in less than 1 minute using a powdered graphite admixture with 20 milligrams of the pulverized sample. The Zn 3345.02 line was used in all the work.

A variety of exposure conditions were tested to establish the best conditions requiring the least critical adjustments. These conditions are summarized in table 1. It should be mentioned that the undercut sample electrode (anode), designated "S-13" by the ASTM (1964), is produced with either carbon or graphite material. At first carbon was selected because of its relatively low heat conductivity. Its use resulted in slightly faster volatilization of the sample components. However, certain samples were subject to a welling-up in the electrode crater, causing continuous light

emission from the resulting incandescent particles. The resultant spectrum had a prohibitively heavy background and line broadening, preventing accurate Zn determinations. Use of the graphite S-13 electrode, with lower heat retention, eliminated this difficulty.

Table 1.--Spectrographic conditions

Electrodes	Undercut 1/4-in. graphite anode, type S-13; and a 1/8-in. graphite counter electrode. A 3-mm analytical gap.
Excitation	An 8 amp d-c arc for 5 sec, then switched to 25 amp for the remaining 85 sec. A 6.6 liter per min flow of argon around the electrode.
Spectrograph	An Eagle-mount, 3-m grating spectrograph set for 2d order in the 3,000-3,680 A spectral region. A 45-cm cylindrical quartz lens at the 25-μ slit focusing the middle 3d of the arc gap on the grating.
Photography	Eastman III-O emulsion, plate. Developed for 4 min at 18°C in D-19 developer.
Calibration	2 step, 50/100 percent T, Fe spectrum recommended method of ASTM (1964).

STANDARDS

A series of zinc standards was prepared by successively diluting the standard granite, G-1 (Zn = 45 ppm), and the standard diabase, W-1 (Zn = 82 ppm) (Fleischer, 1965), with pure SiO_2 quartz, using equal parts of each preceding standard and SiO_2. These standards were used to establish a detection limit for Zn at 4 ppm, using 20 mg sample and 20 mg powdered graphite, tamped firmly into the cavity of an S-13 type electrode.

Another set of standards was made using the opal glass standard NBS-91, which has a recorded zinc concentration of 640 ppb. The zinc content of NBS-91 was reanalyzed using both X-ray fluorescence

and atomic absorption techniques. A Zn concentration of 670 ppm was obtained (F. Cuttitta, oral commun.).

These silicate standards contain Zn in a matrix approximating chemical composition of tektite glasses. Dilution of the standard was made with a synthetic tektite-base matrix of tektite composition consisting of Johnson-Mathey "Specpure" chemicals and a pure quartz as shown in table 2.

Table 2.--Synthetic tektite-base matrix

	Percent
SiO_2 (quartz), N. C.	76
Al_2O_3	14
Fe_2O_3	3
K_2CO_3	2.5
$CaCO_3$	2
MgO	1
Na_2CO_3	1
TiO_2	.5
Total	100.0

This mixture was sintered at 900°C for half an hour in a muffle furnace. The matrix was ground and then mixed with NBS-91, providing a diluted standard containing 67 ppm Zn. Subsequent dilutions were made with equal parts of matrix to give a series of graded Zn concentrations down to 1.0 ppm.

A comparison of the analytical curves obtained with the carbon and graphite anodes is shown in figure 1. The slightly steeper slope is obtained with the graphite, which might be indicative of a more efficient excitation (less self-reversal) in the cooler electrode.

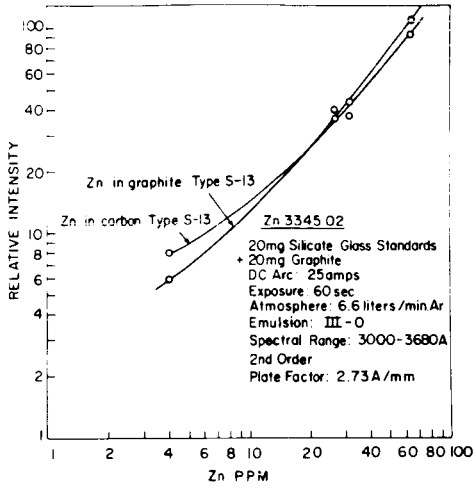

Figure 1 Analytical curves for Zn obtained with carbon and graphite electrodes.

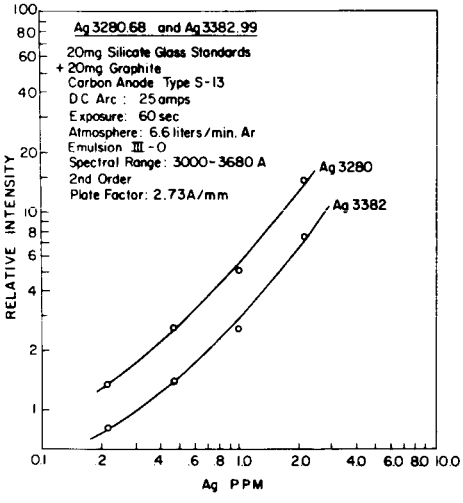

Figure 2 Analytical curves obtained with two different silver lines.

SILVER DETERMINATIONS

After the optimum conditions were established for the determination of zinc, an attempt was made to find an internal standard which might provide high accuracy. Although Wedepohl (1953) found cadmium to be a satisfactory internal standard with his "boiler" enrichment method for the determination of zinc, several moving or jumping plate tests with Cd (as CdO) and Ge (as GeO_2) added as internal standards indicated Cd to be more volatile and Ge less volatile than Zn, under the arcing conditions described above. However, it was noted that a silver impurity, as detected by the Ag 3382.99 and Ag 3280.683 lines, was volatilized beyond detectability in approximately 60 seconds.

A series of standards in a pegmatite base matrix (Bastron and others, 1960), which contained as little as 0.215 ppm Ag, was arced under the same conditions used for the determination of zinc. The analytical curves for both sensitive Ag lines are shown in figure 2. Since no modification of the Zn procedure is necessary, Ag can be determined to as low as 0.2 ppm at the same time. Care must be taken, however, to use the Ag 3382.99 line when Mn is present, especially when Mn 3280.75 is visible. This line causes a slight background difficulty for Ag determinations below 1 ppm. Precision of determinations for Zn was checked by arcing 10 replicate samples of a G-1:SiO_2 standard (Zn = 22.5 ppm). A coefficient of variations for the method was approximately 6 percent.

REFERENCES CITED

American Society for Testing and Materials, 1964, Methods for emission spectrochemical analysis: 4th ed., Philadelphia, Am. Soc. Testing Materials, 862 p.

Bastron, H., Barnett, P. R., and Murata, K. J., 1960, Method for the quantitative spectrochemical analysis of rocks, minerals, ores, and other materials by a powder d-c arc technique: U.S. Geol. Survey Bull. 1084-G, p. 165-182.

Fleischer, M., 1965, Summary of new data on rock samples G-1 and W-1, 1962-1965: Geochim. et Cosmochim. Acta, v. 29, p. 1263-1283.

Helz, A. W., 1964, A gas jet for d-c arc spectroscopy: U.S. Geol. Survey Prof. Paper 475-D, p. D176-D178.

Morrison, G. H., Rupp, R. L., and Klecak, G. L., 1960, Spectrographic analysis of high purity silicon carbide: Anal. Chemistry, v. 32, p. 933-935.

Schnetzler, C. C., and Pinson, W. H., Jr., 1963, The chemical composition of tektites, in O'Keefe, J. A., Tektites: Chicago, Univ. Chicago Press, p. 95-129.

Vallee, B. L., and Baker, M. R., 1956, Anode temperatures and characteristics of the dc arc in noble gases: Optical Soc. America Jour., v. 46, p. 77-82.

Vallee, B. L., and Peattie, R. W., 1952, Volatilization rates of elements in the helium direct current arc: Anal. Chemistry, v. 24, p. 434-444.

Vallee, B. L., Reimer, C. B., and Loofbourow, J. R., 1950, The influence of argon, helium, oxygen, and carbon dioxide on emission spectra in the dc arc: Optical Soc. America Jour., v. 40, p. 751-754.

Wedepohl, K. H., 1953, Investigations into the geochemistry of zinc [in German]: Geochim. et Cosmochim. Acta, v. 3, p. 93-142.